UNIVERSITÀ DEGLI STUDI DI PADOVA

Corso di Laurea Magistrale in Bioingegneria

Biomechanical analysis of sport performance of Wheelchair Rugby Italian National Team players

Tesi di laurea di: **Maria Laura Magrini**
Dipartimento di Ingegneria dell'Informazione

Relatore: **Prof. Nicola Petrone**
Dipartimento di Ingegneria Industriale

ANNO ACCADEMICO 2015/2016

Summary

ABSTRACT

A project with the aim of assessing how Wheelchair Rugby can improve neuromuscular activity of disabled people, was started in Padova in October 2015, with the participation of Italian National Team players. Within its 2 years duration, an engineering, medical and sportive group evaluates biomechanical, medical and sport training aspects to improve players' sport performance on court, with personal training and therapeutic programs which give advantages also in daily activities. The present work describes the biomechanical analysis performed on 19 players. The investigation of maximal isometric force in unilateral and bilateral pushing forward and shoulder/elbow flexion/extension allowed assessing the presence of asymmetries in contralateral joints, and determine force rankings of athletes. Tests of sprint, rotation, eight track, and the analysis of a match assessed their ability in dynamic sport performance. Pressure tests on the wheelchair seats allowed identifying the presence of incorrect postures.

INTRODUTCION

Sport has many powers: it gives the chance to express personal abilities, meet new people, fight for the same goal together, and go beyond physical and mental limits. For people with physical impairments, caused by an accident or a disease, sport becomes even more: a challenge with themselves, a need, a mean to overcome their limits, to acquire a deeper knowledge of their body, able to help them also in daily life.

In this contest, Wheelchair Rugby was born as a Paralympic sport for people with spinal cord injuries or with impairments that can be associated to tetraplegia. Started from Canada in the late 70s, it spread all over the world, reaching Italy in 2011. A group of enthusiastic people started to believe in this sport and to spread it, bringing to the foundation of different sportive association and teams, from which the Italian National Team was born.

After some years of training, national and European competitions, in October 2015 a project aimed at acquiring a deeper knowledge of this sport, was started in Padova, with the participation of some athletes of the Wheelchair Rugby Italian Team. The aim of this ambitious project is to observe the Wheelchair Rugby athlete on his totality, in order to improve his performance by bringing him to exploit at best his abilities.

An athlete is a complex system, involving many different aspects: first the motivation and the spirit of the team, then wheelchair, technique, force, ability, state of health, and many other features (*figure 1*). For this reason, the study analyses each participant from different points of view: medical, engineering, sportive and psychologic. A team composed by engineers, doctors, physiotherapists and sport scientists, work in strict contact with the athletes, to improve their sportive and physical performance with the investigation of the great number of involved aspects. In the present work, the biomechanical measures, performed by the engineering group from November 2015 to February 2016, will be described.

Figure 1. *Wheelchair Rugby athlete is a system involving many different aspects.*

CHAPTER 1

Wheelchair Rugby

Wheelchair Rugby was born in Canada in 1977: it developed as a Paralympic sport for people with tetraplegia. It grown intensively during the following years, and after being presented as a demonstration sport at the Atlanta 1996 Paralympic Games, it finally made its debut as a medal sport at the Sydney 2000 Paralympic Games. The sport is now practiced in more than 25 different countries all over the world, and includes men and women on the same team.

Wheelchair Rugby was first conceived for athletes with spinal cord injury: however, in the following years, people with a wide variety of impairments started competing in this sport. For this reason, a system of classification has the task of dividing roles within the game, by taking into account physical and psychological features of the athletes, together with their performance on court. In this chapter, the system of classification will be described, together with the Wheelchair Rugby court, rules and wheelchairs features and specifications.

1.1 Classification

Classification in Paralympic sport exists since the mid-1940s. Early classification was based only on medical diagnoses, such as spinal cord injury, amputation or other neurologic or orthopaedic conditions, conferring each athlete a sport class. However, recent reviews have taken into account a more functional classification, determining the sport class not only by health condition, but also by the relevance of an athlete's impairment to carry out fundamental activities to sport performance.

In the beginning of Wheelchair Rugby, according to its classification rules, athletes were divided into three sport classes, largely determined by medical diagnosis and neurological level of spinal cord injury. In 1991 a sport-focused classification system for Wheelchair Rugby was started. Although the spinal cord injury examination was used as a guideline in classifying the physical assessment, the classification rules were expanded to include, in the determination of the sport class, fundamental activities of Wheelchair Rugby. This change was made, on the other hands, to accommodate the growing number of athletes with different disabilities from spinal cord injury. People with diseases as poliomyelitis, cerebral palsy, muscular dystrophy, multiple sclerosis, multiple amputations and other conditions

with impairment in muscle strength similar to tetraplegia, started to be classified and compete in Wheelchair Rugby.

Classification is a continuous updating progress: the last review of the classification rules, by the International Wheelchair Rugby Federation (IWRF), dates to February 2015. All athletes are under regular observation by classifiers, to ensure two important goals:

1. to determine eligibility to competition;
2. to divide athletes into classes, assigning them a point (0.5, 1.0, 1.5,…3.5). The highest point values are given to players with the least movement restrictions. The lowest point are assigned to those players with the most severe impairments.

People who want to compete in Wheelchair Rugby have to perform different tests and evaluations, to determine the point of classification:

1. physical assessment by bench test;
2. technical assessment, including a range of sport specific tests and novel non-sport tests;
3. observation assessment, consisting of observation of sport-specific activities on court.

A system of classification is necessary both for the athlete and for the team: the assigned point often determines the role of the athlete on court and the type of wheelchair he uses; moreover, according to Wheelchair Rugby rules, the classification point has to be taken into account in the formation of the team playing on court [1].

1.2 On court rules

Wheelchair Rugby combines elements of rugby, basketball, football and ice hockey and it is played indoor in a basketball court, with a soft-cover volleyball ball. Each team is composed by 4 players and 8 substitutes. For each team, the sum of athletes' classification points playing on court cannot pass 8. During the match, each athlete is assigned a defensive or offensive role.

The field of play is a 15 x 28 m (*figure 2*), marked by end and side lines and is divided into two halves by the centre line on which the centre circle is also located. On the end lines two cones mark the goal line. At a distance of 1.75 m from the end lines, the key areas are signed. Only 3 defenders are allowed to remain inside these areas while no player is allowed to remain in the opponent's key area for more than 10 seconds when their team is in possession of the ball. On the sides of the court near the side lines penalty areas are marked out.

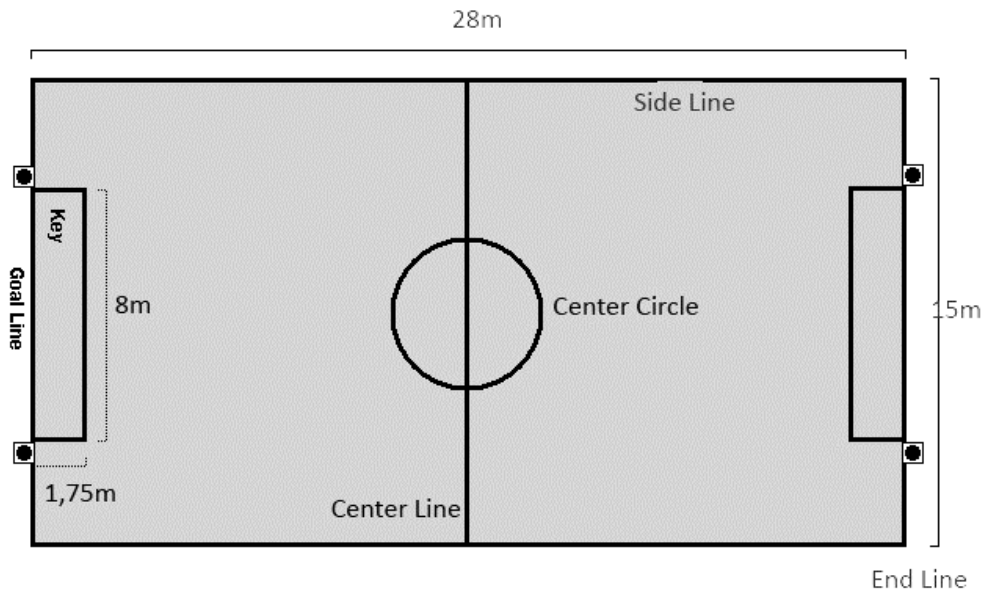

***Figure 2**. Wheelchair rugby field.*

The aim of the game is to score a goal by passing or touching the opponent's goal line with two wheels while holding the ball: the team with the highest score at the end of the match, wins. A match is played in 4 quarters of 8 minutes each, with 1 minute break at the end of the first and third quarter and a 5 minute break at the end of the second one. In the case of a tie, 3 minutes extra time is provided. Each team is entitled to 4 time-outs of one minute during the normal length of the game, and one time-out during extended time. If not all the time-outs are used, they can be transferred to extra time.

The game starts in the centre circle of the court: a referee launches the ball vertically between two opponent players. The remaining players take position outside the circle. The ball can be carried, dribbled, passed or stolen in any way, avoiding physical contact between athletes. When moving, players can hold the ball on their thighs, pass it to a team mate or bounce it, but it must be bounced or passed at least once every 10 seconds. Moreover, the team in possession of the ball must pass it to the other half of the court within 15 seconds. After a goal, foul or time-out, the ball is brought back into the game from the end line (when a goal is scored) or from the side lines.

Many unfair sportive behaviours are interrupted by the referees commanding the game. An offensive foul is punished by the loss of the ball, while a defensive foul is punished with one minute out of the game (in the penalty area). A player under the penalty of leaving the game cannot substitute an injured player. Instead of the one-minute penalty, the referee can award a penalty goal when a player is fouled while in possession of the ball and in position to score a goal [2,3].

Finally, it is worth to remember that Wheelchair Rugby would not exist without the great number of people that help athletes in their primary necessities, inside and outside the game: referees, staff members and volunteers.

1.3 Wheelchairs

The wheelchair is considered part of the player. It is the mean to move ad to express the athletes' specific talents and abilities within the game. At a first sight, it is possible to identify two types of chair: offensive and defensive, as shown in *figure 3.* Nevertheless, the chair does not automatically determine the role of the athlete during the match.

Figure 3. *Offcarr Go Try Rugby Wheelchair. Left: Offensive chair; right: defensive chair.*

An offensive chair is set up for speed and mobility, and equipped with a front bumper and wings to prevent other wheelchairs from hooking it. In most cases, players with higher points (more than 2.0) use this type of chair. Defensive wheelchairs contain bumpers set up to hook and hold opponents players. These wheelchairs are most often used by players with lower points (less than 1.5).

According to the sport rules, wheelchairs must meet some specifications, for reasons of equality and safety: the athlete is responsible of respecting them. The player who does not meet these specifications, is automatically banned from the game, until he returns on the established standards. The main specifications coming from IWRF Rugby International Rules are reported as follows.

- **Wheels**: the wheelchair shall have four wheels.
    - Two large wheels at the back (main wheels), used to propel the wheelchair; their maximum diameter shall be 70cm (*figure 4a*). Each main wheel must be fitted with a spoke guard protecting the area of contact by another

wheelchair, and a push rim. There shall be no bars or plates extending around the main wheels. The rearmost part of the main wheel shall be considered the back of the wheelchair and nothing can extend past this point.

- Two small wheels at the front (casters): they must be on separate axles positioned a minimum of 20 cm apart, measured centre to centre. The housing that holds the caster must be positioned no more than 2.5 cm away from the main frame of the wheelchair, measured from the inside edge of the housing to the outside edge of the mainframe.

- **Anti-tip devices:** the wheelchair shall be fitted with an anti-tip device attached at the rear of the wheelchair, consisting in two wheels a minimum of 40 cm apart. If the wheels of the anti-tip device are fixed, they cannot project further to the rear than the rearmost point of the main wheels. The bottom of the wheels of the anti-tip device must be no more than 2 cm above the floor (*figure 4b*).

- **Width**: there is no maximum width; no point on the wheelchair may extend in width beyond the widest point of the push rims.

- **Length**: the length of the wheelchair, as measured from the front-most part of the main wheel to the front-most part of the wheelchair, cannot exceed 46 cm (*figure 4b*).

- **Height**: the height of the wheelchair, as measured from the floor to the midpoint of the seat side rail tubing halfway between the front and back of the side rail, cannot exceed 53 cm (*figure 4b*).

Other specifications, not reported in this work, refer to bumpers, wings and other general standards about comfort and safety. Considering this rules, the athlete can make personal adjustments, in order to satisfy his/her physical and functional needs [3].

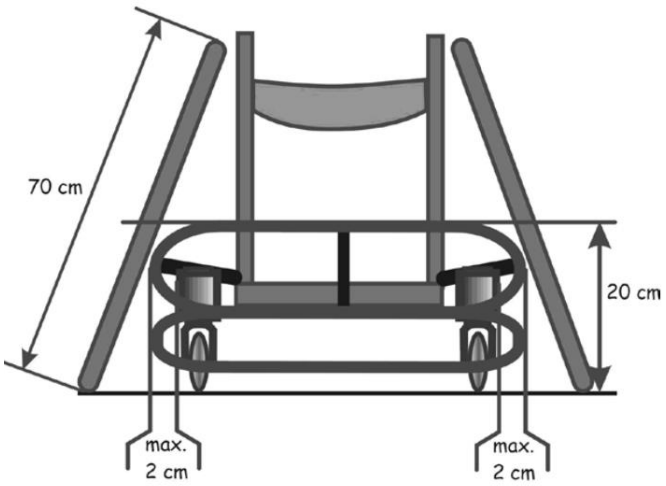

Figure 4. *a) Front view.*

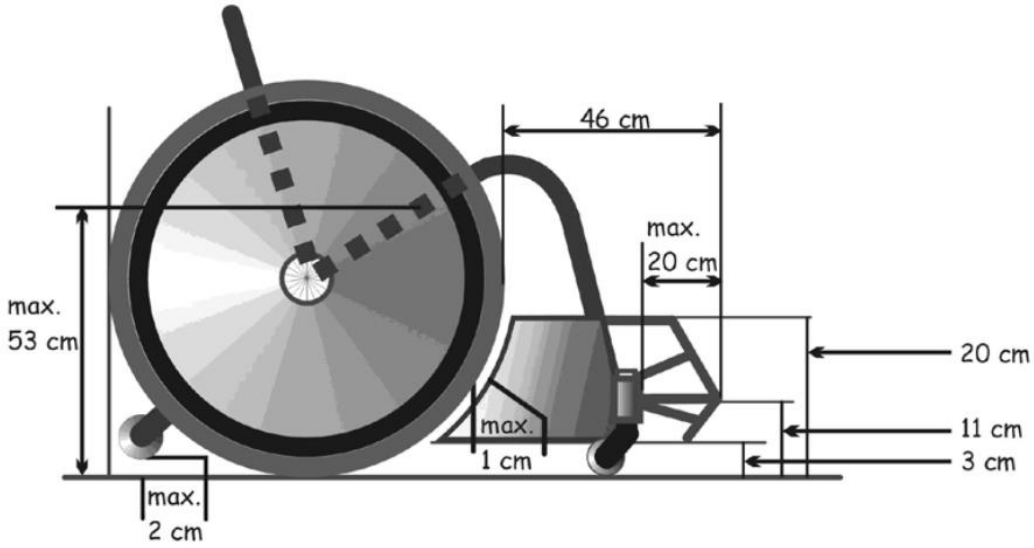

Figure 4*. b) Side view.*

1.4 Athlete equipment

Since wheelchair manoeuvrability is essential to guarantee the best performance on court, players are provided with a specific equipment ensuring safety, comfort and functionality during the game:

- **gloves**: mostly covered with rubber on the palm and taped to the wrist, they create additional grip in pushing, starting and stopping, and prevent skin injuries. Sometimes they can also help compensating the loss of hand and finger function associated with the particular disability of the athlete.

- **Straps**: athletes are firmly strapped to the wheelchair frame to improve their stability and balance. The three common strapped areas are the trunk, to eventually

compensate the lack of trunk control and to prevent the risk of falling forward during a high strike; the thighs, to prevent shifting from the seat; the feet for a more comfortable position.

- **Additional protections and equipment:** any kind of protection or device can be wear to prevent the risk of injuries or to compensate the loss of determinate physical function, without giving an additional advantage or creating risk for the other athletes [4].

***Figure 5**. An action during a match.*

CHAPTER 2

Project: “Improvement of the residual neuromuscular capacities in Wheelchair Rugby athletes”

In October 2015 a scientific project started in Padova, with the aim to assess how Wheelchair Rugby can improve the residual neuromuscular capacities in people with different physical disabilities. A scientific team composed by engineers, doctors, physiotherapists and motor scientists collaborates with the Italian Wheelchair Rugby National Team to perform physical, sportive and metabolic measures, in order to get information about their physical state from a medical and biomechanical point of view. These measures are collected to enhance their sportive performance, with the final goal of entering in the international rankings and participate to the Paralympic Games (Tokyo 2020).

2.1 Partners

Several partners finance and support the project:

- HPNR (Human Potential Network Research Onlus Via Toblino 53, Padova) the proposer company, managing the financial and organizational aspects;
- Industrial Engineering department (DIM) of University of Padova;
- Physiology department of University of Padova;
- FISPES (Italian Federation for Paralympic and Experimental Sports) providing a representation of the Wheelchair Rugby Italian National Team and its supporting staff;
- Offcarr SRL (Via dell’Artigianato 29, Villa del Conte, Padova), the main provider of Italian rugby wheelchairs, also interested in the investigation of biomechanical properties of movement and posture, and on the improvement of the structural frame of wheelchairs.
- OIC foundation (Opera Immacolata Concezione, via Toblino 53, Padova), providing the structures, and the equipment for the athletic preparation.
- Microgate (Via Stradivari 4, Bolzano) providing instruments for the biomechanical study;

- Tecnogym (Via Calcinaro 2861, Cesena, FC) providing instruments for the personal training;
- DJO Italia SRL (Via Leonardo da Vinci 97, Trezzano sul Naviglio MI)
- CIP (Italian Paralympic Committee).

2.2 Aims of the project

The project has a 2 years duration (from October 2015) and within this time, there are three main goals that it aims to achieve:

- ➲ improving the motor-functional sportive abilities of Wheelchair Rugby athletes, trying to promote at best their residual capacities;
- ➲ identifying individual rehabilitation programs;
- ➲ producing scientific protocols in order to classify athletes and supervise their performances during the rehabilitation programs.

Once the project is concluded, the results will be used with spinal unities and other related associations, in order to exploit at best the collected information. The results may be extended for other sports for people with disabilities. Moreover, two or more official classifiers, formed during the project duration, may work together with FISPES and IWRF (International Wheelchair Rugby Federation). Finally, the project may bring to the creation of an Italian reference centre for study and training of Paralympic sports, in the University of Padova, with an official role given by CIP.

The project aims at an evaluation of players under different points of view: biomechanical, medical and physiological investigations are able to create a general overview of the athletes. A sport engineering research group works for biomechanical measures, a group of doctors and physiotherapists investigates different medical and physiological aspects, and a sport medicine group works for the athletic training. In particular, these aims are divided into three main aspects, described in the following lines.

- **Biomechanical evaluations.**
    1. Study of the athletic performance:
        - measuring of dynamic forward push force and braking;
        - measurement of the ability to spin;
        - evaluation of the effectiveness in applying and sustain blocks;
        - evaluation of the strength of delivering the ball.
    2. Study of the properties of the wheelchair:
        - road load measurement;
        - maximum stress detection.

3. Study of posture and stability:
    - pressure distribution on cushion;
    - calculation of the 3D position of the center of gravity;
    - calculation of stability indexes.

- **Medical evaluations.**
    1. Study of the metabolic consumption:
        - measurement of the metabolic capacity thresholds;
        - estimation of body composition;
        - evaluation of muscle activation.
    2. Study of joint mobility:
        - ROM evaluation of shoulder joint;
        - ultrasound detection of muscle structure in the shoulder.
- **Sport medicine evaluations**.
    1. Identification of individual training schemes:
        - exercises during the team meetings;
        - exercises to individually perform outside the team training;
    2. Study of physiological variables:
        - ability of isometric shoulder and elbow flexion/extension;
        - measuring of VO_2max in ergometer tests;
        - measuring of RR and REE;
        - measuring of lactate and ventilator threshold (IAT);
        - recording of HR in different training situations;
        - EMG recording for different muscle groups.
    3. Study of an appropriate individual diet:
        - Daily calories uptake related to individual consumption and workloads.

2.3 Participants

The participants are 19 male players, with different levels of training. They are part of the Italian Wheelchair Rugby National Team, born in Padova in 2012. The list of players participating in the project, with their anthropometric parameters, classification points and type of wheelchair, is contained in the following *table (1).*

IN	INITIALS	DATE OF BIRTH	BODY WEIGHT [kg]	WCR WEIGHT [kg]	HEIGHT [cm]	POINTS	TYPE OF WCR
1	A.S.	21/09/1981	58	18	178	1.0	defensive
2	B.A.	21/03/1977	90	19	190	3.5	offensive
3	B.N.	21/06/1991	85	17	140	2.0	offensive
4	B.M.	29/10/1973	70	19	182	2.5	offensive
5	C.A.	05/12/1979	90	25	175	1.5	defensive
6	D.A.	16/08/1988	65	17	170	1.5	defensive
7	F.P.	15/01/1974	65	19	174	1.0	defensive
8	F.A.	06/12/1988	86	22	192	0.5	defensive
9	F.S.	23/07/1980	90	20	188	3.5	offensive
10	G.D.	26/01/1975	75	16	185	1.5	defensive
11	G.M.	06/11/1970	61	19	168	2.5	offensive
12	K.H.	05/07/1990	55	12	173	1.0	defensive
13	M.P.	21/11/1986	74	20	183	3.5	offensive
14	Q.V.	18/11/1969	80	19	177	2.5	offensive
15	S.P.	18/06/1992	55	16	177	0.5	defensive
16	T.G.	08/09/1984	68	17	180	1.0	offensive
17	T.N.	09/09/1990	79	21	178	2.5	offensive
18	V.L.	27/06/1977	108	21	185	2.5	offensive
19	Z.L.	26/11/1993	70	14	182	2.5	offensive

Table 1. *List of participants. IN=Identification Number; Initials=Surname+Name; date of birth; body weight; wheelchair weight; Points=classification point.*

2.4 Diary of the project

Each participant is asked to join a team meeting, one per month. Meetings take place at the OIC gym (Padova, via Toblino 53), from Friday to Sunday. The meetings started in October 2015, with the following dates until today:

1) 09-11/10/2015
2) 13-15/11/2015
3) 18-20/12/2015
4) 15-17/01/2016
5) 12-14/02/2016
6) 11-13/03/2016

From November 2015 to January 2016, the engineering group collected biomechanical measures about dynamic performances, isometric force, and posture tests.

Between November and December 2015, the medical group executed shoulder echographies, to analyse the state of the most stressed joint for Wheelchair Rugby players.

Starting from January 2016, a personal program of training was monthly given to the athletes, with the aim of improving their muscular force and resistance; moreover, in February 2016 a personal diet was produced and given to everybody.

Visceral and cardiocirculatory aspects are still under investigation, starting from February 2106, through interviews and questionnaires about the personal habits of the athletes sphincterical management during trainings and matches, and the use of standing instruments at home.

From January to March 2016, metabolic tests were executed by the sport medicine group, to evaluate the VO2 max of each athlete, durgin a test made on the ergometer.

In parallel, from February 2016, a study on the structure of wheelchair's frame is under investigation by the Engineering group.

2.5 Aims of this work and next developments

The project aims at achieving different goals along its two years duration: in this work, the biomechanical results collected during the team meetings from November 2015 to January 2016 are described. A study of Wheelchair Rugby player was carried out, to evaluate their performance on court and their physical abilities. Firstly, with the use of a load cell, the isometric force expressed in the fundamental movements involved in pushing a wheelchair, was tested. With the use of inertial sensors, the athletes' ability of accelerating, spinning and braking was measured in different situations and during a match. Finally, a posture test about the pressure acting on the chairs 'seat was performed. The present paper describes the protocols of acquisition, data analysis and the related results, collected by the Engineering group. The outcome is a general overview of each player's starting point, from a biomechanical point of view.

Nowadays, athletes are undergoing a program of training, based on force improving and compensation of missing abilities, a team training, and an educational program about diet and management of their physiological needs. For this reason, in the following months, the biomechanical measures described in this work will be execute again, to determine whether there have been a physical and performance improvement or not. This is also a motivation for athletes, who have to achieve a goal that can be measured quantitatively. Therefore, starting from the first set of biomechanical measures, with the acquisition of time tests and forces, and the use of rankings for each test, each athlete developed the awareness of his points of strength and the aspects to enhance, also in relationship with the other mates. This lead to a healthy competition, that could also serve as an additional motivation.

The work of the engineering group is still going on. With an Offcarr offensive wheelchair, equipped with strain gauges, the main loads acting on the frame in the case of impacts and during a match, are under measuring. Moreover, in the same conditions an accelerometer at high frequency acquires the longitudinal acceleration. This will be the starting point for a Finite Element Method analysis, with the aim of improving the structure of Rugby chairs produced by Offcarr factory, and to make them more customized for the athlete's specific needs.

CHAPTER 3

Wheelchair propulsion: references

Wheelchair propulsion technique, in daily use as in sport, is determined by three basic features:

I. the user (the motor) who produces energy and power for propulsion;
II. the wheelchair, which determines power requirements;
III. the wheelchair-user interaction, which determines the efficiency of power transfer from the motor to the wheelchair.

The wheelchair-user connection is a system producing an amount of work, to win some resistance forces: some studies demonstrated that the mechanical efficiency of this system in the propulsion movement, is low. The contribution of biomechanics and physiology to the understanding of these elements in improving the performance in wheelchair sports and daily use is fundamental [5]. In the present chapter, a literature research of biomechanical studies about wheelchair propulsion is reported.

3.1 The wheelchair user shoulder: anatomy and problems

The human arm is, contrary to the human leg, not specialized. Leg has very powerful muscles to support the body weight, allowing walking, running, jumping, without a higher range of movement. In contrast, arm has a large range of motion, and can perform many different tasks, from manipulation of small objects to handling of heavy materials. From an anatomical point of view, the functional difference between arms and legs is well visible in the difference of structure between the shoulder joint (*figure 6*) and the pelvis.

The two main bones of the shoulder are the humerus and the scapula, which extends up and around the shoulder joint to form the acromion and the coracoid process. The end of the scapula, called the glenoid, meets the head of the humerus to form a glenohumeral cavity that acts as a flexible ball-and-socket joint. Ligaments connect bones of the shoulder, and tendons join the bones to the surrounding muscles. The biceps tendon attaches the biceps muscle to the shoulder and helps to stabilize the joint.

Shoulder can perform movements of adduction, abduction, flexion, extension, internal rotation, external rotation, and 360° circumduction in the sagittal plane. Furthermore, it allows for scapular protraction, retraction, elevation, and depression. These free of movement also makes the shoulder joint unstable.

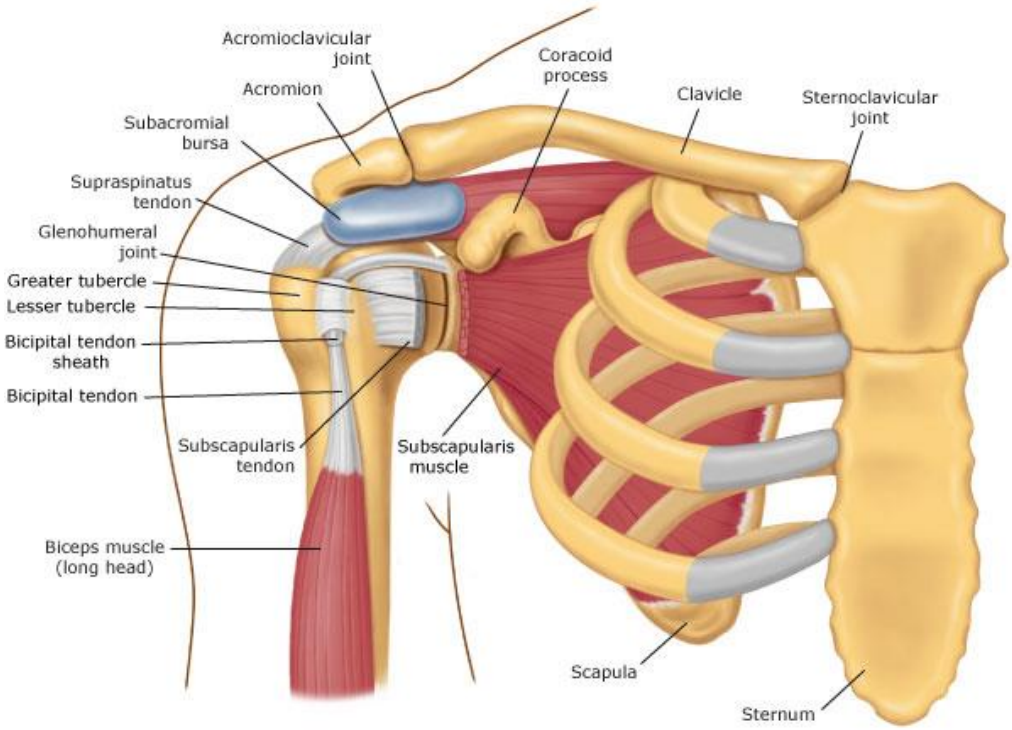

***Figure 6**. Shoulder joint.*

The loose connection of the scapula to the trunk is the main reason for the large range of motion of the arm. Since the scapula is able to slide and rotate over the surface of the rib cage, it is possible to move the base of the arm, the gleno-humeral joint (GH). This leads to a high increase in the range of motion of the arm: making a comparison with the leg, in the hips this is not allowed, since the pelvis does not have a range of movement as it is for the scapula.

A second reason for the large range of motion of the arm is the fact that the GH joint is shaped as a small and shallow cup (the glenoid) and a large saucer (the humeral head). The cup and saucer are connected by strong, but loose ligamentous tissue. The joint structure allows for rotation in three directions, as well as some translation. Despite the fact that the GH joint is loose, spontaneous subluxation can occur: it is assumed that this is the result of muscular control by the rotator cuff muscles. For this reason, a good coordination between these muscles is fundamental.

People seated on a wheelchair use their arms as legs. Therefore, considering the features of arms, high and cyclic loads are not anatomically favourable. Moreover, people competing in wheelchair sports use their arm even more during training: heavier loads, more cycles, higher velocity of movements. Therefore, athletes with an incomplete shoulder muscle system, and for whom muscular control is limited, will be at risk regarding shoulder luxations and other injuries[6]. Shoulder and wrist complaints are very common within the wheelchair users: Campbell and Koris diagnosed 24 patients with a cervical spinal cord injury with acute

and chronic shoulder pain. Some publications state that at least 50% of the wheelchair users suffer of wrist complaints. About 30-50% of this group has problems with their shoulders [7]. In the present study, on 19 Wheelchair Rugby players, shoulder echographies revealed an inflammation of the long head of biceps tendon in 17 of them, and a subacromial bursitis in 18 of them.

The high prevalence of complaints of wheelchair-user is a clear indication that the mechanical load in propulsion is unfavourably high. An explanation of this can be found in the fact that additional muscular effort is needed for the stabilization of the shoulder mechanism in movements that are not usual for the joint, especially for prevention of shoulder luxations. These extra muscular forces would then lead to overload of one or more of shoulder muscles, but also to high compression forces in the GH joint, which in turns might lead to damage the joint cartilage. To a deeper understanding of how a wheelchair user the shoulder works, wheelchair propulsion must be studied in its different aspects [5].

3.2 Basis of wheelchair propulsion

Some studies investigated the propulsion kinematic technique of a wheelchair, in ordinary activities and for different kind of sports. Wheelchair propulsion is studied as a cyclic movement: a given propelling motion is repeated over the time at a given frequency (*f*), to generate a certain linear velocity (*v*). With a first approximation, a cycle of propulsion can be divided into two phases, as shown on *figure 7*:

- push phase: hand in contact with the rim, effective force production;
- recovery phase: non propulsive phase, hand is not in contact with the rim since the arm is preparing to restart the next push.

In each push of the wheel, the user produces an amount of work (*W)*. The product of push frequency (*f*) and work (*W)* gives the average external power output (P_{out}), according to:

$$P_{out} = f \cdot W$$

The work produced in each push constitutes the integral of the momentary torque (*M*) applied by the hands to the handrim over a more or less fixed angular displacement (*Q*). The above equation can be rewritten into:

$$P_{out} = f \cdot \sum M \cdot dQ$$

where torque is the product of the bi-manual tangential force, which is applied on the handrim, and the radius of the hand rim.

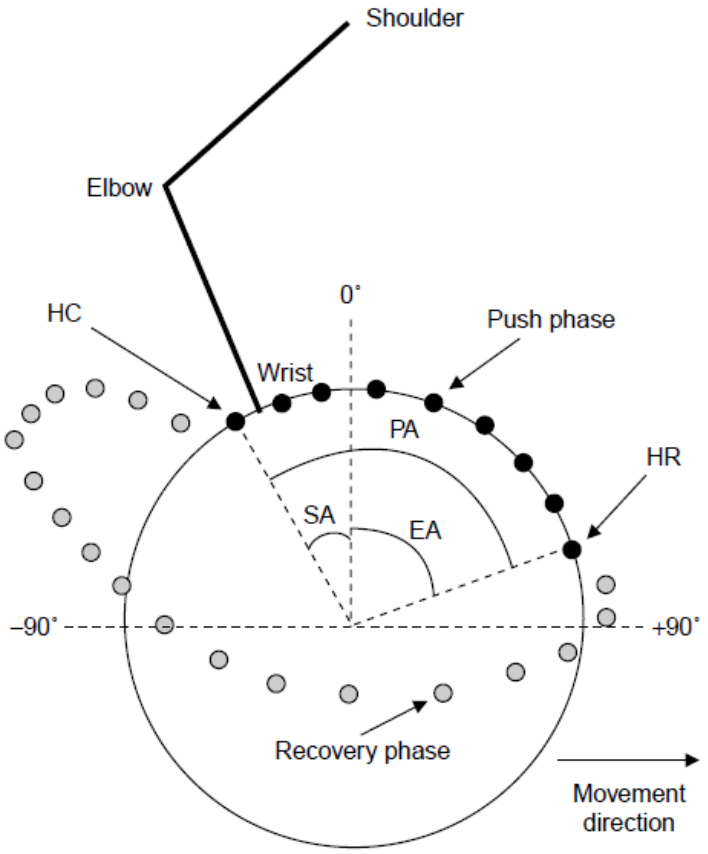

***Figure 7**. Representation of a wheelchair propulsion technique: HC=hand contact; HR=hand release; PA=propulsion angle; SA=start angle; EA=end angle. [8]*

Physiological measures (i.e. energy cost, physical strain) can be linked with biomechanical measures (i.e. power output, work, force and torque production) to obtain a general view of the force acting on the system. Considering wheelchair sports, the wheelchair-user combination is approached as a free body that moves at a given speed (v) and encounters the following resistance forces (F_{drag}): rolling friction (F_{roll}), air resistance (F_{air}), internal friction (F_{int}) and the metabolic consumption of the user (F_{met}). Power production during wheelchair propulsion is achieved by upper body work, primarily the arms. The forces (F_{prop}) acting to propel the system and winning the resistance are: inertial force of the system in movement (F_{inert}), the action produced by arms (F_{arm}) and the push force produced by the movement of the trunk (F_{trunk}). In conclusion, the acting forces are:

$$F_{drag} = F_{roll} + F_{air} + F_{int} + F_{met}$$

$$F_{prop} = F_{inert} + F_{arm} + F_{trunk}$$

The output force is given by:

$$F_{out} = F_{prop} - F_{drag}$$

The power output that must be produced by the system to maintain the velocity v is:

$$P_{out} = F_{out} \cdot v$$

Starting from this statements, it is possible to perform tests in order to obtain a quantitative evaluation of the mechanical efficiency of the movement [5,8].

3.3 Mechanical efficiency

The relatively small muscle mass of the upper extremities and increased tendency for local fatigue lead to a much lower maximal work capacity in comparison to leg work. Peak oxygen uptake is usually 60-85% of that in leg work [9]. Measurement of power output in wheelchair exercise testing, in combination with physiological measurements of the cardio-respiratory strain, gives additional information on the physical capacity of the person, and is also required for the calculation of the efficiency of the wheelchair-user system.

The gross mechanical efficiency (ME) is defined as the ratio between externally produced energy (power output) and internally liberated energy (En) according to:

$$ME=(P_{out}/En)\cdot 100\ (\%)$$

Calculation of energy expenditure during submaximal exercise is based on the measurement of oxygen uptake (VO_2) and simultaneous respiratory exchange ratio (RER) [36]. In the case of handrim propulsion on a wheelchair ergometer, the work done by the upper limb muscles is easily calculated by the tangential force exerted by the subject on the wheels to generate these rotations, usually converted to equivalent work (in W or kcal/min) [10]. In handrim propulsion, ME appears up to 11–12% [11]; In arm crank ergometer, values of ME around 15% are commonly found.

Although there are not many studies about mechanical efficiency in wheelchair propulsion, it appears clear that the value is low: this may be explained by the small muscle mass in comparison with legs, the complex functional anatomy of the upper extremity and the composite movement of propulsion. As described before, the anatomy of arm and shoulder, not specialized in movements involving repetitions, peaks of force and extreme joint deflections, requires some extra work to stabilize the glenohumeral joint. Another important feature is the way in which forces are applied to the hand rims, and the analysis of the acceleration of the system: this can give an explanation of the low mechanical efficiency, and address an effective pushing technique [5].

3.4 Moments and forces at the handrim

In wheelchair pushing, any force that has a tangential component respect to the wheels, contributes to the propulsion. Forces in other directions do not directly give a contribute to

the forward movement. The studies reporting only tangential forces or moments about the hub, do not take into account the components of the handrim forces. For this reason, a three dimensional analysis of the force generation pattern at the handrim, is a prerequisite to relate force application strategies to risk for injuries, and to understand how the propulsion technique can be improved in order to obtain a better sportive performance [8].

3.4.1 Moments and forces measuring

The recording of force acting on the handrim during wheelchair propulsion needs the use of an instrumented wheel; a novel instrument that allows this measures is the Smartwheel®: a modified wheel, instrumented with a 3-beam system that allows the determination of three dimensional forces and moments [12]. As the Smartwheel® can be mounted on the individual's own wheelchair, wheelchair-user interface and external conditions can be simulated. The output of the Smartwheel® consists of forces and moments in three dimensions, determined by a world coordinate frame. The force components *Fx* ,*Fy* and *Fz* are defined as directed horizontally forwards, horizontally outwards and vertically downwards, respectively, in a right-hand coordinate system (*figure 8*); they are combined to give the resultant force F_{tot} .

To relate the forces to the wheel, the coordinate frame can be rotated such that the force components *Fx* and *Fz* represent, respectively, the tangential (*Ft*) and radial (*Fr*) force components of the hand rim.

The tangential force component *Ft* is the only force component that contributes to the forward motion of the wheel. The radial force component *Fr*, and the axial force component *Fy*, create the friction necessary to allow *Ft* to be applied. The resultant force F_{tot}, which is the total force applied to the hand rim, is mathematically calculated by taking the vector sum of the 3 force components *Fx, Fy* and *Fz* [8].

Veeger et al. [13] also introduced a parameter called Fraction of the Effective Force (FEF), as a measure for the effectiveness of force application. FEF is the ratio of the effective propulsion moment measured at the wheel hub (M_{hub}) to the resultant force:

$$FEF = (M_{hub}/r) /F_{tot} \cdot 100\ (\%)$$

where *r* is the radius of the rear wheel.

Some studies analysed the wheelchair propulsion to find a reason why users statistically choose a mechanically disadvantageous movement. An explanation can be found in biomechanics [8].

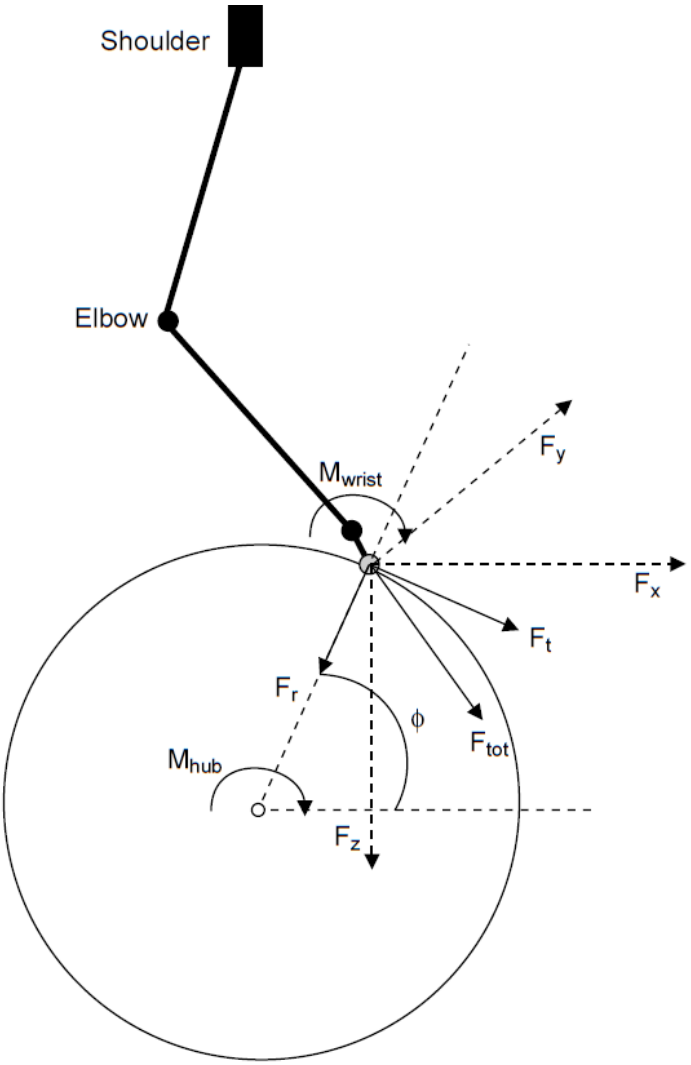

Figure 8. *Coordinate frames on the instrumented wheel [8].*

3.4.2 Effective vs actual force at the handrim

Since, during the push phase, the hands hold the rims, the movement of hands and arms is considered as a guided circular movement. In guided movements, forces applied by the hands do not directly influence the trajectory of the hands. As a consequence, it is possible to apply a force that is not tangential to the hand rims.

Experimental results in which propulsion forces were measured with instrumented wheels, showed that propulsion forces are indeed not tangentially directed. The direction of the forces applied on the handrim does not agree with the most optimal direction in terms of mechanical power production, i.e. the direction tangential to the handrims. Surprisingly, this apparently, in mechanical terms, suboptimal direction of actual force application was found for athletes as well as untrained subjects [13,14,15,16]. It appears that this particular manner of force application is the most efficient force application technique. In other words, subjects appear to adopt the technique that demands them the

least energy, given the mechanical constraints of the wheelchair-user combination [17]. The reason why the users choose this force pattern can be found in the muscle contraction during propulsion.

Veeger and van der Woude [18] studied this concept, represented in *figure 9*.

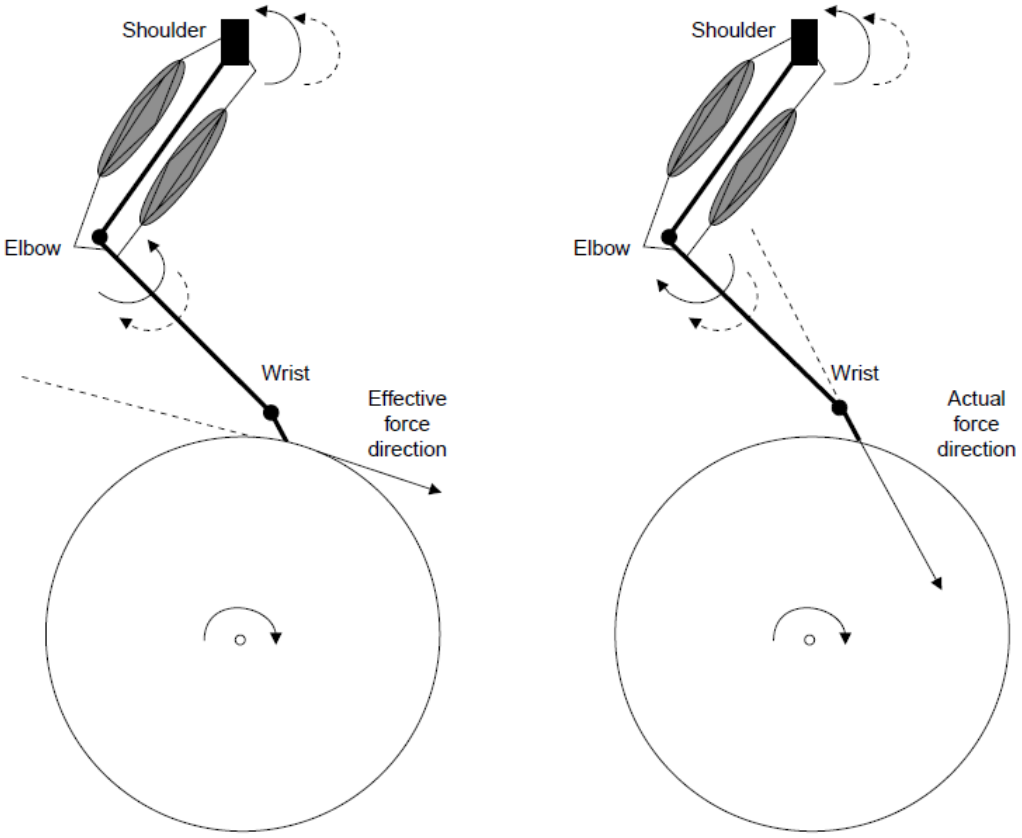

a) *b)*

Figure 9. *Difference between effective a) and actual b) force: relationship between force direction and calculated net joint torques around shoulder and elbow. Solid lines: moment around the joint; dashed lines: rotation direction of movement [8].*

Figure 9a shows that the application of the tangential force (effective force) might lead to a contradictory situation in which the elbow joint is extending while at the same time a flexor moment ought to be generated for a mechanically optimal results. In this case, the elbow has to be extended (dashed lines) to follow the hand rims in order to be able to apply force on those rims. As a consequence, to direct the force only tangentially, the elbow flexors have to apply force against stretch, which is highly inefficient. In this case, the contribution of elbow flexors would increase the effectiveness of the propulsion force, but the total force would be smaller. A second aspect of this force direction is that the strong elbow extensors cannot be used. The condition in *figure 9b* depicts the force direction in which no conflict between torque direction and movement direction occurs. This is the situation that is generally found in the studies. The reason of this mechanical inefficient form of propulsion,

is based on fact that this is the most efficient solution for muscle biomechanics: the production of negative power is prevented and the strong elbow extensors can be used [8].

3.4.3 Moments at the handrim in static propulsion: a study

Some studies measured, with an instrumented wheel, the moments at the rim in wheelchair propulsion. A work by Lan-Yuen Go et al. [19] examined 5 male healthy subjects (non wheelchair-users) during a maximal isometric wheelchair propulsion. The study wanted to demonstrate that, given a subject specific profile of the strengths of each of the upper extremity joints as a function of joint angle, there is an optimal direction of force application in the handrim to maximize the propulsion moment about the wheel axle at each instant of the propulsion cycle. In the experimental setting, the instrumented wheel had a handrim radius of 25.4 cm, and was locked to prevent the forward movement as the subjects pushed with maximum isometric effort. Five hand positions, corresponding to wheel angles θ of 120, 105, 90, 75 ,60° (*figure 10*) were assigned in a random order.

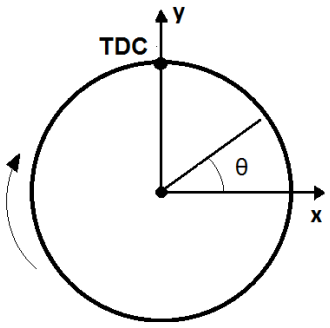

Figure 10. *Definition of angle θ and Top Dead Centre (TDC)*

The subjects performed four trials of maximal wheelchair propulsion effort for each hand position. Applied hand forces in the laboratory reference frame and progression moments about the wheel axle were averaged for the four repetitions to represent each subject's performance at each hand position. The force direction and magnitude of force applied to the handrim were determined.

To estimate the joint strength in an isolated loading condition, the isometric shoulder flexion and extension muscle strength were measured at different angles, using a dynamometer. Muscle strength at each position were determined as the peak force generated during a 3s contraction; three trials of muscle strength were collected.

The optimal force direction was determined at each instant with a linear optimization problem which aims to maximize the moment about the wheel axis, M_0, considering the constraints of the subject's shoulder and elbow joint moment-generation capabilities for the specified joint angles. The results are represented in the following figures (*11,12,13*).

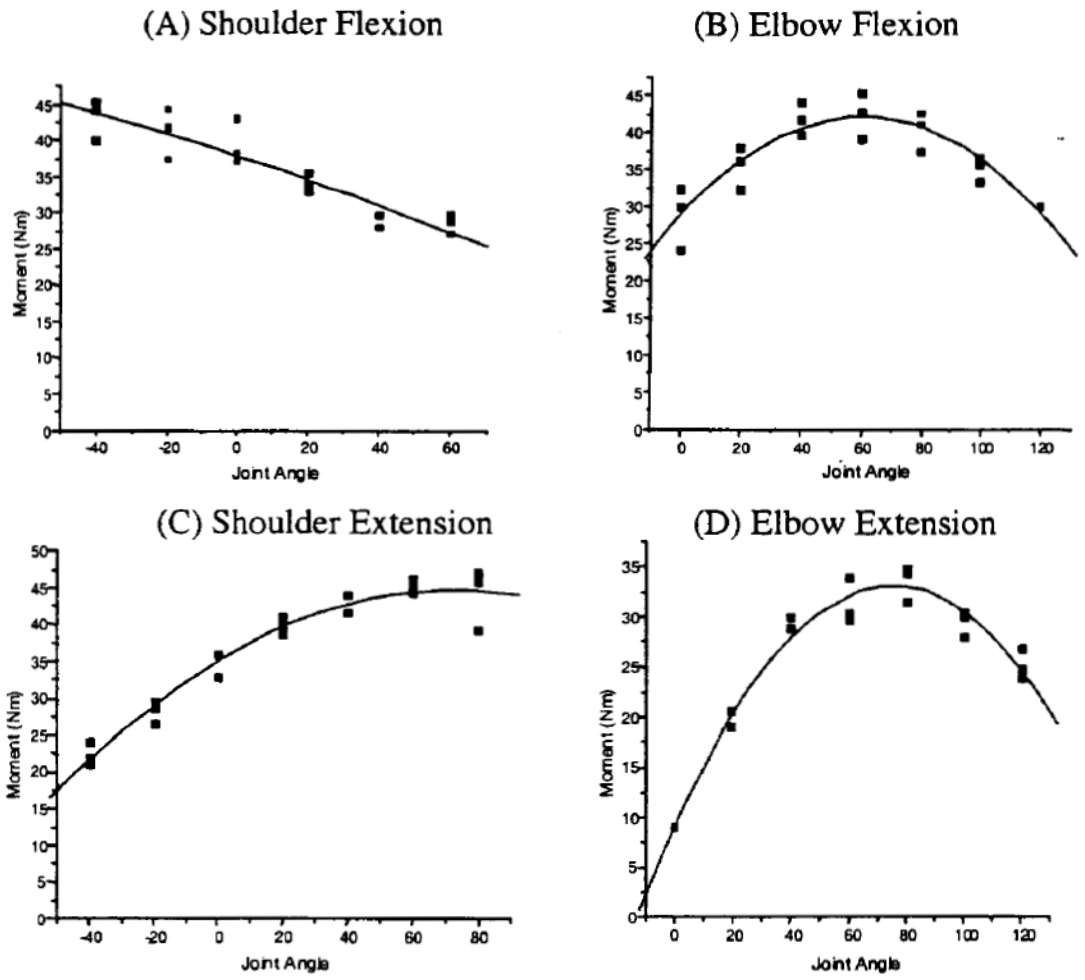

***Figure 11**. Moment of elbow and shoulder flexion/extension during isometric contractions [19].*

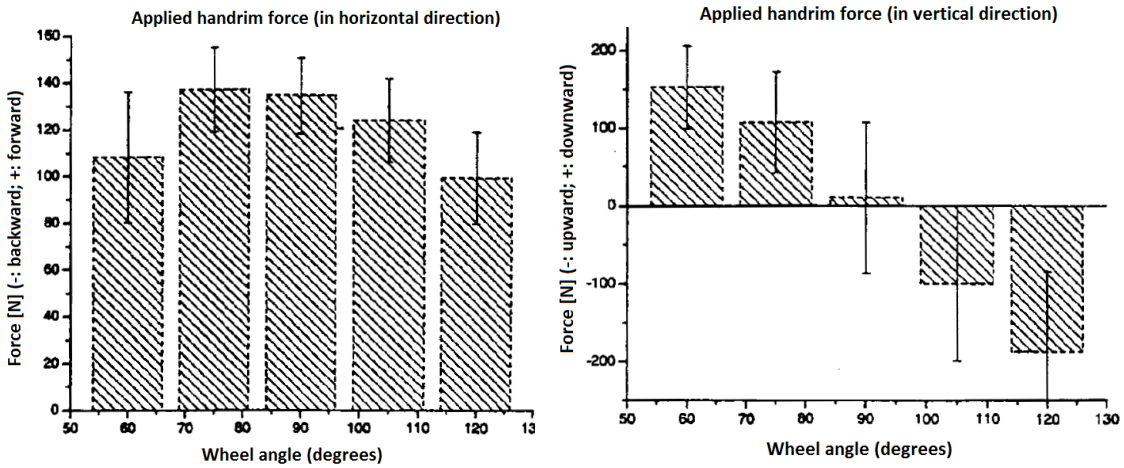

***Figure 12.** Mean and standard deviation of handrim force in the horizontal (left) and vertical (right) directions [19].*

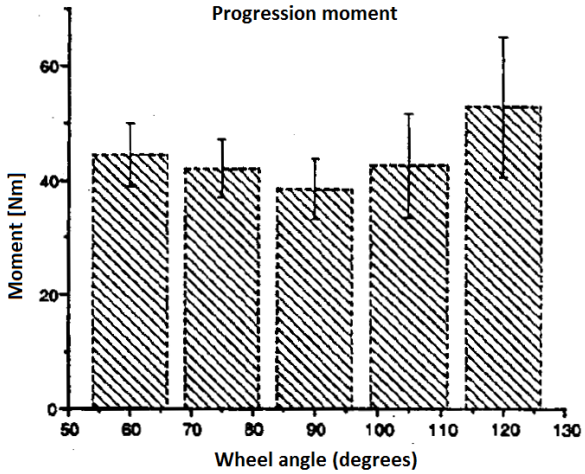

***Figure 13**. Mean and standart deviation of progression moment ath the hand rim, at five hand positions [19].*

The results revealed that the progression moment was greater at both initial and terminal propulsion positions (wheel angles of 120° and 60° respectively) and smaller in the mid propulsion position (wheel angle of 90°). The applied handrim force in the horizontal direction, however, was smaller in the initial and terminal propulsion positions and larger during mid-propulsion while the applied handrim force in the vertical direction showed a bimodal pattern, negative prior to top dead centre (TDC) position. These vertical and horizontal force directions correspond to a force which is radially away from the wheel axle posterior to the TDC and radially toward the wheel axle anterior to TDC.

3.4.4 Moments in dynamic and static propulsion

The results described in the previous paragraph are an example of the data collected in different studies of static propulsion. Nevertheless, they are in contrats with those documented for dynamic tests: for example, the wheelchair user does not have to initiate acceleration of the wheel at all hand positions as in the static equivalent.

During dynamic wheelchair propulsion, the progression moment reaches its maximum value in mid-propulsion while in experimental models and static studies, the peak in the progression moment is recorded at the beginning and terminal phases of the propulsion cycle. The static analysis reveals that the hand position at TDC may not be optimal to for the upper extremities to generate large forces in the handrim: since the applied handrim force is sperimentally nearly perpendicular to the line from the hand to the shoulder, a large shoulder moment will result. For example, in wheelchair racing, users always flex their trunk anteriorly to propel the handrim with their hand anterior to TDC: this hand position allows larger progression moments to be generated because their lever arms enable the upper extremities to tolerate greater external loading.

Moreover, the force direction posterior to TDC found in static propulsion, differs greatly from the results of dynamic wheelchair propulsion. The direction of handrim force during dynamic wheelchair propulsion is toward the wheel axle during the whole propulsion phase, including the period when the hand position is behind the TDC (*figure 14*).

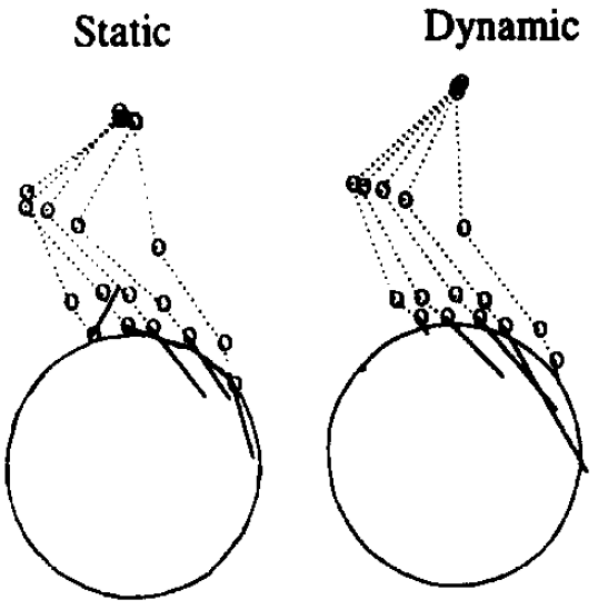

***Figure 14**. Stick diagrams showing the position of the upper extremity during static and dynamic wheelchair propulsion. The force vector at the rim is shown [23].*

To generate a push force directed away from the wheel axle, the elbow flexor must be activated, and this would indeed be beneficial for propulsion as the elbow must flex during this phase of the cycle (behind TDC). However, halfway through the propulsion phase, the applied force must change to progress the wheel and so the elbow extensor needs to be immediately activated at that point in the cycle. During static propulsion, switching from elbow flexion to extension is not difficult, however, the change in muscle activation from elbow flexor to elbow extensor dynamically may result in a more complex and inefficient movement.

It could then be hypothesized that users could be trained through biofeedback to activate their muscles more like that seeing during static analysis, to increase mechanical efficency [19]. Nevertheless, care should be taken when using increasing FEF as a rehabilitation goal, as higher FEF values shift handrim force contributions from muscles crossing the elbow to those crossing the shoulder, which are already susceptible to overuse injuries [20].

Considerable differences in force application during steady-state wheelchair propulsion [21] and sprinting [22] have been demonstrated between people with quadriplegia and those with paraplegia. The FEF in quadriplegics is the consequence of a significantly larger

inwards directed lateromedial force component (*Fy*). Friction at the hand rim is necessary to produce the tangential component and can be generated through hand grasping, wrist moment generation and/or directing the resultant force away from the tangential direction. In quadriplegics without hand function, only the latter option is available. If triceps function is limited, the generation of friction in a downward or outward direction is hampered. Therefore, the inwards-directed lateromedial force component can serve as an effective alternative for friction generation [8].

3.5 Inertial contributes in dynamic propulsion

The results found for static wheelchair propulsion differ from those recorded during dynamic propulsion. For this reason, the research cannot limit to the study on moments and forces at the handrim: the study of dynamic propulsion is necessary. Therefore, the wheelchair-user system is moving: in this contest inertial events, not occurring in static propulsion, highly contributes to the output performance.

3.5.1 Forward acceleration

Wheelchair propulsion under realistic conditions does not merely consist of an active period (the push phase) and a passive period (the recovery phase), as commonly described. It is composed by 3 phases, each with specific energy demands:

I. an acceleration phase caused by forces applied to the hand rims;
II. a second acceleration phase caused by the inertial forces acting on the wheelchair-user system, caused by a backward arm and/or trunk-swing;
III. a deceleration phase during the second part of the recovery phase.

The deceleration is amplified because of inertial forces acting on the wheelchair-user system, caused by an increased forward segmental velocity of the upper limbs to prepare for the hand contact with the hand rims [8].

This fact finds a relevance in the study of forward acceleration of the wheelchair-user system, collected with inertial sensors, in specific points of the wheelchair frame. The typical forward acceleration trend is composed by high peaks of positive acceleration and high peaks of negative acceleration: this is in line with the low mechanical efficiency found for wheelchair propulsion. The acceleration trend gives other explanations about the inefficiency of this system. This can be seen in the difference between experiments on the ergometer and on real dynamic conditions. The acceleration on court is not directly comparable to the acceleration on the ergometer, as on the court the mass of the wheelchair-athlete system is accelerated, whereas on the ergometer only the moment of

inertia of the rotary parts has to be accelerated. Additionally, the breaking torque works against acceleration and thus adds further resistance [24].

In stationary systems, inertial forces acting on the wheelchair, caused by accelerations and decelerations of trunk and arms, are neglected. Vanlandewijck et al.[25] and Spaepen et al. [26] showed that positive mechanical work during the recovery phase at velocities higher than 1.67 m/sec can amount to one-third of the total mechanical work during the propulsion cycle, because of inertial forces acting between the user and the wheelchair.

3.5.2 Trunk Kinematics

The force is not only applied by arms: alterations in trunk inclination, if functionally available, are most likely used as a force generation strategy. There are no biomechanical studies specifically addressing the role of the trunk in hand rim wheelchair propulsion. Nevertheless, trunk motion might be one of the most important force generating mechanisms during fatigue, or high resistance wheeling, such as accelerating from standstill, sprinting or uphill driving. Furthermore, trunk motion will directly affect rolling resistance and air drag. In wheelchair sports classification procedures, trunk range of motion has been determined as one of the key parameters in identifying the functional potential of wheelchair sportsmen [8].

Some studies measured trunk excursions during manual wheelchair propulsion and generally found a forward shift of the trunk as the amount of activity increases [27,28]. Vanlandewijck et al. [25] observed in 40 wheelchair athletes that the change from trunk flexion to extension shifted significantly towards the end of the push phase when velocity was increased from 1.11 to 2.22 m/s (from 68.39 to 93.15% of the PT) [29]. This might be explained with the need of pushing with the hands more anteriorly on the handrim to exploit a bigger lever arm, and with a higher push given by the trunk flexion.

3.5.3 The importance of the recovery time

A number of studies have shown that a mere speed increase leads to a marked decrease in propulsion cycle time (CT), mainly because of a decrease in propulsion time (PT) instead of a decrease in recovery time (RT). The reason why RT, often qualified as a passive period, remains almost constant as velocity increases, has been discussed by Vanlandewijck et al. They investigated the propulsion technique in wheelchair basketball players, in different velocities, at a constant power on a treadmill. The authors demonstrated that, in high velocities, experienced wheelchair users adapt their propulsion technique not by changing their style, but by increasing the amplitude of their movements. In fact, when propulsion

velocity increases, an increased backward arm swing is needed to generate a greater acceleration of the hand before contact with the rim. Both the accelerated backward arm swing and the preparation for hand contact result in an increased muscular activity. This implies a higher muscle contraction velocity and is associated with an increased energy expenditure and, consequently, a lower mechanical efficiency [8]. Decreased mechanical efficiency can be explained by a significant change in the acceleration of the wheelchair-user system during recovery time, caused by arm and trunk movements, inducing inertial forces to act on the wheelchair. Consequently, mechanical work increased significantly during the recovery phase. These findings indicate that studies on mechanical efficiency in wheelchair propulsion should not only be focused on power supply during the push phase, but also on the movement pattern during recovery [25].

CHAPTER 4

Project activity 1: isometric tests

In Wheelchair Rugby, as for all Paralympic sports played in a chair, arms are for athletes their mean to express at best their abilities: the force they can exert with their arms influences the pushing technique, the way of launching the ball, the velocity and acceleration and all the performances within the game. Depending on the impairment, some players miss the control of some muscles. Therefore, it is important to investigate the maximum force they can express in particular movements, to study which muscles are more powerful, which should be trained more, and the presence of eventual asymmetries between left and right side. In this work, an isometric study of muscular force was performed as a starting point to determine a personal program of training for each athlete, with the aim of exploiting at best their residual capacities during the game, and with advantages also in the daily routine. The isometric tests aim at evaluate the muscular ability of players in different kind of exercises: total, left and right push forward using the wheelchair, left and right shoulder flexion and extension, left and right elbow flexion and extension. A MuscleLab load cell was used to collect the force data.

Research question: what is the maximum isometric force developed in unilateral and bilateral pushing forward? What is the maximum isometric force in shoulder flexion/extension and elbow flexion/extension?

4.1 Instrumentation

An efficient instrument to measure the force produced during an isometric contraction is a load cell. In this work a strain gauge MuscleLab S-load cell, 100 kg full scale, provided by its acquisition software, was used (*figure 15).* The principle of function is a force measurement by a system of strain gauges in the configuration of a Wheatstone bridge. The gauges are bond onto a beam that deforms when load is applied: at the application of a force, the strain gauges feel the strain as a variation of the electrical resistance. The variation is very low (few millivolts) so the system is provided with an amplifier. The output is then converted from mV/V to N, to give a measure of the force applied to the transducer.

***Figure 15**. MuscleLab S-load cell.*

The load cell measures the force generated by the application of a tension load in the direction of the longitudinal axis of the "S", so during the exercise performing, the load must be applied in that direction. The load cell is connected to an encoder, which is in turns connected via USB to the PC with the MuscleLab software, allowing data acquisition and elaboration. The data are then exported to Excel for their elaboration.

The system used to perform the isometric tests consists of:

- a wooden platform with an aluminium column fixed on it. The load cell was fixed to the column, and its position was adjustable depending on the type of exercise and the athlete's anthropometry;
- a set of belts, elastic wristbands with Velcro fixations and carabiners;
- deadweights ensuring the system to stay still during isometric exercises;
- MuscleLab load cell;
- MuscleLab acquisition set.

4.2 Methods

This paragraph contains the description of isometric tests, the protocol for force acquisition and the data analysis.

4.2.1 Tests description

Each participant executed a set of exercises involving an isometric maximal contraction: unilateral and bilateral pushing forward, shoulder flexion and extension.

4.2.1.1 Push forward

This exercise evaluates the maximum isometric force an athlete can express in the action of pushing his wheelchair forward. This is a complex movement, involving different groups of muscles and characterizing the pushing technique of the athlete and his performance on court. For example, during the game, blocking an opponent with an isometric action is allowed.

In preparing the subject for the test, the back rest of his wheelchair (posterior handle) was connected to the system through a belt, fixed to the load cell with a carabiner. The height of the load cell in the column was adjusted to assure the belt, and consequently the applied load, in being parallel to the ground, in the direction expected by the load cell. A plastic mat behind the main wheels creates a friction that avoids them moving during the test. This set was used to perform three different exercises *(figure 16):*

- total push forward: the athlete on the wheelchair pushes forward at his maximum strength, with both arms;
- right push forward: the athlete pushes at his maximum strength with the right arm;
- left push forward: the athlete pushes at his maximum strength with the left arm.

The subject was asked to execute the exercise choosing for the position of their hands and arms, the one in which he feels to push with the higher force. In this way, it was possible to obtain an evaluation of the maximum force in that specific movement. Moreover, depending on the impairment and the capacity of muscular control, the positions assumed by the subjects varied.

Figure 16*. Pushing forward with both arms.*

4.2.1.2 Shoulder flexion-extension

During wheelchair propulsion the largest net joint moments and powers are generated around the shoulder: the action of pushing a wheelchair involves, at this joint, the work of

several movements and muscles but the main actions can be considered flexion and extension. For this reason in this work, maximum isometric force of shoulder flexion/extension were investigated.

According to the test procedure, the athlete wore a wristband, with a carabiner that allowed it to be connected to the bend; the last was still connected with the load cell, which was set at the proper height to ensure the bend and the applied load in being parallel to the ground. Before starting the test, the wheels of the wheelchair were eventually removed, to avoid any kind of obstacle to correctly perform the exercise. For those athletes (mostly low points) who do not have the total control of their triceps, the wristband was put in the arm, just above the elbow. The load cell needed to be positioned in the same side for the left-shoulder-flexion/right-shoulder-extension and for right-shoulder flexion/left-shoulder-extension. Therefore, to optimize the time of the exercise, the session was executed in the following order:

1. right shoulder flexion (*figure 17);*
2. left shoulder extension *(figure 17);*
3. left shoulder flexion *(figure 18);*
4. right shoulder extension *(figure 18).*

Subjects were asked to perform the movement, as much as possible, with a zero degree of shoulder flexion/extension, with the arm straight and perpendicular to the ground, and a zero degree of trunk flexion/extension.

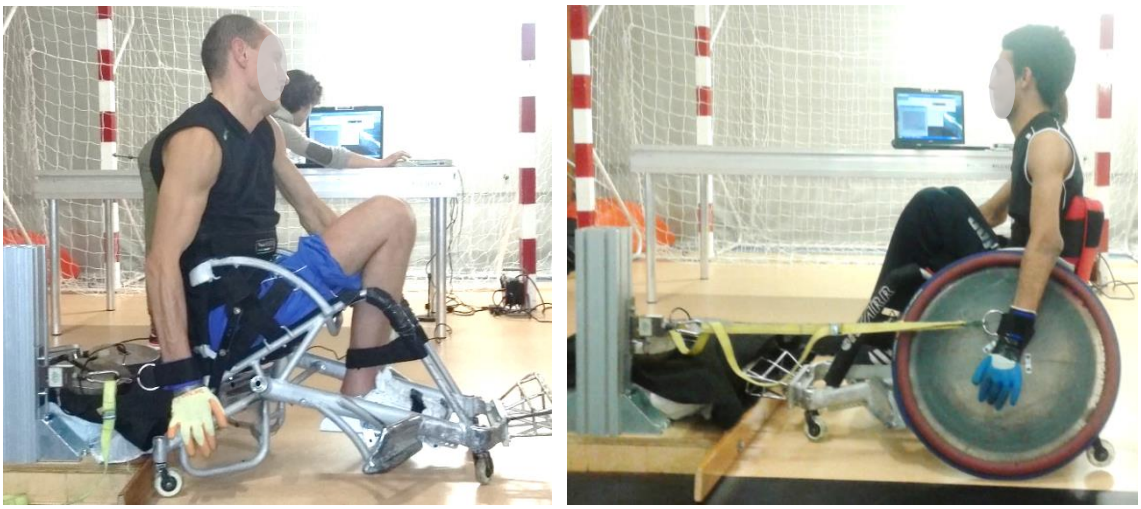

Figure 17. *Right shoulder flexion; left shoulder extension.*


***Figure 18**. Left shoulder flexion; right shoulder extension.*

4.2.1.3 Elbow flexion-extension

The elbow is a joint with two degrees of freedom: at this joint, the most relevant movement for wheelchair pushing is flexion/extension. To evaluate the maximal isometric force at the elbow, according to the adopted protocol, the load cell was screwed directly to the wooden platform, in vertical position. A beam was screwed to the load cell: the beam had a plastic sliding disc, with a hole on his edge to which a carabiner could be attached and connected to the wristband, to execute movements of elbow flexion/extension. This configuration allowed people with tetraplegia, who do not have the possibility to hold the handle, to perform the exercise. The load cell remained in this position for all the elbow exercises. In this case, there was the need to remove the wheels, to correctly execute the movements. The session was performed as:

1. right elbow flexion (*figure 19);*
2. right elbow extension;
3. left elbow flexion;
4. left elbow extension (*figure 19).*

In all the elbow exercises, subjects were asked to perform a maximal isometric contraction starting from a 90° of elbow flexion.

***Figure19**. Right elbow flexion; left elbow extension.*

4.2.2 Acquisition protocol

The protocol for the acquisition of the force signal was the same for each isometric test. After the load cell fixation in the proper position and before attaching the belt, the load cell signal was zeroed by a proper command in the MuscleLab software. The subject maintained the same posture during the exercise, performing the following actions:

- 5 seconds of maximal isometric contraction;
- 5 seconds of rest.

This session was repeated three times, consecutively, for each exercise.

4.5 Data analysis

The force trend of each exercise can be visualized in the MuscleLab software, which gives the possibility to perform a preliminary data analysis. Force signals of different exercises recorded by the load cell differs in force values, but since the acquisition protocol is the same, trends are homogeneous: the typical force trend is represented in *figure 20.* It is possible to notice the growing trend when the isometric contraction starts, kept for 5 s; the following 5 s of null force correspond to the rest period. This session was repeated three times. The period of contraction generally contains initial spikes and oscillations since the contraction cannot be maintained at the same level for the whole period. For this reason, for each part of the signal corresponding to a contraction, a period of 3 s was averaged, considering values in which trend remains constant, and avoiding initial peaks and strikes. After exporting this data as an Excel file, the three mean values of each isometric period

were averaged, obtaining for each player an estimation of the maximal isometric force of contraction, in the different cases.

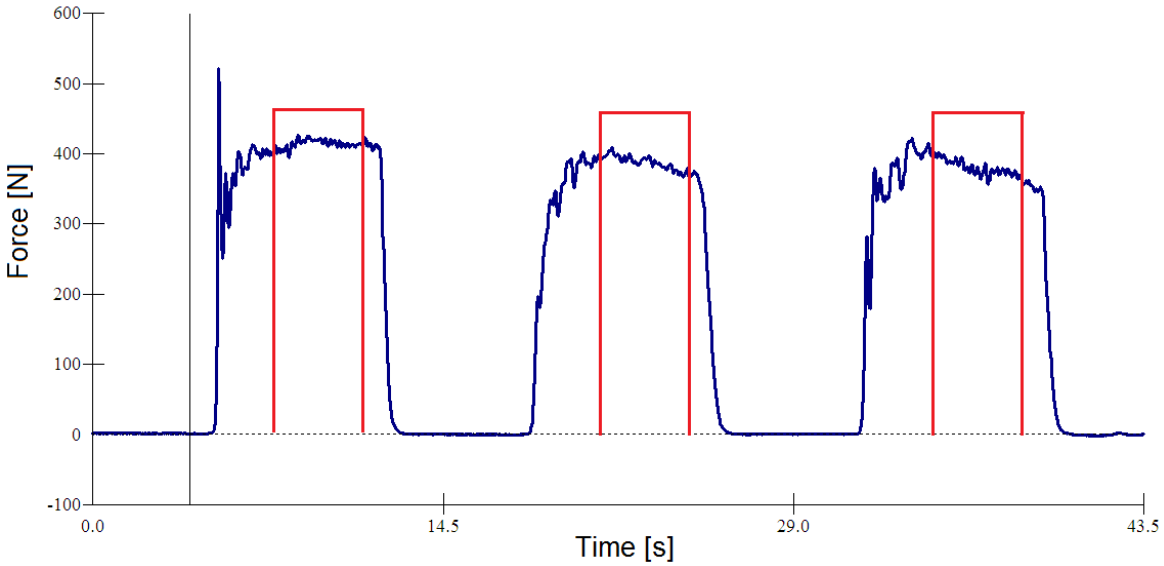

***Figure 20**. Isometric contraction trend (example of a total push force); blue: force trend; red: averaged periods.*

4.3 Results

After the data analysis, each subject was assigned one value for each isometric test, representing the maximum isometric force he could express in different and controlled situations. This served as a starting point to assess the force of each subject at the beginning of the program, the presence of asymmetries between the left and the right side, eventual phenomenon of compensation, or the loss of control of some muscles. This paragraph contains the isometric results collected for the participants, their position in the total ranking, and the comparison between different exercises. Each player was given a report containing his personal results and his position in the total ranking.

Table 2 represents the values of the isometric push force for each player, *figure 21* shows values in descending order, and *figure 22* puts in relation force values with the classification point.

	F PUSH FWD TOT	F PUSH FWD LEFT	F PUSH FWD RIGHT	
INITIALS	MEAN [N] ± SD	MEAN [N] ± SD	MEAN [N] ± SD	Fright= tot(%) Fleft
A.S.	268,95 ± 0,07	137,27 ± 4,75	199,20 ± 18,53	-45,12
B.A.	452,00 ± 8,02	239,07 ± 11,58	286,03 ± 16,88	-19,65
B.N.	324,30 ± 34,17	99,74 ± 2,01	130,80 ± 1,55	-31,15
B.M.	335,20 ± 14,25	155,23 ± 17,98	141,48 ± 39,96	8,86
C.A.	318,90 ± 25,76	156,97 ± 11,68	207,93 ± 29,21	-32,47
D.A.	198,10 ± 26,99	330,97 ± 8,97	283,47 ± 7,52	14,35
F.P.	250,00 ± 26,16	88,67 ± 1,79	104,67 ± 2,65	-18,05
F.A.	195,00 ± 11,37	150,07 ± 10,06	149,00 ± 13,31	0,71
F.S.	469,30 ± 19,68	347,03 ± 8,03	119,77 ± 5,46	65,49
G.D.	391,80 ± 20,79	284,80 ± 11,70	342,27 ± 18,11	-20,18
G.M.	271,10 ± 11,54	164,30 ± 4,17	222,27 ± 10,78	-35,28
K.H.	218,60 ± 17,26	165,90 ± 5,33	145,23 ± 8,59	12,46
M.P.	563,83 ± 35,32	514,93 ± 33,21	506,23 ± 18,74	1,69
Q.V.	384,03 ± 29,88	302,07 ± 17,45	166,30 ± 14,96	44,95
S.P.	148,30 ± 16,80	65,24 ± 2,52	71,23 ± 4,40	-9,18
T.G.	341,07 ± 35,20	159,17 ± 19,13	226,50 ± 41,11	-42,30
T.N.	417,83 ± 20,60	163,83 ± 20,26	228,33 ± 24,81	-39,37
V.L.	83,77 ± 16,50	235,53 ± 10,33	116,80 ± 1,90	50,41
Z.L.	457,47 ± 23,01	191,77 ± 14,64	171,27 ± 24,92	10,69

***Table 2**. Push forward force values [N]: mean and standard deviation. Difference between left and right side (%.)*

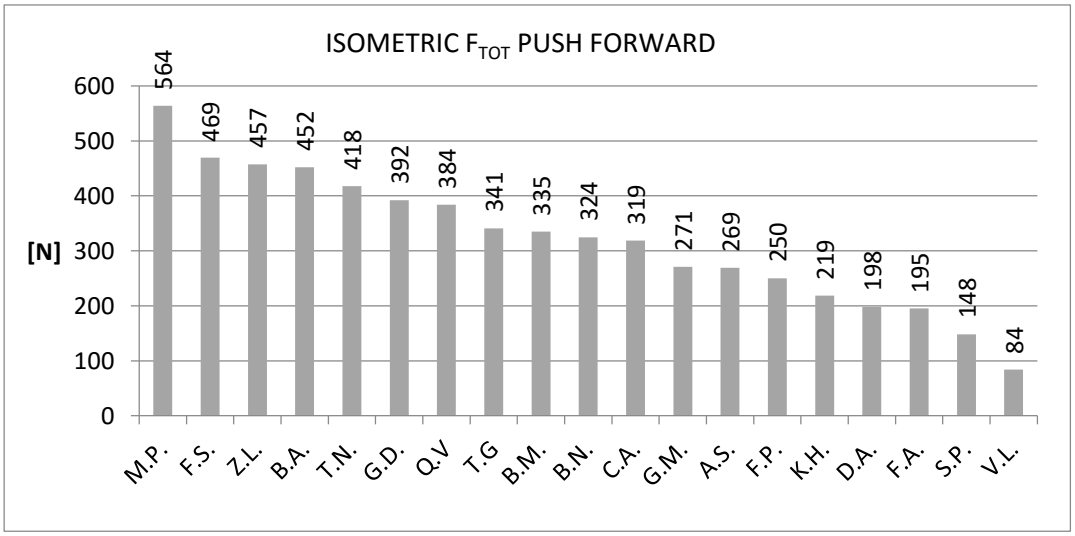

***Figure 21.** Isometric push forward total force (both arms).*

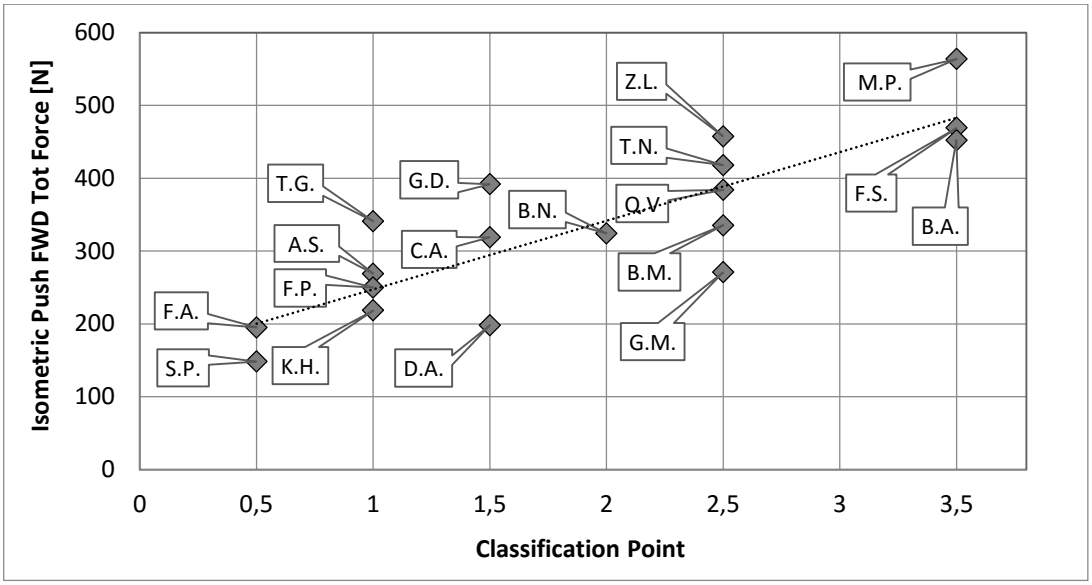

***Figure 22**. Isometric push forward total force in relation to the classification point.*

The ranking of the maximum isometric force in the test of total pushing forward (*figures 21, 22*) generally agrees with the point of classification: points from 3.5 to 2.5 (with one exception of V.L. due to a wrong measure) are in the first half of the ranking; points from 1.5 to 0.5 are in the second half. Therefore, people with more severe impairments develop less force, because of the weakness of some muscles. In average, 3.5 points develop the greater force; some of 2.5 points (Z.L., T.N.) exert the same force as 3.5 points (F.S., B.A.). Some 1 and 1.5 points develop force values that are comparable to 2.5 points: this might mean that 2.5, with some training, could increase their maximal force.

The following graphs (*figures 23, 24*) represent the ranking for the unilateral tests of pushing forward.

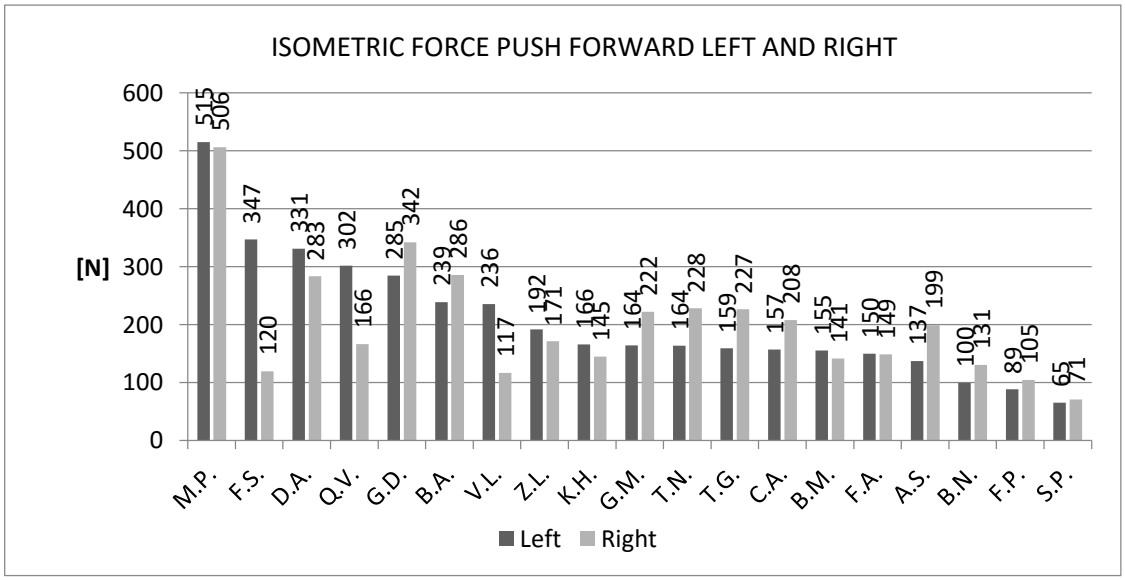

***Figure 23**. Isometric push forward force with left and right arm (force values are sorted by the left side).*

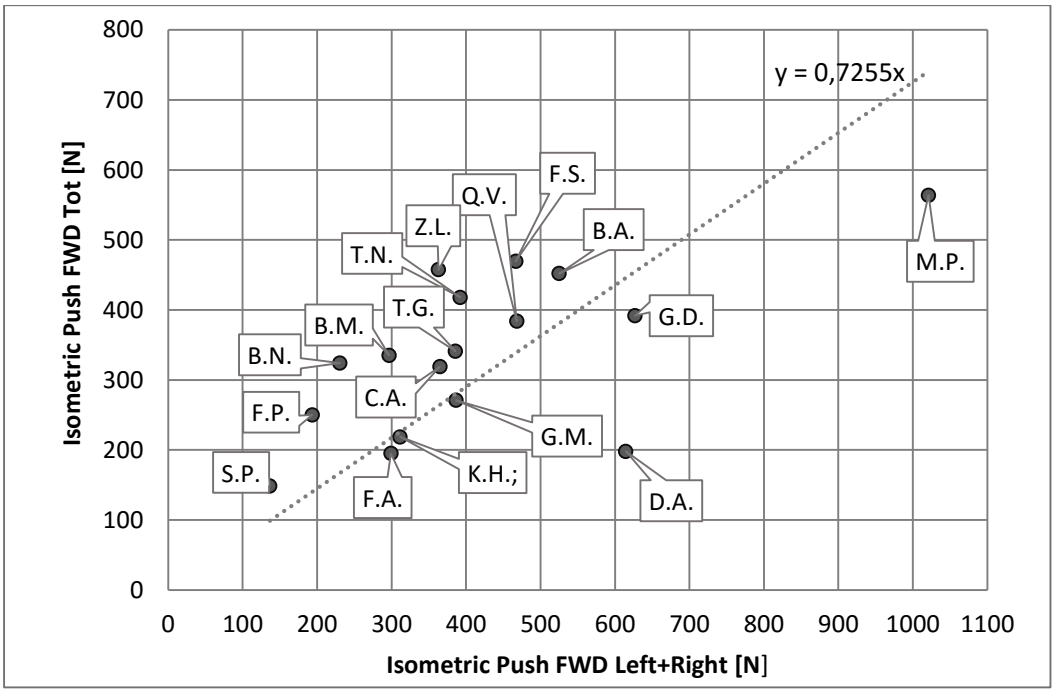

Figure 24. *Sum of isometric left and right push forward force in relation to total push forward force.*

Unilateral pushing forward tests give information about the difference between the left and right side (*table 2*): values with the negative sign indicate that right force is higher than the left force. For subjects where the difference among left and right side is high (apart from the sign, more than 50%) it must be determined whether there is a diagnosed problem or not, and eventually prepare a program of training for the weaker side.

Differently from bilateral tests, the unilateral push forward values do not follow the ranking of classification (*figure 23*): this could be expected, because in pushing forward with both arms, some mechanism of compensation can occur: on the contrary, the unilateral exercises underline the personal impairments and can be read only in accord to the single person's disease.

Figure 24 represents the sum of left and right push forward values in relation to total push forward values: the regression line reveals that the sum of left and right isometric push force is in average 27% higher than the total push force (in this case, the wrong value of V.L. was not considered to avoid altering the regression line).

The following *tables* (*3,4)* contain force values, with their standard deviation, for shoulder and elbow flexion/extension.

	SHOULDER FLEX LEFT			SHOULDER EXT LEFT			SHOULDER FLEX RIGHT			SHOULDER EXT RIGHT		
INITIALS	MEAN [N]	±	SD	MEAN [N]	±	SD	MEAN [N]	±	SD	MEAN [N]	±	SD
A.S.	-	±	-	155,60	±	5,11	209,17	±	5,69	179,57	±	7,51
B.A.	317,77	±	20,71	265,67	±	9,76	237,80	±	11,10	251,57	±	6,30
B.N.	133,60	±	1,56	34,26	±	3,90	137,47	±	11,34	49,69	±	8,30
B.M.	76,33	±	9,31	87,04	±	1,18	62,68	±	5,09	75,87	±	2,66
C.A.	302,20	±	4,33	151,63	±	3,71	302,60	±	4,42	67,97	±	11,26
D.A.	152,13	±	12,36	99,85	±	10,19	209,57	±	17,74	120,83	±	0,76
F.P.	175,87	±	5,64	79,00	±	3,27	185,17	±	11,10	62,66	±	2,05
F.A.	146,87	±	1,99	135,83	±	6,80	112,33	±	5,95	96,86	±	9,84
F.S.	208,53	±	6,00	150,87	±	9,38	138,00	±	3,27	66,65	±	9,43
G.D.	132,00	±	12,42	100,55	±	3,98	120,40	±	3,44	112,17	±	5,26
G.M.	75,23	±	16,22	88,58	±	0,81	101,65	±	4,81	57,80	±	8,53
K.H.	109,70	±	1,71	48,72	±	4,12	91,66	±	5,03	41,19	±	1,25
M.P.	116,07	±	11,18	120,83	±	6,09	156,67	±	9,90	125,50	±	7,13
Q.V.	128,20	±	13,48	124,17	±	5,32	123,47	±	5,35	113,00	±	2,19
S.P.	33,20	±	2,76	62,67	±	0,93	96,45	±	1,73	43,63	±	8,25
T.G.	225,43	±	10,97	95,32	±	1,81	182,50	±	41,40	82,06	±	9,00
T.N.	129,33	±	16,34	88,80	±	7,98	111,93	±	1,50	100,52	±	15,13
V.L.	191,67	±	19,52	108,78	±	12,36	178,30	±	10,50	91,90	±	10,53
Z.L.	114,03	±	16,24	91,79	±	6,17	125,83	±	18,07	95,96	±	0,46

Table 3. *Force values of shoulder flexion/extension left and right (A.S., F.P., F.A., S.P., T.G. performed the exercises with the wristband above the elbow).*

	ELBOW FLEX LEFT			ELBOW EXT LEFT			ELBOW FLEX RIGHT			ELBOW EXT RIGHT		
INITIALS	MEAN [N]	±	SD	MEAN [N]	±	SD	MEAN [N]	±	SD	MEAN [N]	±	SD
A.S.	211,97	±	8,90	-51,46	±	7,02	234,07	±	32,60	-45,63	±	1,58
B.A.	352,50	±	77,17	-189,40	±	16,81	186,60	±	46,84	-118,73	±	19,09
B.N.	243,00	±	13,19	-193,63	±	28,94	236,83	±	60,23	-232,47	±	10,87
B.M.	156,37	±	17,41	-122,53	±	17,70	226,37	±	15,24	-105,37	±	2,83
C.A.	87,84	±	5,58	-127,07	±	17,84	111,03	±	11,91	-161,17	±	5,90
D.A.	251,00	±	5,75	-70,34	±	5,41	281,87	±	24,47	-204,87	±	12,79
F.P.	184,87	±	12,88	-18,71	±	3,06	145,27	±	18,32	-45,79	±	4,16
F.A.	199,30	±	57,03	-41,10	±	6,60	187,57	±	30,58	-75,71	±	3,10
F.S.	260,43	±	19,75	-176,30	±	20,92	281,23	±	17,89	-129,83	±	14,23
G.D.	227,33	±	6,00	-102,26	±	3,61	260,63	±	33,92	-217,00	±	9,56
G.M.	171,00	±	11,23	-115,73	±	3,13	32,16	±	7,17	-133,67	±	3,28
K.H.	190,90	±	13,05	-27,25	±	1,01	89,08	±	22,79	-22,93	±	0,22
M.P.	290,25	±	1,34	-287,85	±	22,27	325,05	±	7,57	-250,10	±	7,07
Q.V.	220,40	±	25,43	-183,23	±	15,33	316,57	±	12,99	-117,54	±	17,85
S.P.	102,20	±	7,22	-58,32	±	2,87	159,10	±	4,95	-14,81	±	1,25
T.G.	199,97	±	21,00	-55,30	±	1,03	191,83	±	13,04	-73,32	±	7,52
T.N.	309,77	±	10,23	-186,27	±	11,10	309,33	±	13,48	-134,00	±	3,08
V.L.	301,07	±	17,11	-169,33	±	4,24	414,63	±	7,91	-141,90	±	27,21
Z.L.	238,87	±	7,13	-213,97	±	7,84	233,80	±	27,35	-164,77	±	2,73

Table 4. *Force values of elbow flexion/extension left and right.*

The following graphs (*figures 25, 26*) contain the ranking for the isometric force of shoulder and elbow flexion/extension collected by the load cell, in descending order.

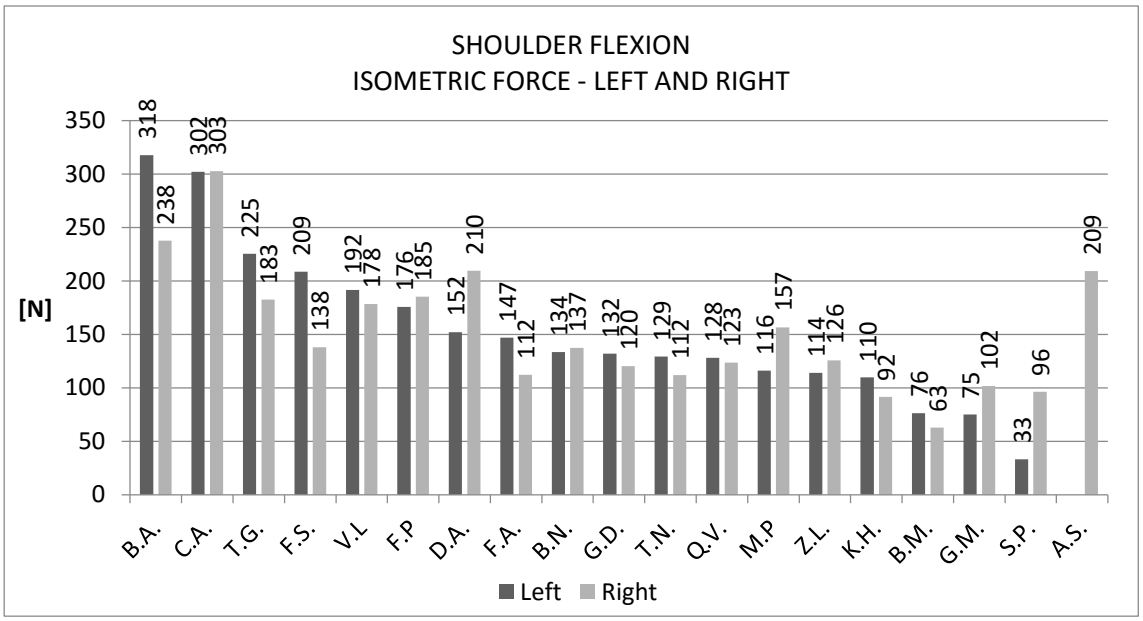

Figure 25. *Shoulder flexion isometric force left and right (values are sorted by the left side).*

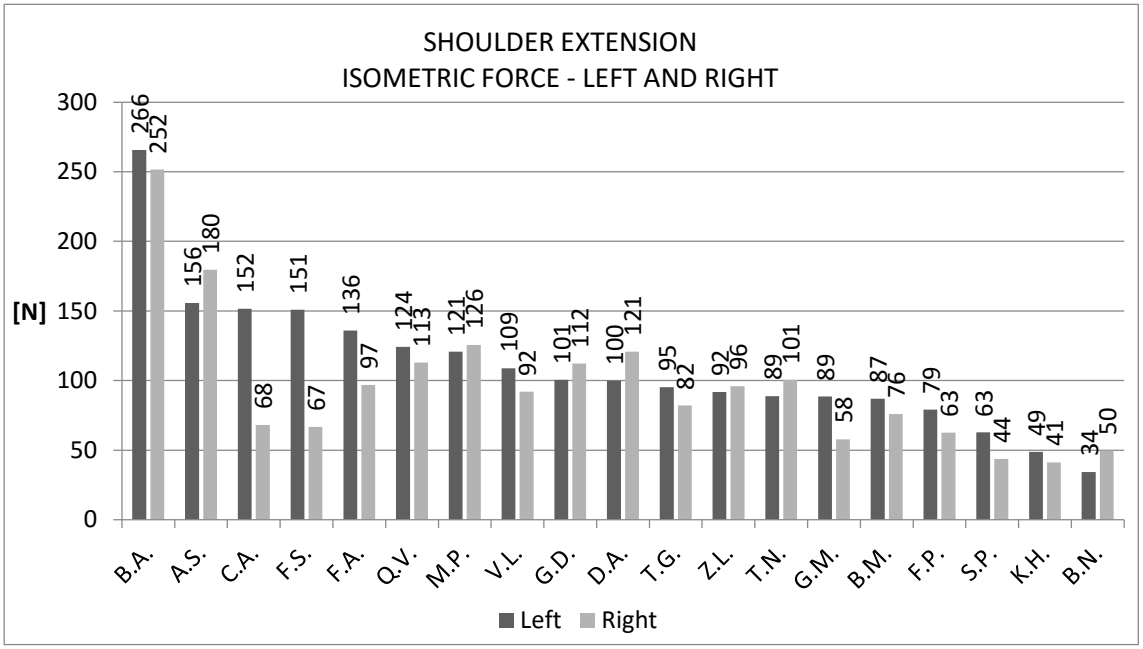

Figure26*. Shoulder extension isometric force left and right (values are sorted by the left side).*

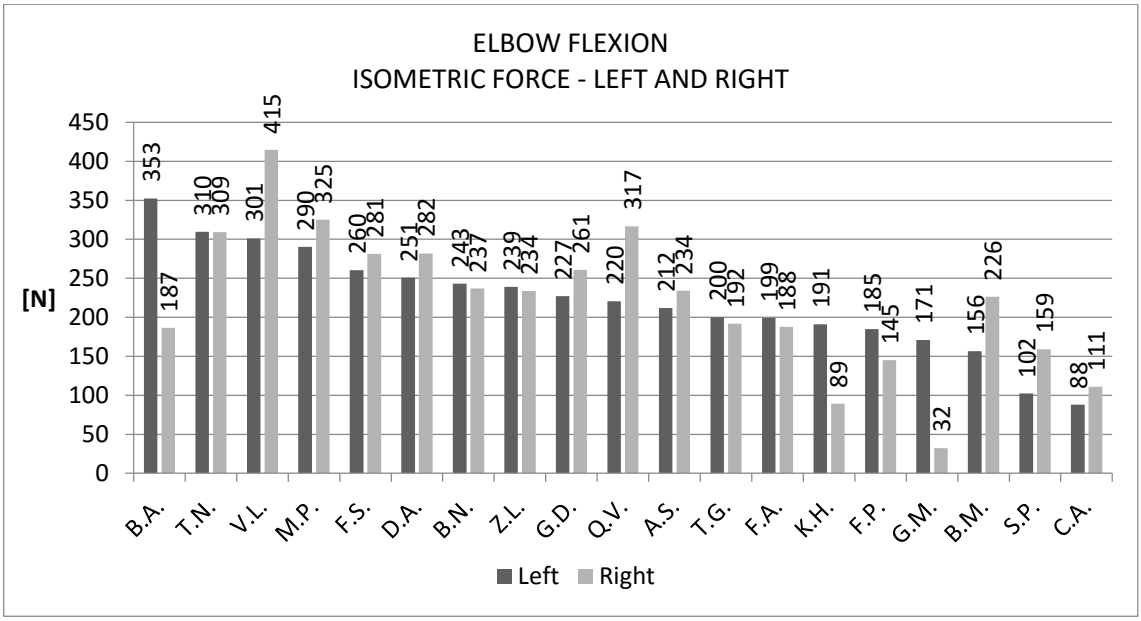

Figure 27. *Elbow flexion isometric force left and right (values are sorted by the left side).*

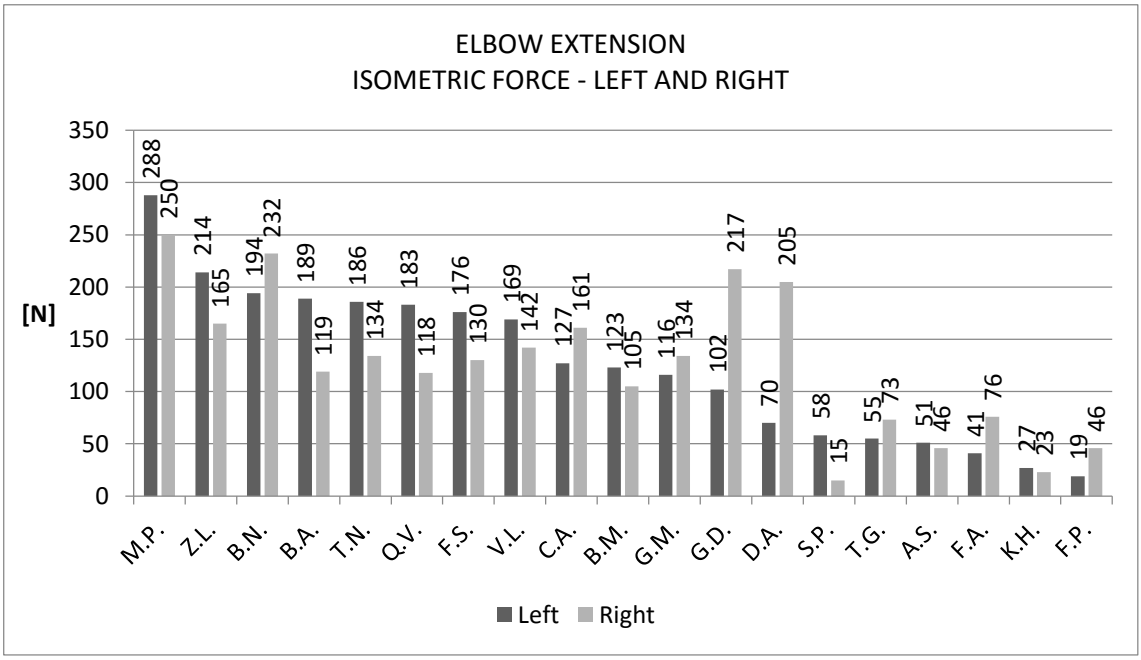

Figure 28*. Elbow extension isometric force left and right (values are sorted by the left side).*

The results for isometric force rankings at elbow and shoulder do not follow the points of classification. This was expected, since these values are strictly connected to each personal disease. In some case, values highly differ between the left and right side. Considering the shoulder flexion, for example, B.A., D.A. and G.M. have a high difference between the left and the right side. This is due to the missing of the control of some muscles of one side, in relation to the pathology. All these results must be correlated with medical information, to find explanations for asymmetries or unexpected values.

Finally, moments at the joints were calculated with the multiplication of the force collected by the load cell for the lever arm. Considering the conditions of zero shoulder flexion for shoulder exercise, the lever arm for the shoulder moment is the total length of the superior limb; considering the isometric exercises at the elbow as executed with 90° of elbow flexion, lever arm for the elbow moment is represented by forearm length. Arm and forearm lengths were measured for each participant, and represented in *table 5.* Arm length was taken from acromion to the most proximal point on the lateral edge of the radius, and forearm length from the latter point to stylus.

	ARM [cm]		FOREARM [cm]	
INITIALS	**RIGHT**	**LEFT**	**RIGHT**	**LEFT**
A.S.	300	260	300	260
B.A.	310	310	280	280
B.N.	320	320	280	250
B.M.	310	320	260	260
C.A.	310	300	250	220
D.A.	290	290	230	220
F.P.	310	320	260	260
F.A.	320	320	280	280
F.S.	320	320	280	280
G.D.	340	330	290	290
G.M.	310	300	250	220
K.H.	310	260	310	260
M.P.	350	340	290	280
Q.V.	320	280	320	280
S.P.	290	300	260	250
T.G.	310	310	270	270
T.N.	310	330	270	260
V.L.	330	330	280	290
Z.L.	310	320	280	270

Table 5. *Anthropometric measures.*

INITIALS	SHOULD FLEX LEFT MOM [Nm]	SHOULD FLEX RIGHT MOM [Nm]	SHOULD EXT LEFT MOM [Nm]	SHOULD EXT RIGHT MOM [Nm]	ELB FLEX LEFT MOM [Nm]	ELB FLEX RIGHT MOM [Nm]	ELB EXT LEFT MOM [Nm]	ELB EXT RIGHT MOM [Nm]
A.S.	-	125,50	80,91	93,37	55,11	60,86	-13,38	-13,69
B.A.	187,48	140,30	156,74	148,42	98,70	52,25	-53,03	-33,25
B.N.	76,15	82,48	19,53	28,32	60,75	59,21	-48,41	-65,09
B.M.	44,27	35,73	50,49	44,01	40,66	58,86	-31,86	-27,40
C.A.	157,14	169,46	78,85	35,34	19,32	24,43	-27,95	-40,29
D.A.	77,59	108,97	50,93	61,63	55,22	62,01	-15,48	-47,12
F.P.	102,00	105,55	45,82	36,34	48,07	37,77	-4,87	-11,91
F.A.	88,12	67,40	81,50	58,12	55,80	52,52	-11,51	-21,20
F.S.	125,12	82,80	90,52	39,99	72,92	78,75	-49,36	-36,35
G.D.	81,84	75,85	62,34	69,54	65,93	75,58	-29,66	-62,93
G.M.	39,12	56,93	46,06	30,05	37,62	7,08	-25,46	-33,42
K.H.	57,04	56,83	25,34	21,42	49,63	23,16	-7,09	-7,11
M.P.	71,96	100,27	74,92	77,81	81,27	91,01	-80,60	-72,53
Q.V.	71,79	79,02	69,53	63,28	61,71	88,64	-51,31	-37,61
S.P.	18,26	53,05	34,47	24,00	25,55	39,78	-14,58	-3,85
T.G.	130,75	105,85	55,29	47,59	53,99	51,80	-14,93	-19,80
T.N.	76,31	64,92	52,39	59,30	80,54	80,43	-48,43	-36,18
V.L.	118,83	108,76	67,44	56,98	87,31	120,24	-49,11	-39,73
Z.L.	67,28	74,24	54,15	56,61	64,49	63,13	-57,77	-46,13

Table 6. *Moments at the joints in isometric elbow and shoulder flexion/extension.*

In some cases, moment values found for flexion/extension at the shoulder do not agree with the results found in the literature (consider paragraph *3.4.3*). This could be partially imputable to an incorrect way of executing the exercise. Considering shoulder flexion, the subject was asked to flex their arms seated on his sport chair, with a zero degree of shoulder and trunk flexion: this situation did not always occur, since in some cases, to perform the exercise, the subject flexed his trunk thus starting from a positive angle of shoulder flexion (*figure 29*). Moreover, according to the execution protocol, the application of the wristband to the wrist, to which the load cell was connected, allowed for an elbow flexion thus adding an eventual moment generated by the biceps: this force was recorded by the load cell, but was not imputable to the shoulder joint. In future measures, there is the need of applying the wristband above the elbow, to make sure the recorded force in being the one exerted by the shoulder flexion. Moreover, this would standardize the test according to those people who do not have the control of his triceps and necessary need a fixation above the elbow, to execute a movement of isometric shoulder flexion/extension.

Also the moments of elbow flexion/extension do not always agree with literature results. This is probably still due, partially, to a wrong phenomenon of compensation occurring during the movement of some subjects. Moreover, the force was exerted through a carabiner attached on the external part of a plastic disk: in this way, the force was not parallel to the load cell direction, and the beam flexed. Some people performed the exercises with an elbow extension different from 90° (*figure 30*). In elbow flexion, some subjects helped the movement with a shoulder extension and elevation; in elbow extension, some people helped the movement with a shoulder adduction. This could add some advantage on the force, especially in those cases in which muscular control is weak, and is recorded by the load cell.

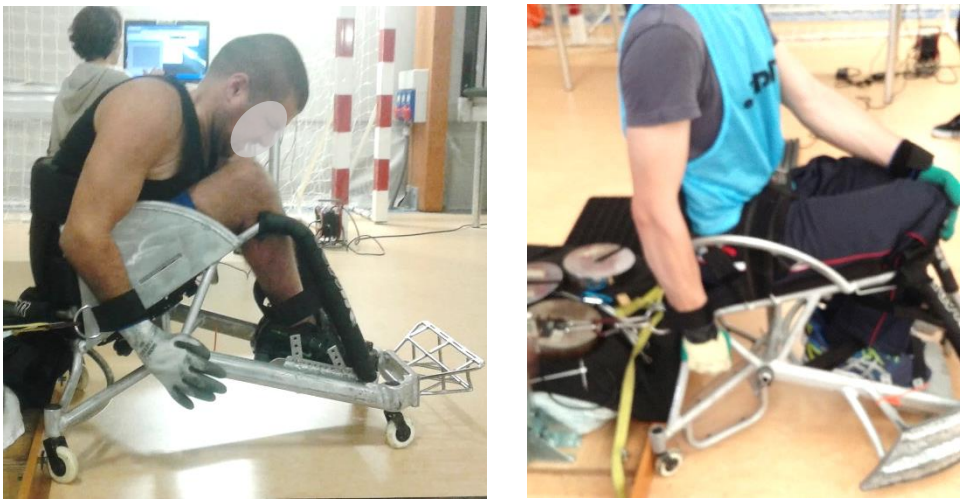

***Figure 29**. Shoulder flexion test. Left: wrong way of execution (positive angles of elbow and trunk flexion). Right: right way of execution (zero elbow and trunk flexion).*

***Figure 30**. Elbow extension test. Left: wrong way of execution (shoulder abduction, less than 90° of elbow flexion, the applied force is not parallel to the beam). Right: right way of execution (no trunk rotation, 90° of elbow flexion, force parallel to the beam).*

For these reasons, the whole set of isometric measure must be repeated assuring the movement to be pure as much as possible, avoiding effects of compensation and extra forces not related to the specific joint moment.

The result reported in literature [19,23] also differ for the fact that in cited studies, isometric tests were executed in healthy and non-trained people: the present study, on the contrary, is based on wheelchair-users athlete, so their level of training of the upper limbs in some cases (as B.A., T.G., M.P., F.S.) is very high.

CHAPTER 5

Project activity 2: dynamic tests

Wheelchair Rugby is a very tactic game, based not only on mere athletes' muscular force, but much more on the way the athlete can use his force to express particular abilities and skills within the game. Impressing a good acceleration, velocity, and spinning, combined with a team play, are some of the most important features that a Wheelchair Rugby athlete has to learn and improve. Therefore, some situations present the necessity of impressing a big acceleration from a still position, for example to reach to the goal line or to receive the ball from a mate; another necessity is the ability of turning quickly, in situations as blocking an opponent or freeing from a blockage position.

This sport was born to give people with an incomplete upper limbs and trunk muscular control, the chance to compete using their residual capacities at best: in this way, athletes with low points and most severe impairments can have an essential role within the game. In this work, the dynamic performances of athletes were investigated by measuring their longitudinal acceleration and angular velocities in different situations, through MEMS inertial sensors.

Research question: considering the wheelchair-user system, what are the maximum and mean forward acceleration in a sprint, eight track and during a match? What is the maximum angular velocity in a rotation and in an eight track?

5.1 Instrumentation

This paragraph describes the meaning of MEMS sensors (accelerometers and gyroscopes), and Xsens inertial sensors used in this work for the data acquisition, with the protocol for their fixation in wheelchairs to perform dynamic tests.

5.1.1 MEMS inertial sensors

Micro Electronic Mechanical Systems, or MEMS, is a technology obtained using the techniques of microfabrication. The physical dimensions of MEMS devices range from below one micron to several millimetres. The types of MEMS devices vary from simple structures having no moving elements, to extremely complex electromechanical systems with multiple

moving elements under the control of integrated microelectronics. The main property of MEMS is the presence of some elements having a mechanical functionality, whether or not these elements can move. Their use and application have become fundamental in different areas such as industrial, mechanical, biomechanical, electronic. For this work is important to describe the function of MEMS inertial sensors: accelerometers and gyroscopes [33].

5.1.1.1 MEMS Accelerometers

A MEMS inertial accelerometer consists of a mass-spring system, which is located in a vacuum. The system lies on a case, which is attached to the moving object: an acceleration of the accelerometer causes a displacement of the mass in the spring system. One way to realize the read out is a capacitive system: in this case, when the geometry of the capacitor is changing, the system senses a changing of the capacitance. The parallel-plate capacitance is:

$$C_0 = \epsilon \epsilon_0 \frac{A}{d}$$

where *A* is the area of the electrodes, *d* the distance between them and ϵ the permittivity of the material separating them. Accelerometers are based on a change in *d* or in *A*, which is measured as a change of capacitance.

The typical MEMS accelerometer is composed of movable proof mass with plates, attached through a mechanical suspension system to a reference frame, as shown in *figure 31*. Movable plates and fixed outer plates represent capacitors. The deflection of proof mass is measured using the capacitance difference. The free-space (air) capacitances between the movable plate and two stationary outer plates C1 and C2 are functions of the corresponding displacements x1 and x2.

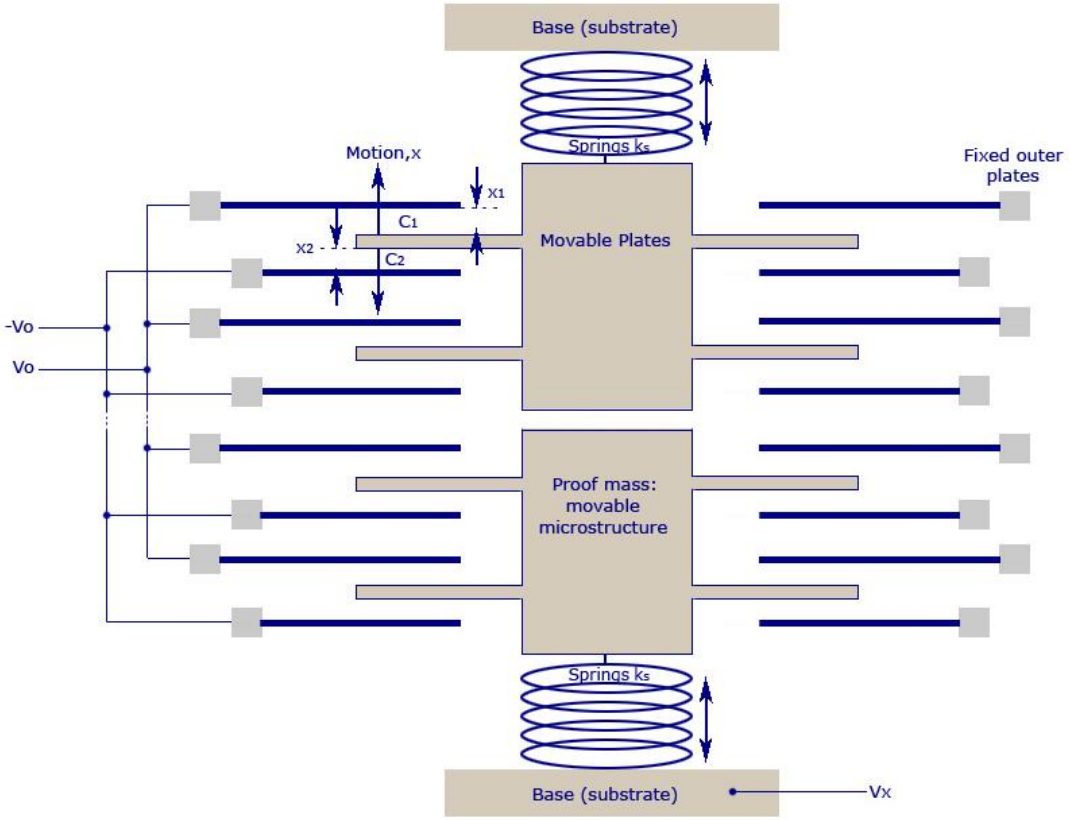

Figure 31. *Typical MEMS accelerometer structure. The proof mass is attached through springs (k_S is the spring constant) at the base substrate. It can move only up and down. Movable and fixed plates form capacitors.*

This was an example of one axis accelerometer. If one circuit includes sets of capacitors in perpendicular directions, it is possible to obtain a two or three axis accelerometer, as shown in *figure 32* [34].

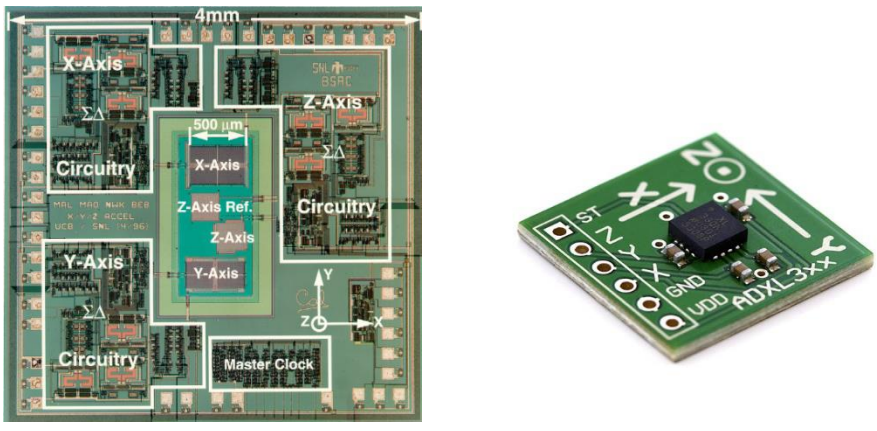

Figure 32. *Left: 3D accelerometer structure. It has three different sensors for x-y-z axis acceleration and three different electronic circuitry for each axis. Right: An ADXL 320 accelerometer.*

5.1.1.2 MEMS Gyroscopes

A MEMS gyroscope uses the Coriolis effect to measure an angular velocity. This effect states that an object with mass m and velocity $\boldsymbol{v}(t)$ in a rotating plane with angular velocity $\omega(t)$, receives an apparent force $\boldsymbol{F_{Co}}(t)$, the Corilois force, proportional to $\omega(t)$ and $\boldsymbol{v}(t)$:

$$\boldsymbol{a_{Co}}(t) = 2\omega(t) \times \boldsymbol{v}(t) \qquad \boldsymbol{F_{Co}}(t) = -m\,\boldsymbol{a_{Co}}(t)$$

Measuring the effects of this force on the oscillating object, the characteristics of the movement can be obtained. According to this physical law, a MEMS gyroscope can be realized in many ways (an example on *figure 33*): vibrating ring, macro laser ring, piezoelectric plate ring, fiber optic and tuning fork gyroscope, which is one of the most widely used gyroscope. Tuning fork gyroscope is composed by two proof masses that are built in such a way as to oscillate with the same intensity but in opposite directions. When rotated, a Coriolis force is generated, that it is bigger when mass is further away from the spin: this creates an orthogonal vibration that can be detected by different methods.

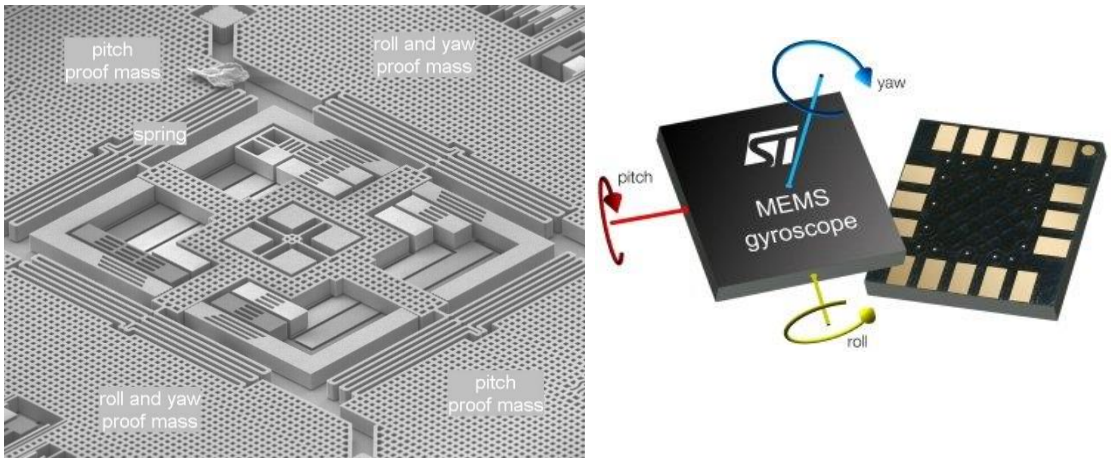

***Figure 33**. Left: SEM tilt view of a MEMS gyroscope; right: L3G4IS, the first three-axis MEMS gyroscope.*

The Xsens inertial sensor used in this work, has a MEMS rate gyroscope, with a beam structure and capacitive readout.

5.1.2 Xsens technology

The Xsens wireless Motion Tracker (MTw™) is a miniature wireless inertial measurement unit (IMU) realized with MEMS technology. It contains 3D accelerometers, 3D rate gyroscopes, 3D magnetometers and a barometer (pressure sensor). The embedded processor handles sampling, buffering, calibration and Strap Down Integration (SDI) of the inertial data, as well as the wireless network protocol for data transmission. SDI is a method to compute an orientation or position changing given an angular velocity or acceleration of

a rigid body. The Xsens provides real time 3D orientation for wireless motion trackers in a network, returns 3D linear acceleration, angular velocity and (earth) magnetic field and atmospheric pressure data. The system used in this work consists in:

- **Motion Tracker wireless sensors (MTw's™):** portable sensors with their own battery (*figure 34*). All wireless motion trackers send data wirelessly to the PC, via the Awinda Station™, placed on the desk next to the recording PC.

Figure 34. *MTw™ inertial sensor.*

- **Awinda Station**™ that controls the reception of synchronised wireless data from all wirelessly connected MTw™ sensors, and charges up to 6 of them simultaneously (*figure 35*); it is connected via USB with the PC for data acquisition;

Figure 35. *Awinda Station™.*

- **MT Manager™ Software** for visualising and recording data; it is possible to see the real time orientation of the connected sensor, together with their angles values, acceleration trend, magnetic field.

Sensors specifications are represented in the following *table:*

	Angular Velocity	Acceleration	Magnetic Field	Pressure
Dimensions	3 axes	3 axes	3 axes	-
Full Scale	± 1200 deg/s	± 160 m/s2	± 1.5 Gauss	300 -1100 mBar[4]
Linearity	0.1% of FS	0.2% of FS	0.2% of FS	0.05% of FS
Bias stability[5]	20 deg/hr	-	-	100 Pa/year
Noise	0.05 deg/s/√Hz	0.003 m/s²/√Hz	0.15 mGauss/√Hz	0.85 Pa/√Hz
Alignment error	0.1 deg	0.1 deg	0.1 deg	-
Internal Sampling Rate	1800 Hz	1800 Hz	120 Hz (max.)	-
Bandwidth (analogue)	~120 Hz	~140 Hz	10-60 Hz[6]	-

Table 7. *Main sensing specifications.*

The patent-pending Awinda™ radio protocol is based on the IEEE 802.15.4 PHY. Using this basis, ensures that standard 2.4 GHz ISM chipsets can be used. The Awinda protocol

provides time synchronisation of up to 32 MTw's across the wireless network to within 10 µs. With Awinda, the data are initially sampled at 1800Hz, down-sampled on the processor of the MTw to 600Hz, and using Strap Down Integration (SDI) the data are transmitted to the Awinda Station. Output sample rate of the MTw's™ can be chosen by the user and changes with the number of connected sensors: with one MTw™ connected, the maximum frequency is 120 Hz; with two, the higher frequency automatically decreases to 100 Hz, and so on. The lower frequency is 20 Hz. Each MTw™ is powered with its own LiPo battery. At its current state of use, the battery lasts for almost 2 hours and can be recharged after one hour docked in the Awinda Station™ [35].

5.1.2.1 Xsens system of orientation

Each MTw™ has a right handed fixed coordinate system, that defines the sensor coordinate frame ***S*** (figure tot). This frame is aligned with the sensor's external box but the real reference is inside and, of course, this may cause an error and a loss of accuracy. The internal angles are defined as Euler "aerospace" angles, called in this way because they are frequently used in aerospace field, defined the RPY convention, where R is *"Roll"*, P is *"Pitch"* and Y is *"Yaw"*. Following to the right hand rule, the *Roll* angle is around X axis, *Pitch* is around Y, *Yaw* is around Z.

The alignment between the coordinate system ***S*** and the bottom of the MTw™'s box is guaranteed less within than 3°. Another problem of the inertial sensors in the orthogonality of the reference system's axes, but regarding Xsens MTw™ the non-orthogonality is less than 0.1°. In default conditions each MTw™ returns angles between the coordinate system ***S*** and the "Earth" coordinate system ***E***, with ***E*** as reference coordinate system. ***E*** coordinate frame is called "Earth" because it is "created" by Earth with its magnetic field and its gravity acceleration axis, it is defined as a right handed coordinate system as follows:

- *X* axis has the same direction and orientation of a vector that points to the Earth magnetic North;
- *Y* axis is calculated according to the right hand rule;
- *Z* axis has the same direction of gravity force but opposite orientation.

The ***E*** coordinate system is invariable, therefore to perform a clearly and more intuitive description of the reset operations, it has been created a new coordinate system called *Fixed coordinate system **F***. Hence ***F*** is taken as the reference coordinate system and in default conditions coincides with ***E*** (*figure 36*).

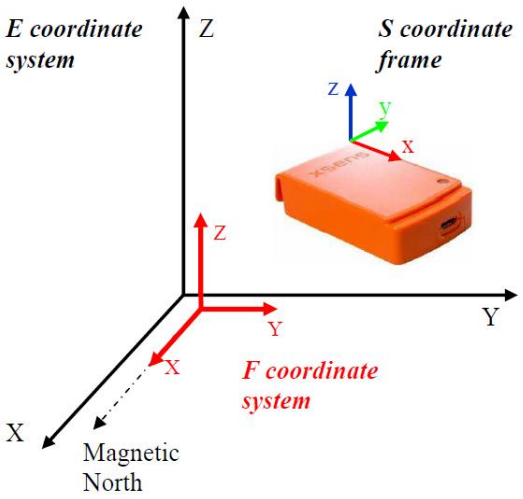

***Figure 36**. MTw's coordinate system*

The software offers several options of reset, that differ for the output angles of the ***S*** coordinate frame. The most complete option is the *alignment reset (figure 37)*: with this operation, the MTw's™ output angles of *Roll, Pitch* and *Yaw* are put at zero degrees. As shown in *figure 37*, a new internal frame ***S'*** is aligned with the new ***F'*** fixed coordinate system. In this work, this option was chose to perform the measures.

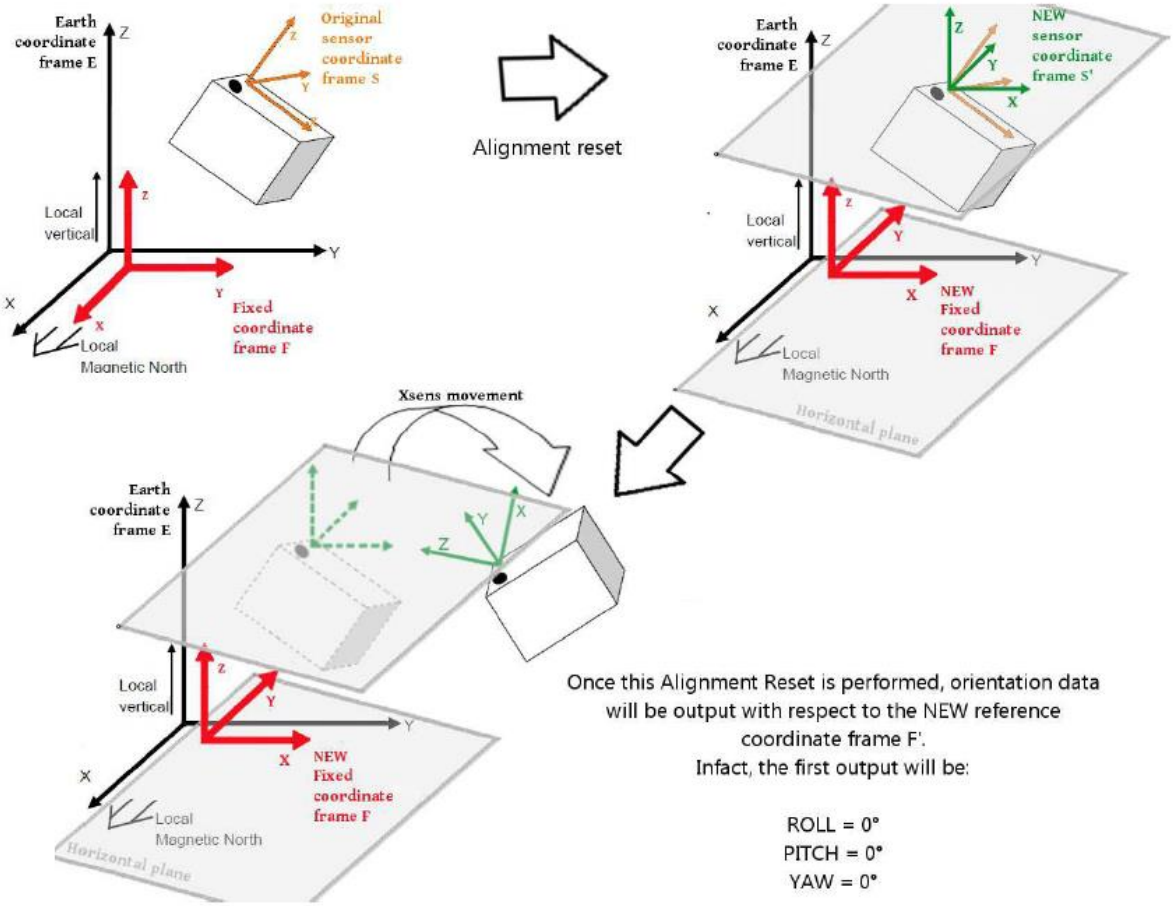

***Figure 37**. Alignment reset of an MTws™.*

5.1.3 Sensor fixation

To perform dynamic measures, Xsens MTws™ were put in the same positions for each wheelchair: one on the frame, and one for each main wheel, as described in the following paragraphs.

5.1.3.1 Wheelchair frame sensor

The wheelchair frame sensor allows recording the forward acceleration and angular velocity of the system in movement. Considering the wheelchair-player system, its reference frame is considered with the origin in its Centre of Mass (COM), the X axis in the direction of movement (horizontal), the Z axis in the vertical plane and the Y axis obtained with the right hand rule. To measure the forward acceleration of the system and its angular velocity, the sensor must be ideally placed in the COM, but since its spatial coordinates are unknown, this is not possible: therefore, its position in the wheelchair frame is given by the centre of the beam connecting the wheels' axles. The Xsens is placed in a horizontal plane, with the X axis parallel to the wheelchair-user's X axis, as represented in *figure 38.*

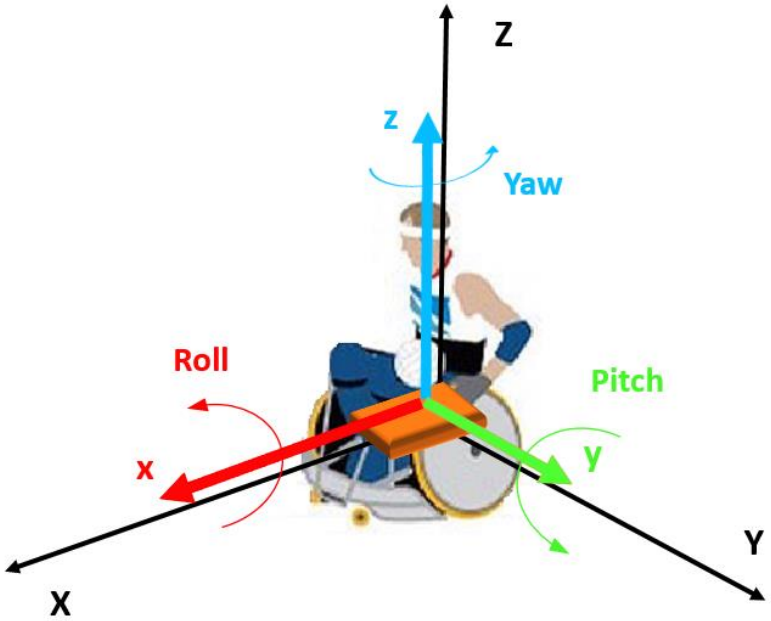

Figure 38*. Player in its reference frame (black); Xsens reference frame with Roll, Pitch and Yaw angles.*

A support was attached to the wheelchair frame to fix the sensor. Since each frame had a slightly different structure, the support and its fixation were adaptable. We used the bends given from the Xsens set, which are provided with a click-mechanism that allows the sensor to be easily fixed. The protocol for the fixation is described in the following points:

1. Sensor connection to the Awinda Station. After choosing a full-battery Xsens, it was connected to the radio station.
2. Sensor reset: the sensor used for the test was placed on the floor (after verifying it to be horizontal with a level), with the X axis parallel to a straight line (e.g. following a line of the court). Using the option of the *alignment reset*, we assured that the internal system of orientation of the sensor was concordant with the global system of reference. Moreover, it was important to assure that there was no flipping phenomenon: the software can register an axis rotation even if the sensor is not moving. In this case is better leaving that sensor resting for some minute, waiting this phenomenon to be over.
3. Support and sensor placement. There were some needs to correctly position an Xsens with its support in the wheelchair frame:
    - the sensor has to be placed in the longitudinal-middle plane of the wheelchair frame (ideally in the point of intersection of the wheels' axles). The support was fixed in the beam just under the seat, which connects the wheels' axles.
    - Xsens' X axis has to be aligned in the longitudinal direction of the wheelchair: in this way the acceleration recorded in that direction is the forward acceleration. To do this, the wheelchair was placed following a court line as its longitudinal line (*figure 39*). In this way we knew that when the Yaw angle is zero, the X axis of the sensor is aligned in the longitudinal direction.

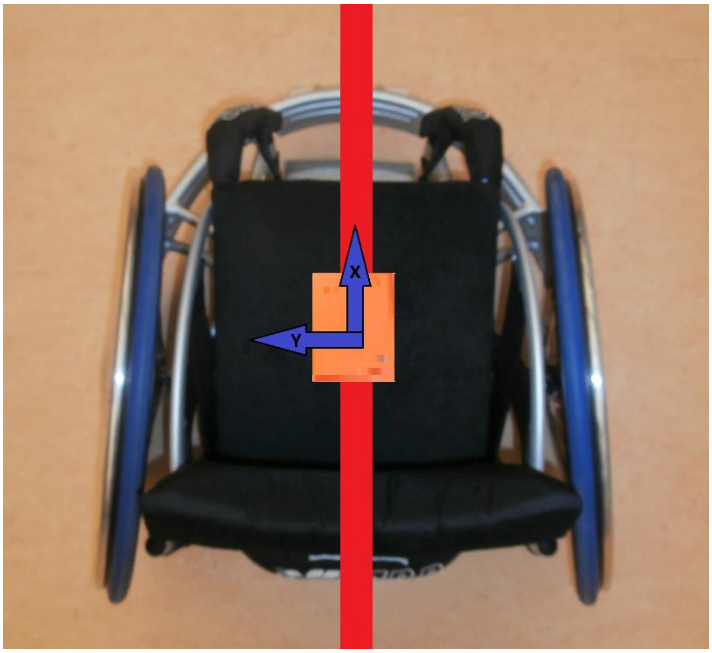

Figure 39. *The red line is a hypothetical court line; the Xsens' X axis is aligned with the red line.*

We used the sensor's system of reference to correctly align it: with the sensor on the support, not yet fixed, we identify its correct position when *Roll* and *Pitch* angles are zero (with a tolerance error of ±4°), we first fixed the support and then attach the Xsens on it. Even if there was the aim of placing the sensor minimizing the

horizontal (*Pitch*) angle, an error of some degrees was always committed. But, as verified in signal analysis, this did not affect the measures.

***Figure 40**. Wheelchair with sensors (frame and wheels).*

5.1.3.2 Wheel sensors

An Xsens was placed on each wheel, to evaluate the velocity of rotation and the number of turns. After removing the wheels, a plastic support was fixed in the axle, and on it, an Xsense with the X axis in the direction of the axis of rotation of the wheel, oriented externally, to record wheel angular velocity (*Ang vel* X_w). The setting is shown in *figure 41*.

***Figure 41.** Sensors in the wheels. Left: wheel system of reference; right: sensors fixation.*

5.3 Methods

In this work, the Xsens was used to measure the longitudinal acceleration and the angular velocity of wheelchair rugby players in different kinds of exercise, to obtain a quantitative evaluation of their performance on court.

5.3.1 Tests description

From the literature and the observation of the match, it was decided to evaluate the ability to push and finally brake during a 20 m linear sprint, the ability of turning left and right on spot, an 8 track which is more similar to a real game, combining linear sprint with turning. Finally, a match was analised.

5.3.1.1 20 m sprint

The 20 m sprint is a time exercise assessing the ability of the player to push with his arms, as much and fast as possible. It corresponds to an explosive performance. In this path, the subject was asked to reach his maximum acceleration in 20 m and, once having passed the final point, brake instantaneously. In this way it was possible to measure the trend of the forward acceleration during the push phase, and the negative acceleration given by braking.

Players started from a fixed position (*figure 42*), without moving, with the front castors aligned in a given line.

Figure 42. *An athlete at the starting position for 2the 20m sprint (yellow arrow).*

The Xsens started its acquisition when the subject was well positioned in the start line: in this way, the initial time of the longitudinal acceleration was visible on the recorded signal as an initial high positive value after a time of zero acceleration.

At the signal of "go" the player started pushing: time was counted with a hand chronometer. Once he passed the final cones, time was stopped and the Xsens acquisition was stopped few seconds after the final braking. This exercise was repeated three times, with a brief recovery (almost one minute) after each trial.

5.3.1.2 Rotation

In this exercise, the subject was asked to rotate on place (*figure 43*) to evaluate his ability to turn left and right and the eventual difference on the performance between the left and the right side, measuring the Z angular velocity of the frame sensor.

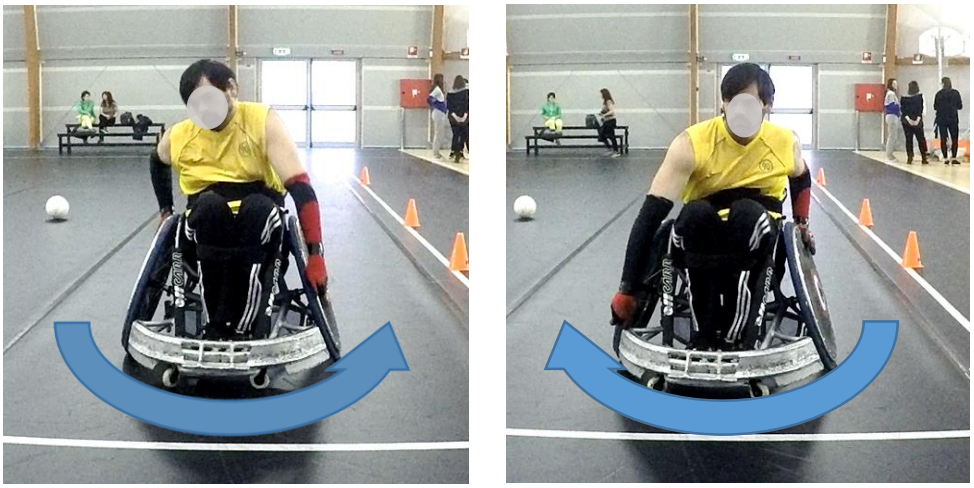

***Figure 43**. Left rotation; right rotation.*

The player started from a given position, and at the signal of start, he executed as fast as he could, a 360° turn on place, in the right direction, trying to turn around the vertical axis that ideally passes through the point of intersection of the wheel axis (the Z axis of wheelchair-player reference frame). Three seconds after the first rotation, he turned on the other direction. This left-and-right session was repeated three times, with a brief recovery (10 s) between each trial. Xsens registered each trial.

5.3.1.3 Eight track

The eight track is a time exercise, described by cones, in which linear acceleration and rotation are combined: this is more similar to a real game situation. During this exercise we measured the linear acceleration and the Z angular velocity of the player.

The path is shown on *figure 44*.

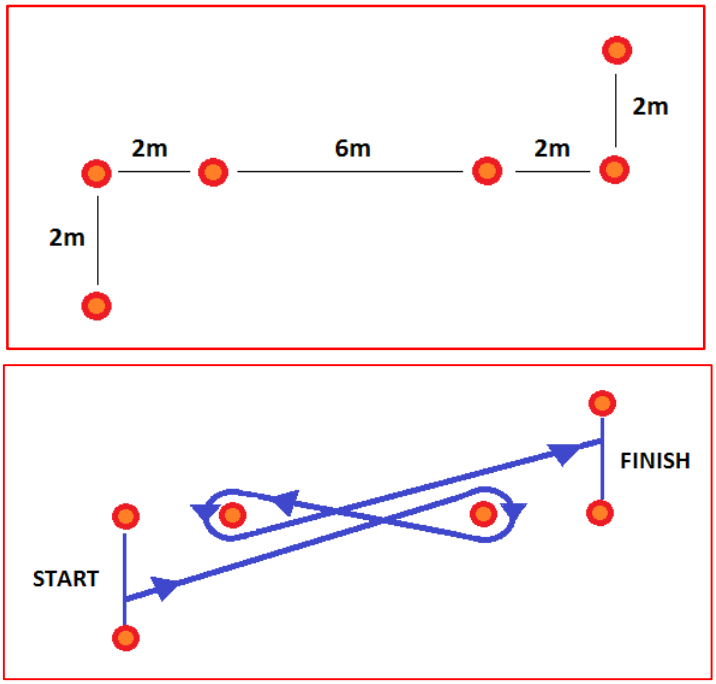

Figure 44. *The red points represents the cones. First: distances between cones; second: 8 track (blue lines) from start to final point.*

The subject started from a given position (*figure 45*) and after the signal of "go", he started pushing. Time was stopped when he passed the last two cones. This exercise was repeated three times, with a brief recovery (almost one minute) between each trial.

Figure 45*. Eight track from starting position.*

5.3.1.4 Match

The most important moment for an athlete is the match: in this contest, he has the chance to express at best all his abilities, with the additional help given by the motivation,

which has a very high impact on the physical performance. Moreover during a match, the game situations are different and complex: sprints, impacts, falls, backward pushes and many others. On the other hand, dynamic tests give information about abilities as accelerating, braking and spinning, in particular controlled conditions, but this parameters acquire another relevance when collected on court, which is the real situation in which the athlete acts. For this reason, in this work, acceleration and angular velocity during a match were recorded and analysed.

To perform these measures, an Xsens was fixed on the wheelchair frame (as described in the previous paragraph) of the 8 athletes on court. The entire match were recorded. A GoPro or a digital camera, to visually synchronise the inertial signals with the event, also recorded the match.

5.3.1.5 Friction

The frame Xsens was used to record some friction tests: the subject was asked to start from a still position and then push for 6 m and let him go without pushing further. The aim was to determine the deceleration which was totally imputable to the numerous factors which creates friction. Nevertheless, it was impossible for the subject to go straight because of the shape of the wheels, which are generally bent for overuse. Therefore, the necessity to correct the direction touching the wheel distorted the measure. This test will be executed in different conditions.

5.3.2 Signal analysis

The MT manager software saves the Xsens file as MT binary log file (*.mtb*). The aim of the signal analysis is the extraction of:

- max and mean values of forward acceleration for the 20 m sprint;
- maximum value of left and right angular velocity in rotation tests;
- maximum value of forward acceleration and of left and right angular velocity in eight track tests;
- maximum forward acceleration and distribution of acceleration values within a match.

Before dealing with the elaboration, it is important to interpret the recorded signals and associate their characteristics to physical phenomenon occurring during the test.

5.3.2.1 Frame sensor

Considering, as an example, a 20 m sprint test, the MT Manager™ output about inertial data coming from the frame sensor are represented in *figure 46*. The MT Manager™ software gives data about acceleration, angular velocity and magnetic field on the three axis of the sensor; in the present work the magnetic field was not studied.

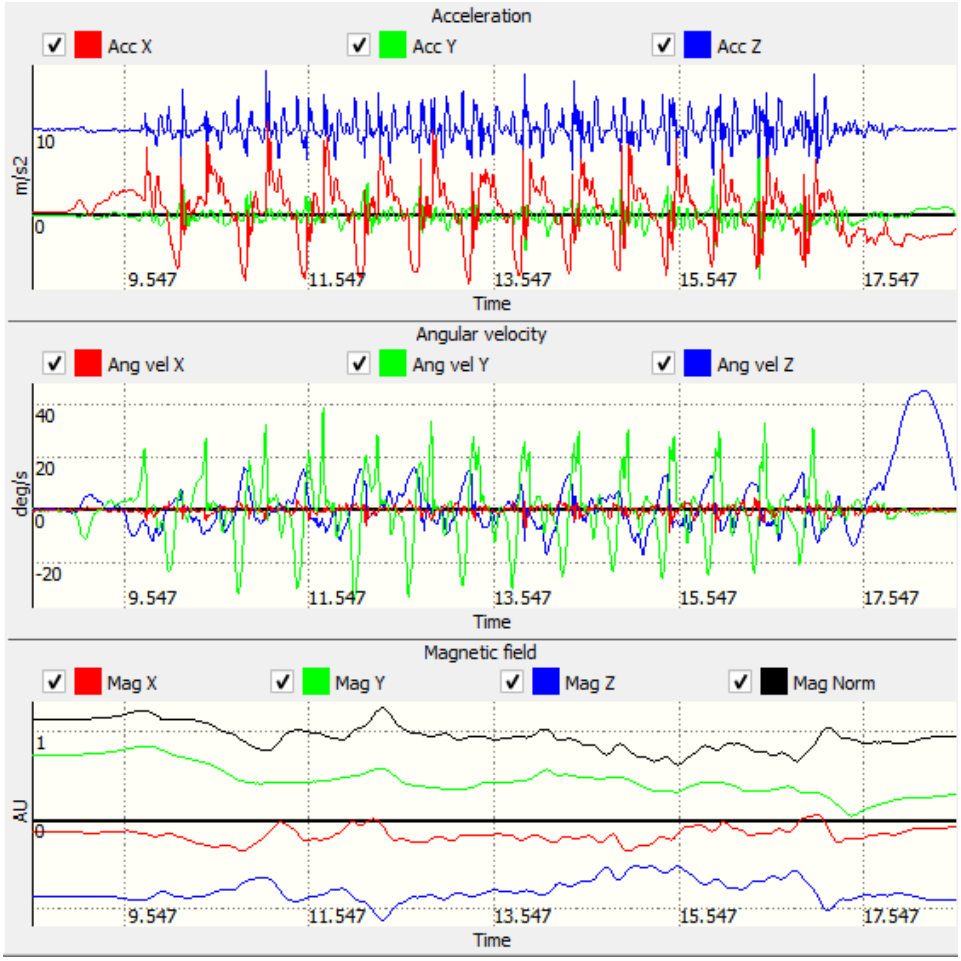

Figure 46. *Frame sensor, inertial data of a 20 m sprint (V.L.): acceleration, angular velocity and magnetic field. X is the forward direction of movement.*

According to the sensor's fixation, longitudinal acceleration of the wheelchair-player system is *Acc X* (with the sign concordant to the direction of movement) while *Acc Y* refers to the transversal direction (directed on the left). The forward acceleration trend, in the propulsion phase, can be considered as periodic: it is possible to notice positive and negative peaks corresponding to the pushes, as described in literature. Pushes visually occur with a given frequency that characterizes the personal subject's propulsion technique.

Oscillations occur also along the transversal direction: *Acc Y* shows an oscillating trend, with a smaller range of values than forward acceleration, and with no periodicity. This component is associated to lateral movements and is always recorded in wheelchair

propulsion. Depending on the player's pushing style, transversal acceleration values vary; nevertheless, in the linear sprint recorded in this work, the maximum *Acc Y* positive peak is always less than 50% of the maximum *Acc X* value.

Xsens is also sensitive to the gravitational acceleration: even if the sensor is not moving, *Acc Z* starts from a positive value (almost 10 m/s^2). Mtw's™ system of reference, after the *alignment reset*, is oriented with the Z axis parallel to the vector of the gravity force, but with opposite sign. After the fixation, the sensor is nearly parallel to the ground: therefore, the gravitational force is only recorded along the sensor's Z axis.

Acc Z trend presents oscillations during the propulsion phase: this is due to player's movements around Y axis. Therefore, during the propulsion, the wheelchair-player system always changes its points of contact with the ground: it shifts from an anterior support on the front casters and posterior support on the main wheels, to an anterior support on the main wheels and posterior support on anti-tip devices. Considering the normal configuration of the wheelchair, that is the anterior support on front casters, anti-tip devices are, for their own function, lifted from the ground (of max 2 cm): for this reason, a posterior support on them, makes the whole system tilt slightly backward. This continuous shifting, caused by the trunk and arm movement of the user, is recorded by the sensor and can be seen in *Acc Z* trend.

Another evidence of this fact is the angular velocity around the Y axis (*Ang vel Y*): it is possible to notice that the trend is characterized by a sequence of positive and negative peaks, at the same frequency of the pushes (as visible in *figure 46*, the number of positive peaks is the same).

Ang vel Z represents the angular velocity around the vertical axis of the wheelchair, concordant (with some degree of error due to the fixation) to the Yaw axis of the sensor. The positive verse corresponds to a left rotation, the negative to a right rotation. From the Z angular velocity trend, is possible to determine a characteristic of the pushing style of the player. Therefore, some players used to propel with an alternate push, especially when starting from a still position: indeed, for some people, it is easier not to use both arms contemporary, but to exert a push with one arm and then a push with the other arm. This is evident in the Z angular velocity, as this style causes higher degrees of rotation of the whole system, if compare with a normal push (*figure 47*).

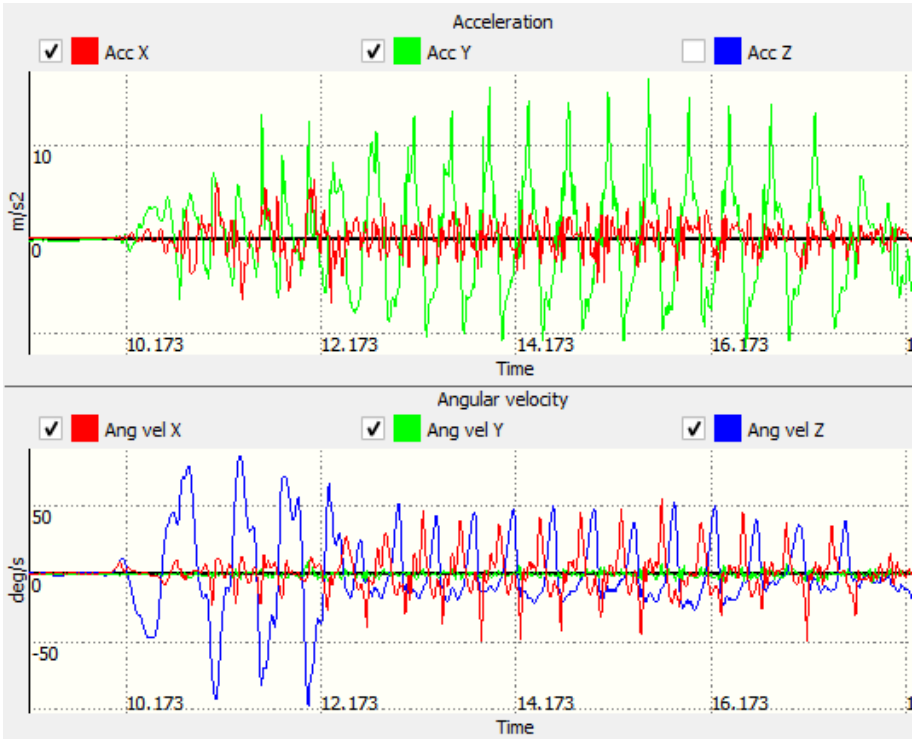

Figure 47. *Acceleration and angular velocity trends of a 20 m sprint (N.B.), for an alternate pushing style, visible in the first three pushes. Forward direction is Y, transversal direction is X.*

In this case, for a particular configuration of the wheelchair frame, the sensor was fixed with a right 90° rotation around the Z axis to allow its fixation: the forward direction is Y and the transversal direction is X. The first three pushes are alternate (*Ang vel Z*), and generate high values of angular velocity around Z (to 90 deg/s), while a normal style generates lower values (50 deg/s). In the first three pushes, the transversal acceleration component has higher values than in the rest of the signal, comparable to the forward acceleration values; the forward acceleration is lower in the first three pushes, to consequently increase and assume a repeatable shape.

The MT Manager™ Software also records the space orientation of the MTw's™, represented in *figure 48*.

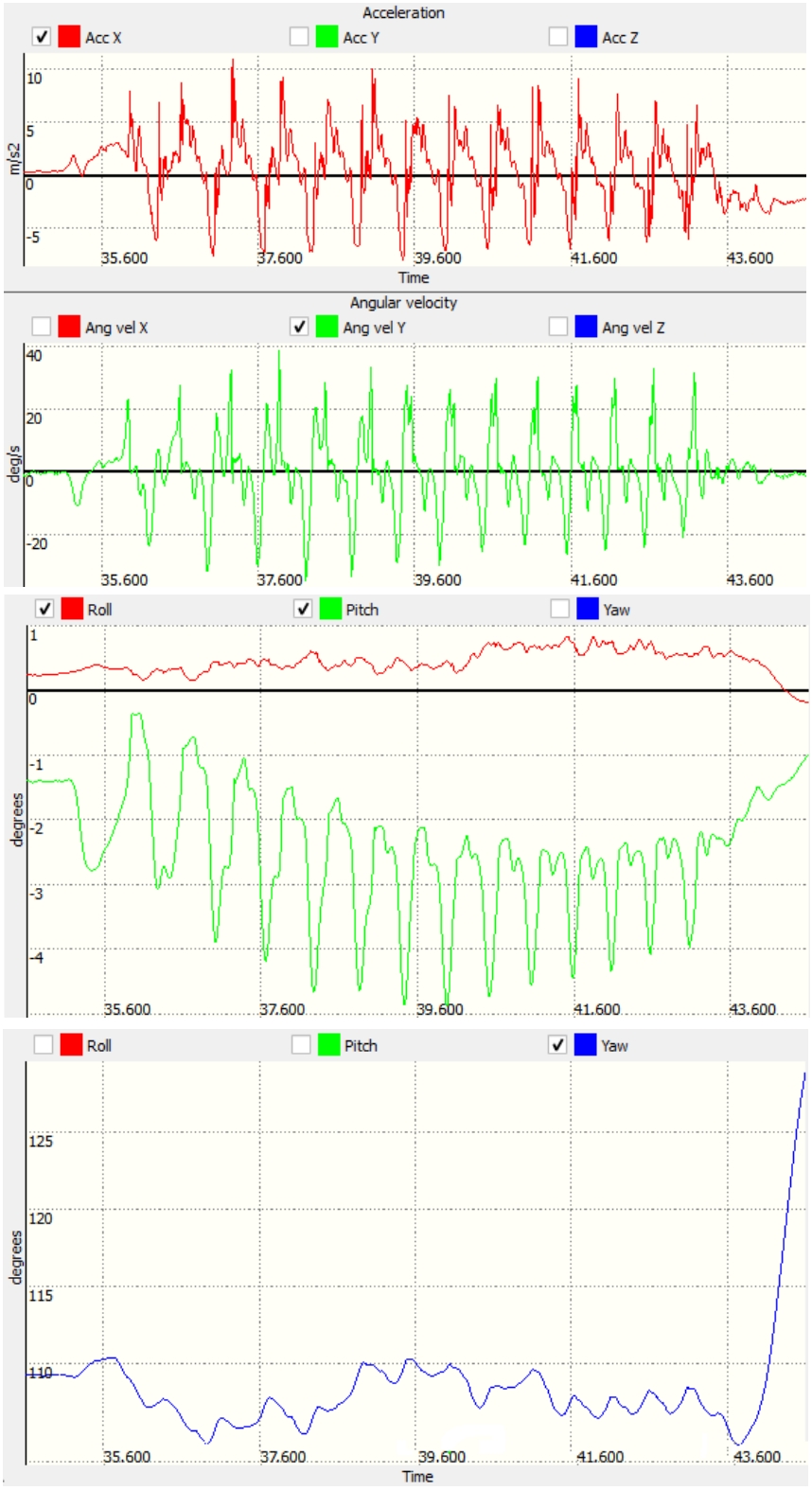

Figure 48. *Forward acceleration (Acc X), angular velocity (Ang vel Y), Pitch, Roll and Yaw angles of a 20 m sprint (V.L.).*

The *Roll* angle trend ranges from 0 to 1° within the propulsion period; the *Pitch* angle presents a different trend, since it shows peaks occurring in the same instants of the Y angular velocity peaks: this is still due to the inclination on the Y plane of the wheelchair. Moreover, *Pitch* and *Roll* present descending and ascending trends that are not imputable

to any physical phenomenon, but seem to be random. The *Yaw* angle registers the rotation around the Z axis. The angles trend can be easily seen in Matlab, as shown in *figure 49*.

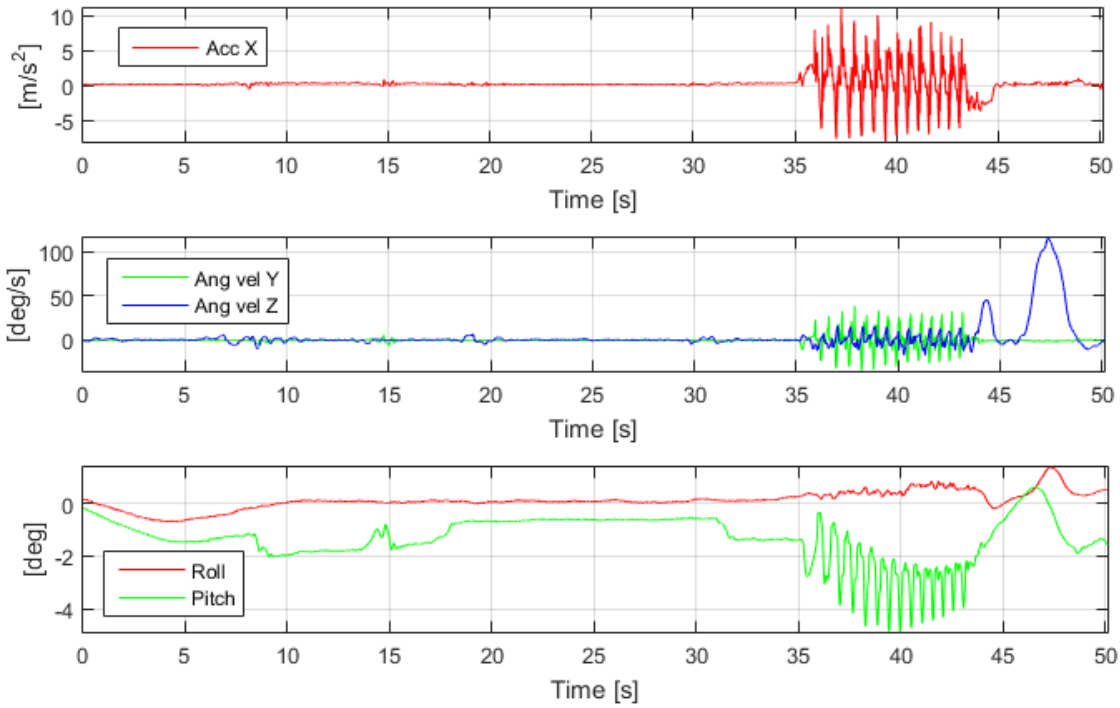

***Figure 49**. Forward acceleration (Acc X), angular velocity and angles of a 20 sprint (L.V.).*

The graphs represent the whole period before the subject executed the test, starting from a still position. It is possible to verify that the *Pitch* angle varies even if the person is not moving in that direction: this seems to be related of some phenomenon internal to MTw's™ gyroscope. Nevertheless, this range of variation of some degree, does not affect the measure, the sensor can be approximated as placed in a horizontal plane, and the X acceleration can be considered as the forward acceleration. In fact, considering *Roll* angle as zero, a *Pitch* inclination error of some degrees does not substantially vary the forward acceleration value. In composing the acceleration, the cosine component should be evaluated:

$$Acc_{horizontal}(t) = AccX(t) \cdot \cos(Pitch(t))$$

In this case, if the *Pitch* maximum value is 4°, cos(4°)=0.9976. The acceleration values vary of a maximum 0.2%. In other situations, *Pitch* value till 10° occurred, bringing an acceleration error of 1.5% that is still acceptable.

Before describing the data analysis, the following paragraph contains some considerations about the wheel sensors.

5.3.2.2 Wheel sensors

The Xsens inertial data coming from the left and right wheel sensor are represented in *figures 50, 51*. The difference of fixation determines the difference of sign, but the values in their module are comparable.

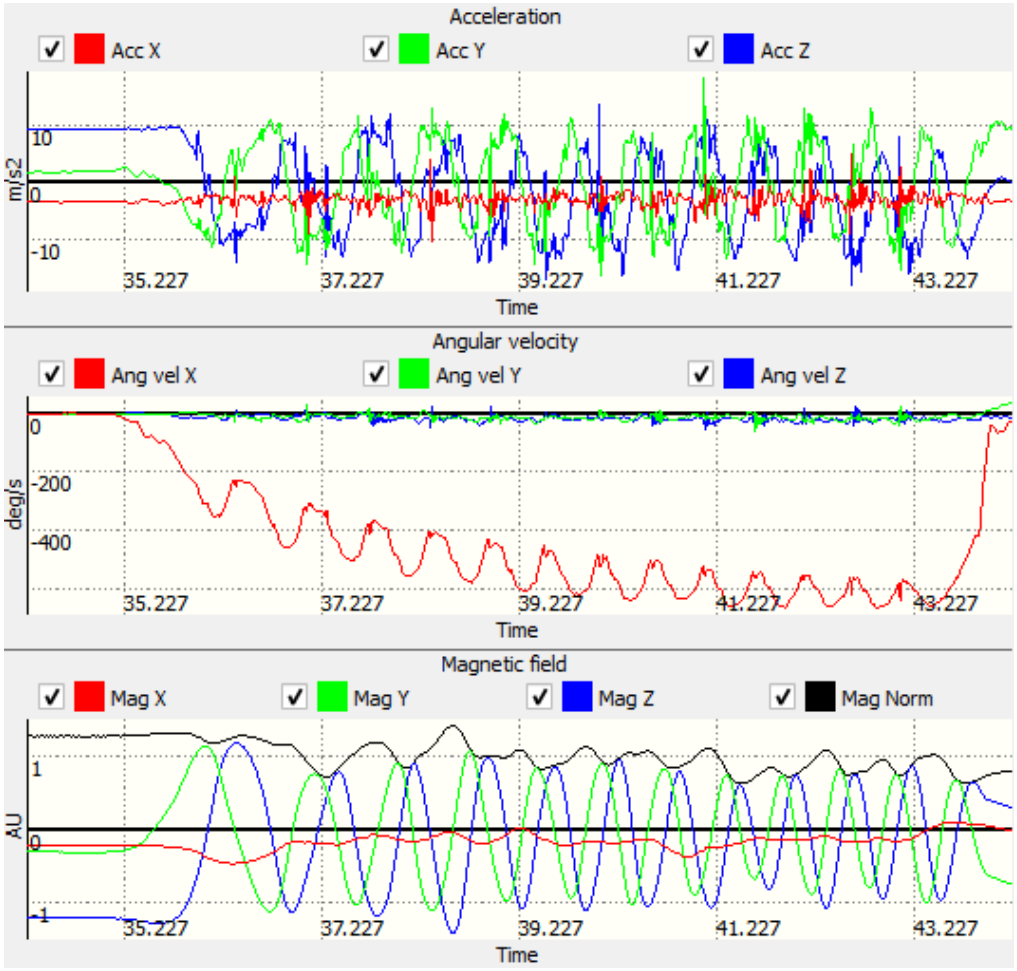

Figure 50. *Right wheel sensor, inertial data of a 20 m sprint (V.L.): acceleration, angular velocity and magnetic field.*

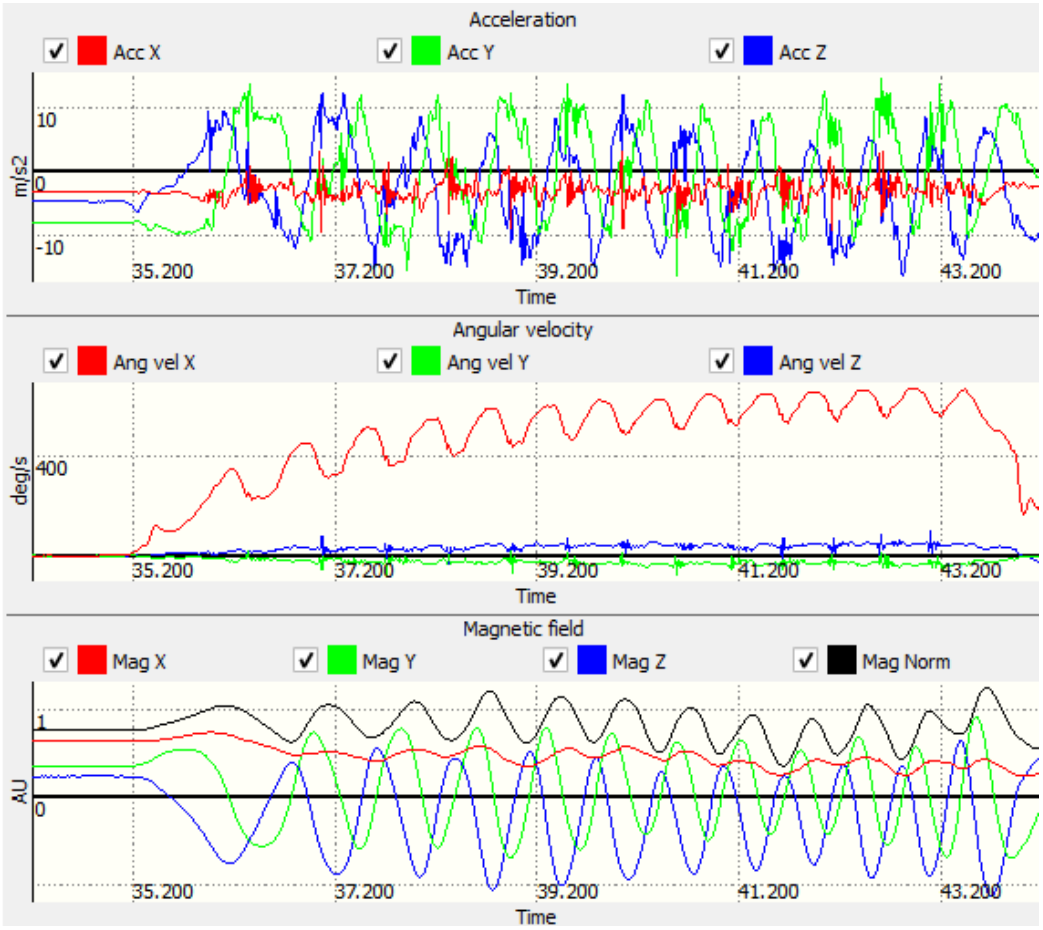

***Figure 51**. Left wheel sensor, inertial data of a 20 m sprint (V.L.): acceleration, angular velocity and magnetic field.*

Acceleration values do not start from zero, even when the sensor is not moving: this is due to the gravitational acceleration, that is recorded by the Xsens. Differently from the frame sensor, a wheel sensor generally presents considerable values of *Roll*, *Pitch* and *Yaw* before the starting moment (*figure 52*): for this reason, even when the sensor is not moving, a component of the gravitational acceleration is felt along all the sensor's axis and recorded as a non zero value.

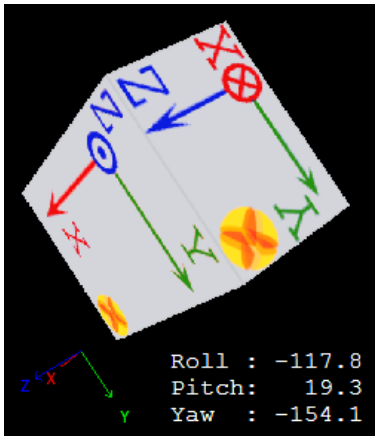

***Figure 52.** Spatial orientation of the left wheel sensor in the fixed position before the start.*

Because of the fixation on the wheel, the sensor's X axis was parallel to the wheel axis, with an error due to the axles' thickness (nearly 2 cm): for this reason, considering the acceleration trends after the start, *Acc X* shows small values if compared with the other two

components of acceleration. *Acc Y* and *Acc Z* present a periodicity at the same frequency, but not in phase because of the rotation of the wheel.

The angular velocity trend is relevant only for the X component: considering the left sensor, it is possible to notice a crescent trend (for the right wheel sensor, this trend is negative) with some oscillation, in phase with the forward acceleration trend of the frame sensor. Visually, the number of pushes is the same and correspond to the variation of velocity of the wheel caused by the push. The crescent trend underlines the fact that the velocity does not remain constant but increases during the whole sprint, more quickly in the first phase and less in the last phase of the sprint. Probably, if the test had been executed in a longer distance, the velocity trend had stabilized at a net constant value, without increasing further.

5.3.2.3 Pre-elaboration

Signals coming from the frame Xsens are then exported as text files and then imported in Matlab MathWorks R2015a. The imported data are acceleration (*Acc_X, Acc_Y, Acc_Z*) and angular velocity (*Gyr_X, Gyr_Y, Gyr_Z*).

Each signal was pre-elaborated to compensate some errors coming from the acquisition. A common error is the drift. The signal always presents an offset error: it registers a non-zero value (positive or negative), even if the sensor is not moving: this value is called drift (*figure 53*). This situation is always occurring: when the error is more than 5% of the signal's SD, the value was algebraically subtracted from the whole signal.

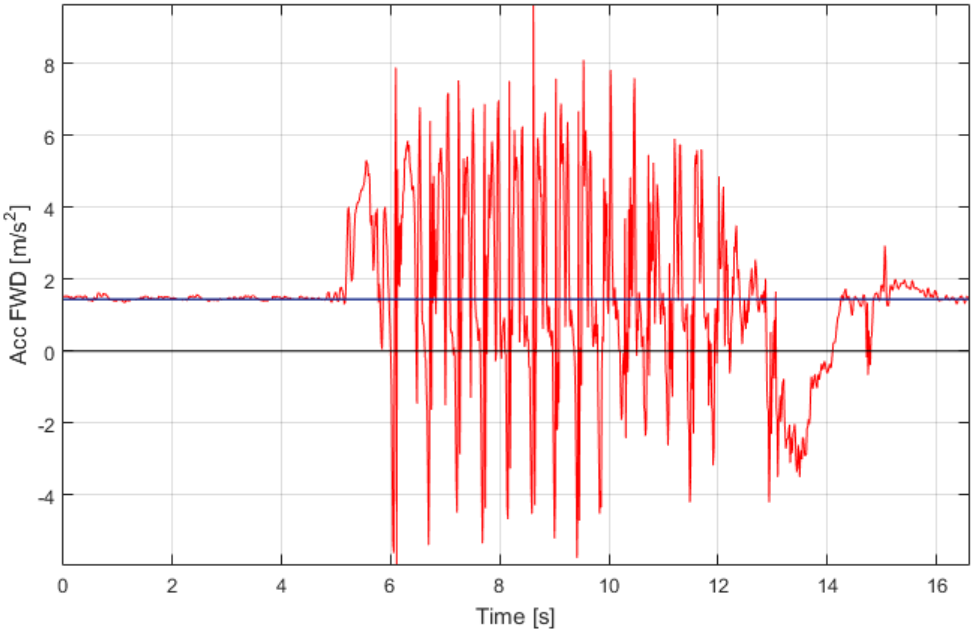

***Figure 53**. Red: Forward acceleration trend during a 20 m sprint (Z.L.); blue: drift value.*

The drift is always easy to identify since during each dynamic test, Xsens acquisition started when the athlete is in a still position: in this way the signal always starts from the zero (drift) value. To evaluate the drift, it was identified an initial interval of samples in which the signal remains stable, and made an average of those values. In most cases, drift was irrelevant but sometimes, it reaches considerable values (even more than SD, as in *figure 53*). This phenomenon seems to be random: it can happen in two consequent acquisitions of the same sensor, with different values.

5.3.2.4 Data analysis of 20 m sprint

The signal that describes the test of 20 m sprint is the longitudinal acceleration of the wheelchair-player system. It has the property of being periodic during the propulsion phase of the test, for this reason it was analysed using the frequency domain and the Power Spectral Density (*Appendix 1*).

For each Xsens file coming from the acquisition of a 20 m sprint, the signal of the longitudinal acceleration was imported in Matlab. The typical graph is shown in *figure 54*. It is possible to notice the propulsion phase characterized by a number of pushes with a maximum peak for each one, and the final braking with a higher negative value of acceleration. The shape of each push is comparable with the other, and during the test, the movement of the athlete itself takes place in a continuous cycle of pushing and recovering: for this reason the signal presents a periodicity.

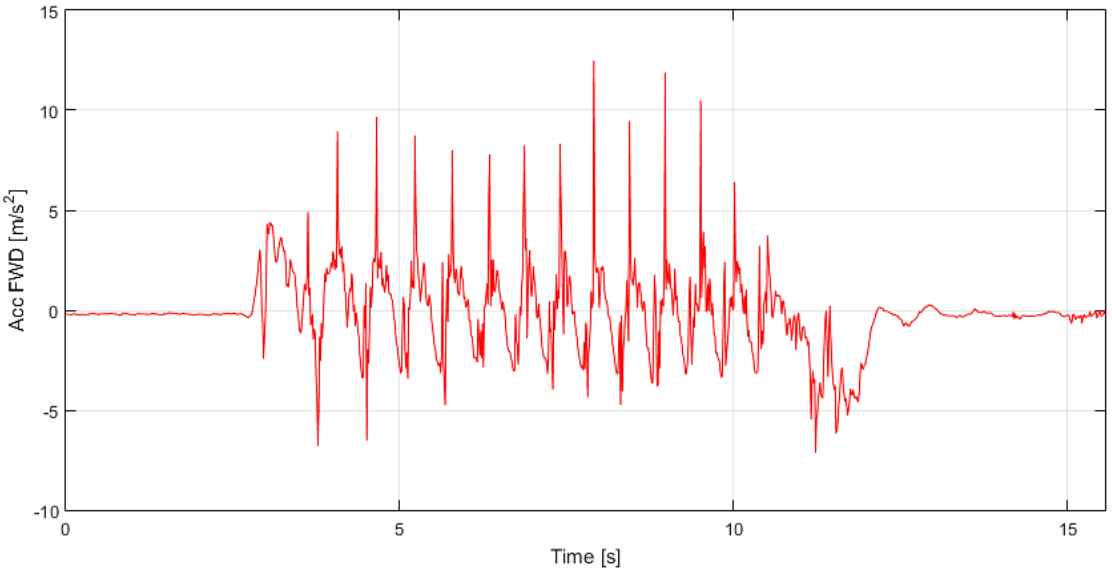

Figure 54. *Trend of the longitudinal acceleration during a 20m sprint (K.H.).*

The parameters chosen to represent this performance are the maximum value of acceleration of the entire signal, mean of the peaks of pushes, and the minimum peak of negative acceleration (deceleration), during braking.

After a pre-elaboration of the signal, to extract these values, the Matab protocol for 20 m acceleration analysis is described in the following lines (in *Appendix 2*, the full code).

1. Graphical identification of the propulsion interval of time. The part of the signal undergoing the analysis is graphically identified from the end of the first push, to the last push (before the braking), as shown in *figure 55*.

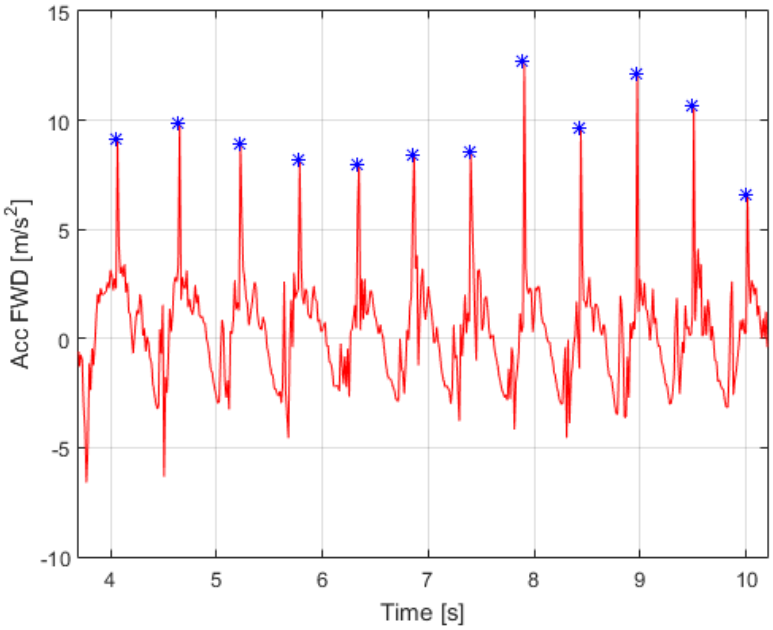

***Figure 55**. Red line: longitudinal acceleration, from the second to the last push (considering the trend represented in figure 54). Blue markers: maximum peak of each push.*

The first push is always different from the others, for shape and duration: it is slower and with a lower peak, so it is not comprised in the Fourier analysis.

2. Fourier transform of the signal. The DFT via the *fft* Matlab function is calculated from the selected part of the signal.
3. Power Spectral Density. The PSD is calculated with the expression in *Appendix 1*.
4. Definition of the frequency domain. The frequency domain is from zero to the sampling frequency.
5. Selection and visualization of the first half of PSD samples. The spectrum is plotted in the frequency domain.
6. Identification of the pushes frequency (PF). In the examined cases, PF was always comprised between 1-3 Hz. Any eventual peak in the spectrum corresponding to lower frequencies was not taken into account.

7. Division of signal into pushes.
8. Peak detection. For each push, the higher value is evaluated as a peak (*figure 55*).
9. Mean of peaks. Mean acceleration is calculated as an average operation between the peaks higher than a chosen threshold (50% of max value of acceleration). After the visualization, it is possible to eliminate any eventual wrong peak.
10. Braking identification. The negative value of braking is identified graphically as the lower value of the negative trend, after the last push.

The values of maximum, mean acceleration and braking of each of the three trials were then averaged.

5.3.2.5 Data analysis of Rotation

The signal considered to evaluate the ability of rotating on place is the angular velocity around the Z axis of the frame sensor (*Ang vel Z*). The MT Manager™ software automatically exports values in rad/s so the first operation is their conversion in deg/s: *figure 56* represents the typical trend.

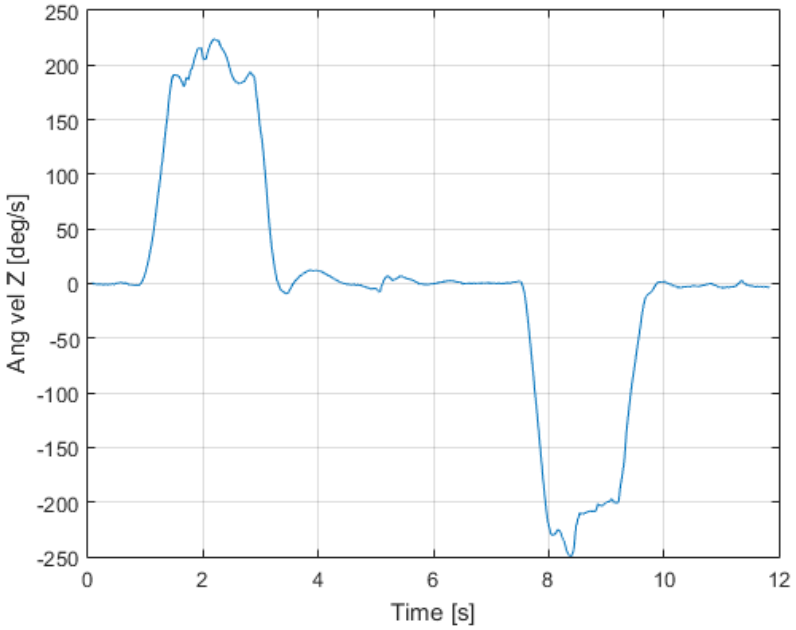

***Figure 56**. Z angular velocity trend in a rotation test (K.H.).*

The positive values correspond to the left rotation: according to the orientation of the Xsens in the wheelchair frame, and to the right-hand rule, left angular velocity has the positive sign. The negative values represent right angular velocity. In those cases in which the sensor

fixation was different, its orientation has to be taken into account to correctly identify the right and left peak values.

For each trial, the maximum and the minimum value (in module) of the angular velocity were identified with the proper Matlab function. The values extracted from each trial were averaged, giving a maximum left and right angular velocity value for each player.

5.3.2.6 Data analysis of 8 Track

Eight track performance parameters are determined as maximum acceleration and maximum left and right angular velocity values during a trial. Angular velocity was converted in deg/s, and its values were extracted as for the rotation test. The typical trend is represented in *figure 57*.

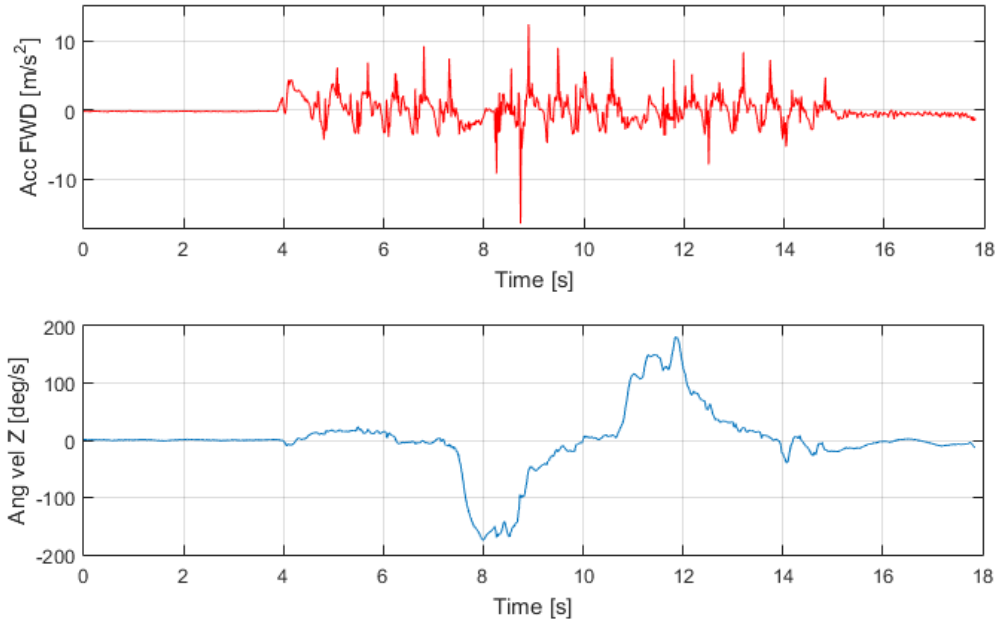

Figure 57. *Eight track acceleration and angular velocity (K.H.).*

The first set of pushes is visible in the acceleration trend, then in the velocity trend there is the right rotation around the second cone and the left rotation around the first cone, and finally the last set of pushes with lower values due to the deceleration. The temporal location of the maximum value of acceleration differs among the players: it could be reached during the first pushes before turning around the first cone, after the rotation around the last cone, or as shown in *figure 57*, between the two middle cones rotation. It was never recorded a situation in which the maximum acceleration value corresponds to significant values of rotation.

The values extracted from each of the three trials were then averaged, and the standard deviation of the measures was evaluated. The result was a unique value of max acceleration

and max left and right angular velocity, which characterize that type of performance, for each player.

From the wheel sensors data, recorded during the eight track, the angular velocity around the wheel axis was extracted (*Ang vel* X_w). To calculate the distance covered by the wheels in the track, the velocity signal was integrated, obtaining the number of degrees of each wheel during the test, and consequently the total number of turnings. The multiplication for the circumference of the wheel gives the total path (in metres) made by each wheel. For the analysed cases, this distance of both wheels is near 22 m, since the path was symmetrical.

Figure 58 shows the frame signals of forward acceleration and angular velocity, and the correspondent wheel sensors signals of angular velocity, with the trend of the space made by the wheels, in metres. The sing of right angular velocity was turned into positive, to allow representing for both wheels a positive angular velocity while the system is going forward.

It is possible to notice that after the first set of pushes, in which wheels angular velocity increases with a comparable trend, the left trend of angular velocity quickly decreases, reaching small values: in that moment the system is starting turning left (around the first cone) so the left wheel is braking (maintaining the same rotation direction). The same situation occurs for the right wheel, before the right rotation around the second cone.

At the end of the track, wheels covered distance is comparable since the 8 track path is symmetrical: in this case, any difference in wheels covered distance can be imputable to phenomenon of slipping.

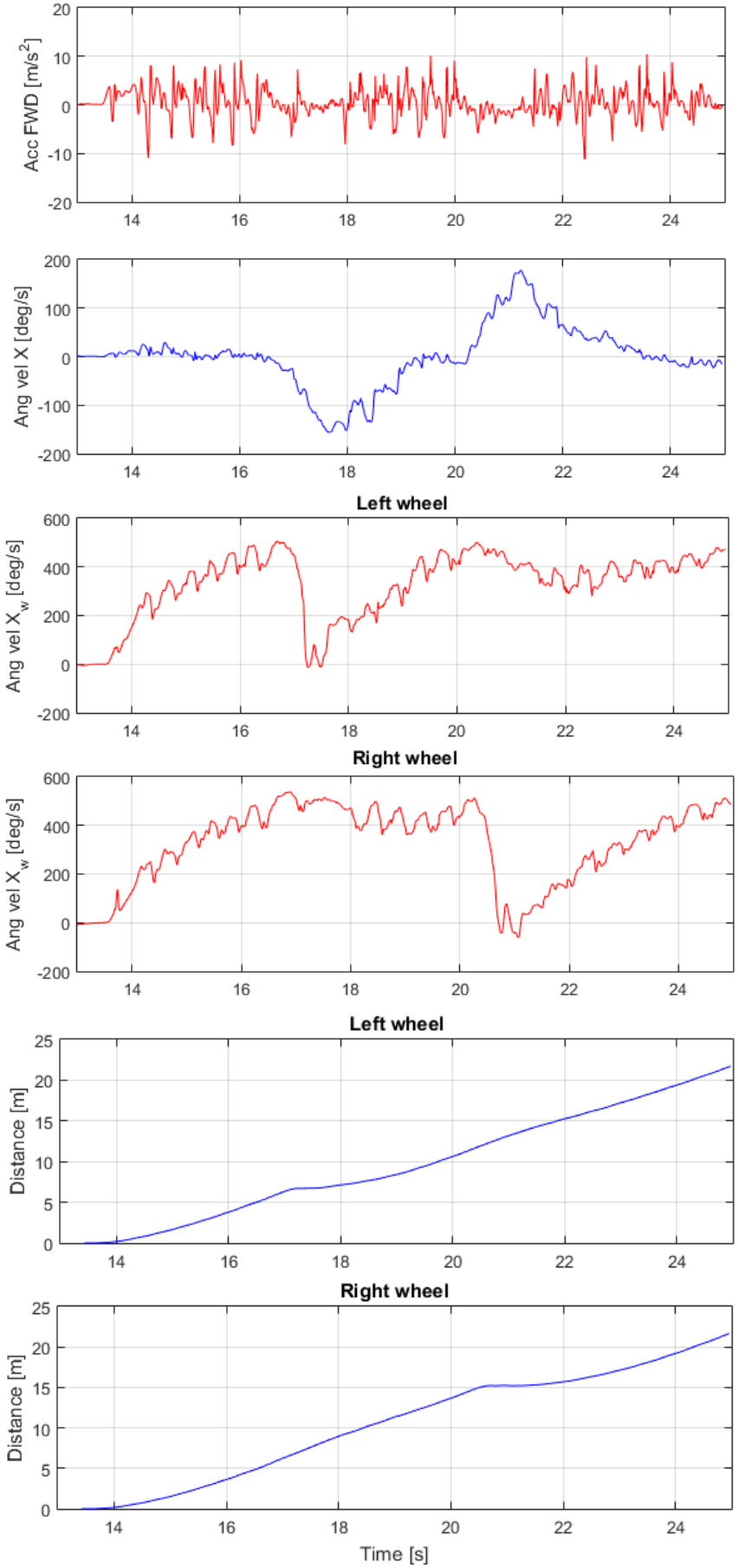

***Figure 58**. Eight track signals from frame and wheels sensors (Q.V.).*

Data analysis of wheel sensors in eight track was made for a future development, to determine the distance covered by the wheelchair-player system in a match: since COM position is unknown, it was approximated as placed in the middle point (MP) of the beam connecting wheel axles, that is the point of fixation of the frame sensor.

Considering forward acceleration of an eight track, after a first integration to obtain velocity and a second integration to determine the space, the final result is a difference (till 30%) between the distance obtained by integration of wheels angular velocity, and that obtained by the frame sensor. This occurred because the space covered by the MP can be obtained from forward acceleration only if the person is going straight, without rotating: therefore, in the same analysis made for the 20 m sprint, distance from wheels and from MP coincide, since the movement takes place in an unique direction. Eight track is a different situation: considering the MP, there are parts of the forward acceleration signal in which the trend is very close to zero, in relation to the fact that the player is, for example, turning around the cone and consequently not impressing a positive acceleration. An integration on that signal, to obtain space, would bring to wrong results.

Considering the signal of angular wheel velocity, three situations can occur:

- player is going straight: wheels are turning in the same direction, with the same angular velocity. Distance covered by the MP is equal to wheels distance.
- Player is making a circular trajectory around an external centre of rotation: wheels are turning in the same direction; considering the centre of rotation of the system, the inner wheel has a lower velocity with respect to the external wheel. Distance covered by the MP is an average between distances covered by wheels.
- Player is turning on place: wheels are turning in opposite direction, their angular velocity has same module but opposite sign. Distance covered by MP is zero, while wheels cover a certain space.

After these considerations, to determine MP distance in eight track, wheels angular velocities were averaged, obtaining *Ang_vel_med*: in this way, if player is turning on place, the result is zero. Then, *Ang_vel_med* was integrated to obtain the space. These results applied are represented in *figure 59*. It is possible to notice that in the first and last part of the space trend, when player is pushing straight, wheels trends coincide, while in the middle part corresponding to the rotation around the cones, wheels signals differ, as expected. This algorithm, reported in appendix 2, can be used in next analysis, when sensor will be put on both wheels of some players, during a match.

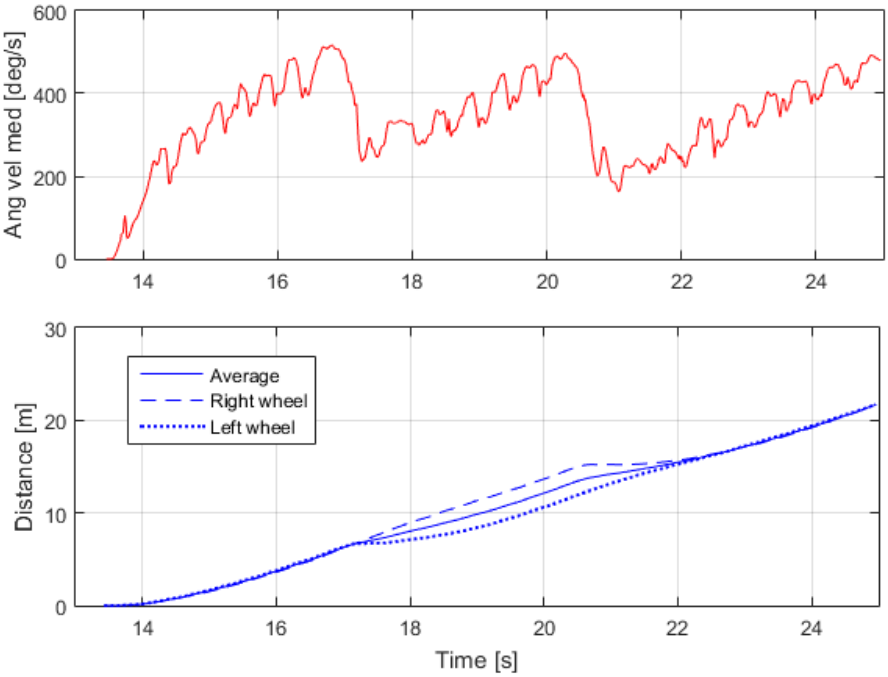

***Figure 59**. Ang vel med obtain by average of wheels angular velocities; distance covered by the MP (average) and by wheels.*

A last observation is that the difference between left and right angular velocities wheels, has a trend which corresponds to the system angular velocity trend (*Ang vel Z*), as shown in *figure 60*.

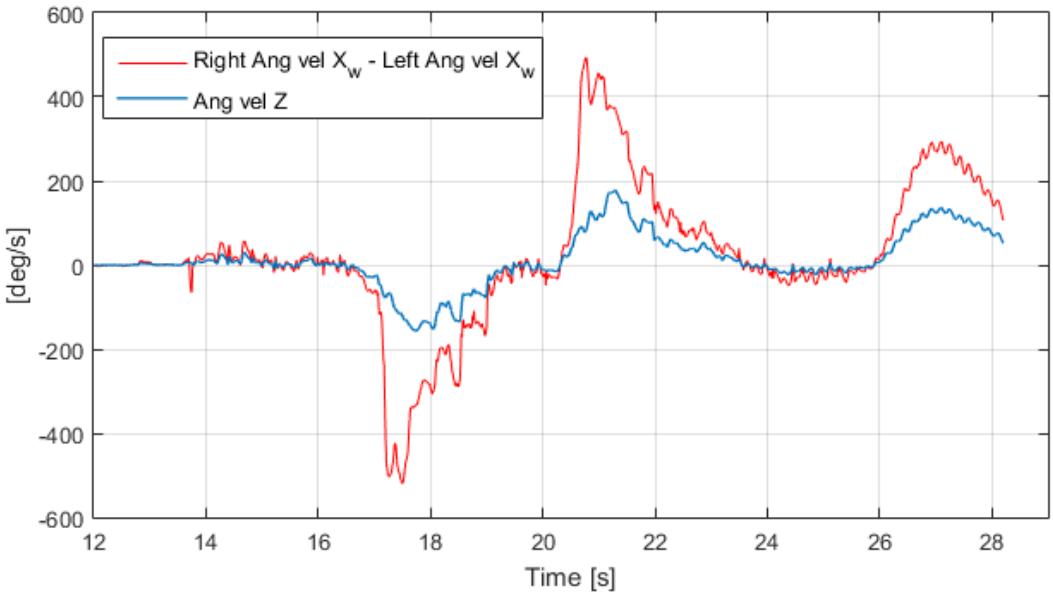

***Figure 60.** Red: difference between wheels angular velocities; blue: angular velocity from frame sensor.*

5.3.2.7 Data analysis of a match

Considering the data recorded during a match, the forward acceleration was evaluated with the following aims:

- individuating the maximum acceleration value;
- determining the distribution of pushes within the match, after considering a threshold based on increasing percentage of the maximum acceleration value.

Differently from the dynamic tests, performed in controlled conditions, match is a very complex situation: the forward acceleration signal itself, presents a high complexity and it is difficult to evaluate it without a video comparison.

Before describing the data analysis, some considerations must be done in this case. During a match, strikes are very frequent: they are recorded as very high positive and/or negative peaks. In recording a match with the Xsens, the sample frequency of the MTw™ is 50 Hz because of the contemporary connection of 8 sensors. This frequency is very low to catch a strike, that is a phenomenon occurring at high frequencies (more than 10000 Hz). For this reason, in the evaluation of the forward acceleration signal, peaks far from the typical range of acceleration are hits that cannot be considered because of the low sample frequency, and must be eliminated.

Even if the sample frequency is too low to catch an impulse, the phenomenon is recorded as fast and high variations of forward acceleration. The calculation of the power spectrum could individuate which are, in that signal, the frequencies of hits: nevertheless, there would be some problems. The spectrum does not locate these components in time, moreover, an eventual low pass filter with proper cut-off frequency, able to eliminate those components, would alter the whole signal eliminating parts that do not correspond to impulses: for example, it would lower the value of the maximum acceleration. Therefore, the first instrument chosen in this work to the elimination of hits is the first derivative.

The acquisition of each player signal was divided into first and second time of the match. The steps for the Matlab protocol for the signal analysis are described in the following lines:

- First discrete derivative of forward acceleration. The function used in Matlab environment was *diff*, which, given a vector of data, calculates the difference between two adjacent values: the division of this new vector by the sampling time, gives the first discrete derivative.
- Elimination of impulse peaks. This was performed in two steps:
    - Threshold on the derivative. A proper threshold on the derivative allows

eliminating all values that overpass it. Considered the sampling time as 0.02 s, the threshold value was: *18/sampling_time= 900 m/s^3* (*figure 61*).

- Elimination of outliers values. Even if many values were eliminated by the previous step, others might still do not agree with the normal acceleration trend. The reference is, for each player, the max acceleration value recorded during the dynamic tests (*Acc_max_DIN*): values that are more than *1.5*Acc_max_DIN*, were considered as not reliable, and eliminated.

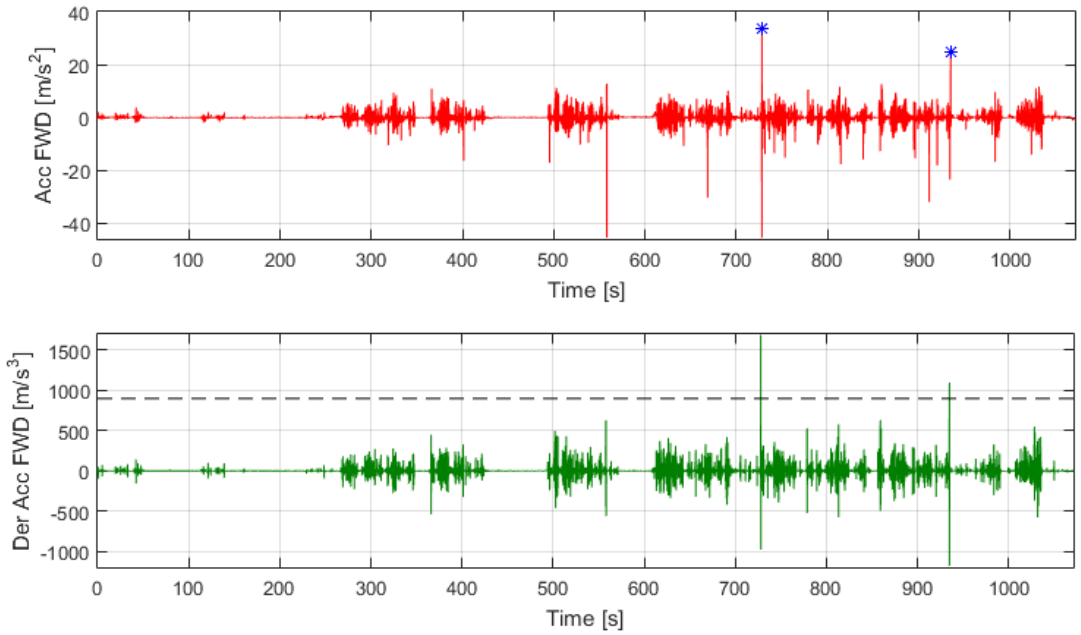

Figure 61. *First time of a match: forward acceleration (Acc FWD) and its derivative (Der Acc FWD). Dashed line on the second graph: threshold on the derivative; markers on the first graph: strikes values.*

- Individuation of the maximum value. The maximum forward acceleration of the signal was extracted (*Acc_max*), and its multiplication for the player's body weight, gave the maximum forward force (*FWD Force_max*).
- Individuation of peaks of pushes. Each push has the characteristic trend described in the previous paragraphs, and can be associated to its maximum positive peak value. Moreover, it was noticed that the peak of push presents a higher value of derivative with respect to the other samples of the same push: therefore, considering the first derivative of the whole signal, a proper threshold on it (between 100 and 200 m/s^3) individuates the maximum positive peaks of the pushes. This also allows counting the number of pushes. Nevertheless, this method committed errors since some peaks are not recognized, but for this analysis the approximation is considered good.
- Pushes distribution. A first histogram divides the pushes into intervals of values: each bar contains the number of pushes with the peak values in a specific range. The intervals

are *0.20-0.25*Acc_max, 0.25-0.30*Acc_max* and so on: moving of 5%, 16 intervals of values were extracted (*figure 62*).

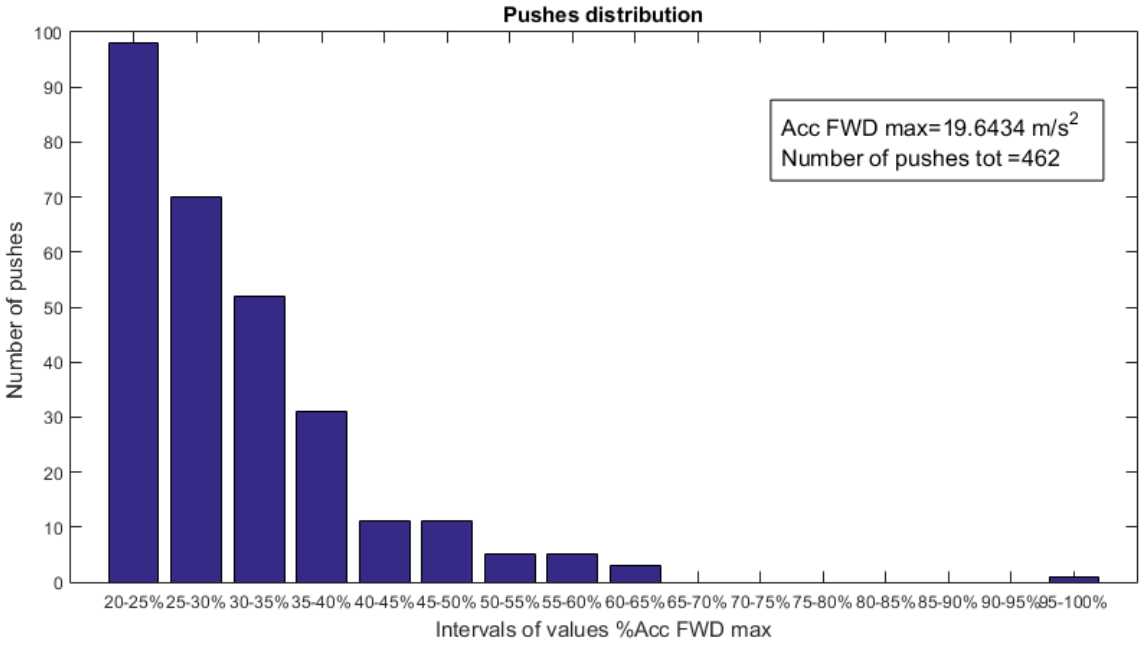

Figure 62. *Pushes distribution in the first time of the match (T.N.).*

- Cumulative pushes distribution. A second histogram contains, for each bar, the number of pushes that overcome the threshold of 20% of *Acc_max*, 25% of *Acc_max* and so on, and then related to the force values. This allows also tracking a descending curve, obtained with a polynomial interpolation (*figure 63*).

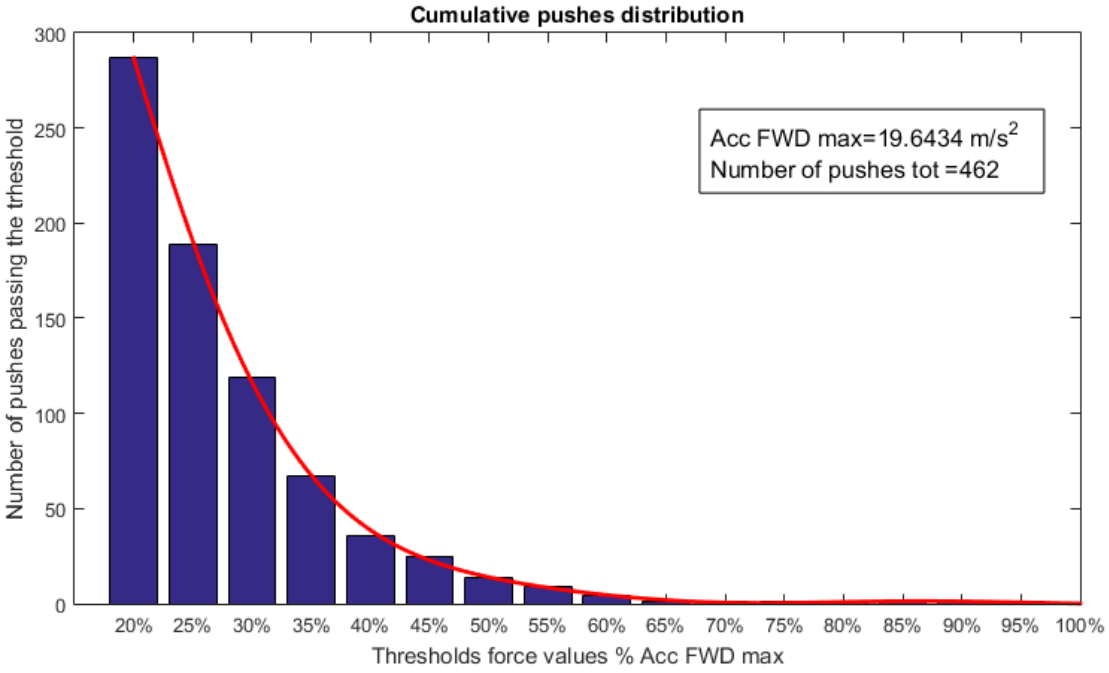

Figure 63. *Cumulative pushes distribution in the first time of the match (T.N.).*

5.4 Results

The present paragraph describes the results about the dynamic test: push shape and frequency, and the data coming from the Matlab analysis.

5.4.1 Push shape

Data analysis of forward acceleration trend revealed that each player has his personal pushing style. One push is defined from the lower negative point of the previous push to the lower negative point after the final descending trend. With a first approximation, a push of acceleration can be described as an initial growing trend and a consecutive decreasing trend. Nevertheless, this description is not complete, since in this work, the forward acceleration signal of the majority of players present a more complex trend.

Figure 64 represents the pushing trends found in the present analysis, during the middle part of a 20 m sprint (without considering initial and last pushes).

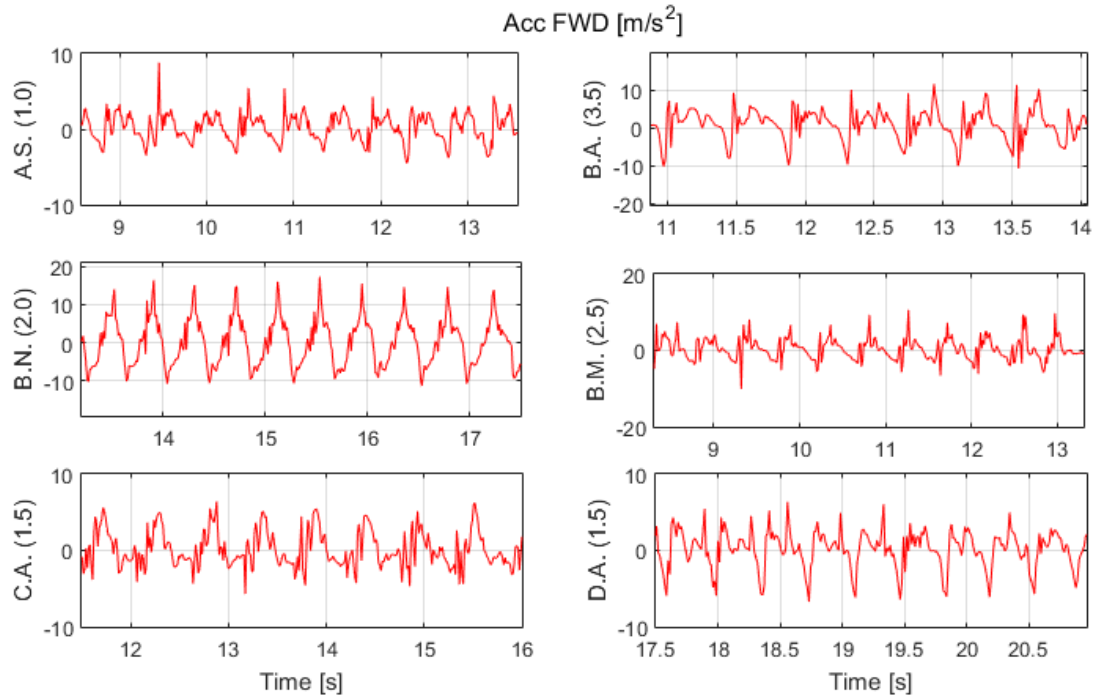

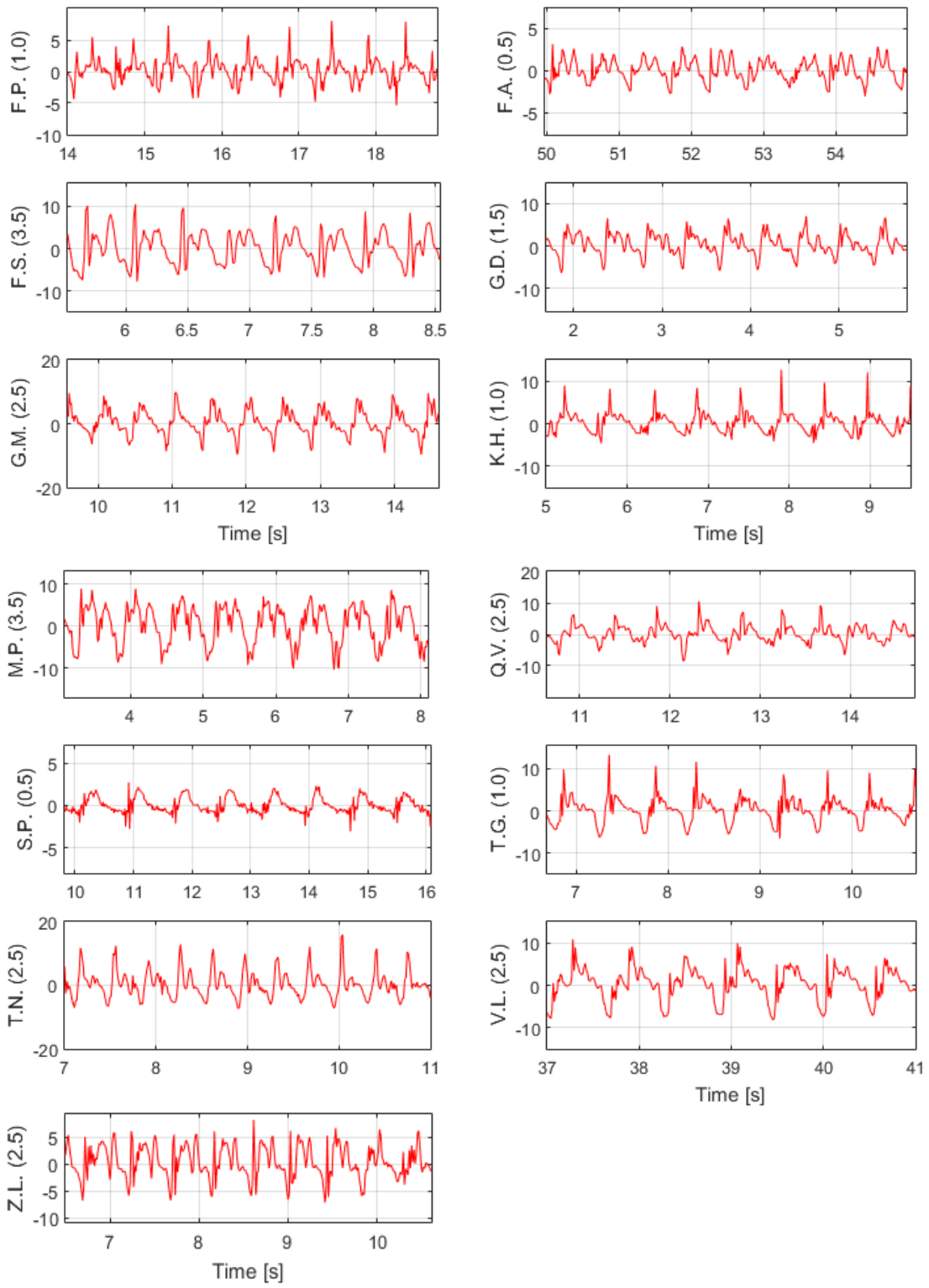

***Figure 64**. Comparison between forward acceleration trends in a 20 m sprint. For each player is represented the point of classification.*

Some players have a more regular push shape, for others shape is not very repeatable. B.N. and G.M. present a clear regular and unimodal push trend. Other situations (as C.A., Q.V.) are heterogeneous; others present a clear bimodal trend (B.A., M.P.).

In correlating this data with the point of classification, the results show that all 3.5 points (B.A., F.S., M.P.) present a very remarkable double positive peak, as two of the 2.5 points (T.N., Z.L.). Three of the 2.5 points (B.M., Q.V., V.L.) present an heterogeneous trend; the other 2.5 point (G.M.) shows an unimodal trend, like the only 2.0 point (B.N.). Between the 1.5 points, D.A. has a bimodal trend, G.Z an oscillating trend and C.A. has a very irregular push style (it may be owed to the fact that he did not use his own wheelchair during the test). The 1.0 points (K.H., T.G.) have comparable trends, with a very high and rapid initial peak within a trend with lower values. Between the 0.5 points, F.A. has many peaks for each push, with very low values, S.P. present a very regular trend, but different from the other shape found in this work.

In conclusion, higher points have a more common and bimodal trend, lower points present different situations. Surely, players with a high control of the trunk, use it as a force generator thus influencing their pushing techniques and acceleration trend.

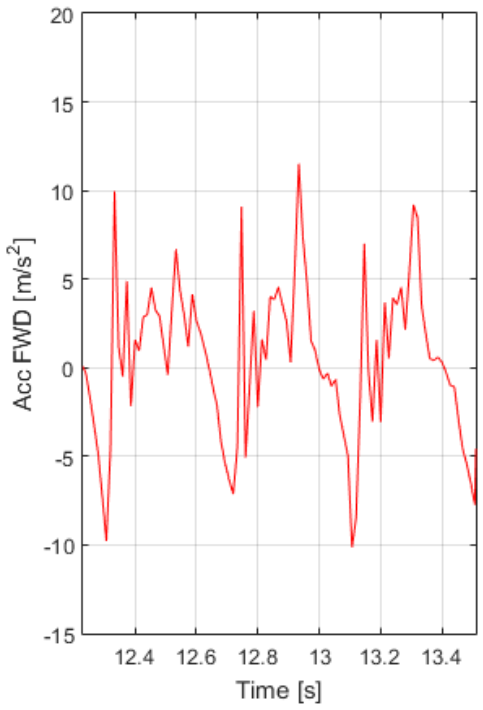

Figure 65. *Three consecutive pushes of forward acceleration in 20 m sprint (B.A.)*

As an example, *figure 65* represents three consecutive pushes during a 20 m sprint of B.A., a 3.5 point. One push is characterized by two positive and higher peaks, and a negative peak: considering the initial time as the lower value after the zero crossing, the push starts with a first rapid increasing and decreasing peak, and a second growing (and oscillating) trend which culminates in a second positive peak, which ends in the lower negative peak. A first explanation of the presence of two distinct positive peaks can be found in a preliminary video analysis: it is clear that arms movement, in particular shoulder flexion/extension, does not correspond to the trunk flexion/extension. In the case represented in figure, starting from the first contact of the hand with the handrim, the shoulder flexes to complete the push angle and at the same time, the trunk extends. Once reached the maximum trunk extension, the player starts extending his shoulder and at the same time, flexing his trunk to prepare to the next push. The increasing and decreasing peaks, can be associated to the fact that when arms are pushing, trunk is braking and when arms are braking in the recovery time, trunk is accelerating. In this work, pushes with only one positive peak are less frequent (2 players over 19). So probably this configuration is due to the full trunk control. Nevertheless, without a movement analysis, it is impossible to associate each acceleration sample to a body configuration: further analysis should be done, to assess in which part of the push the subject reaches the maximum peaks of forward acceleration.

In all cases, negative peak values are comparable to the positive peak ones. In making an average of the whole signal, the value is always positive and very close to zero. This means that the acceleration (force) generated by the player, is almost totally dispersed in the resistance forces, which tend to brake the system. The low total average value is the net part of acceleration which allows the propulsion. This still indicates the low mechanical efficiency of the movement.

5.4.2 Push frequency

In data analysis of 20 m sprints, the calculation of the power spectrum of forward acceleration allowed extracting the push frequency. The common shape is characterized by a first peak at very low frequencies, a second peak at a frequency between 1-3 Hz which is the push frequency, and other peaks. The shape of the spectrum itself, generally presents two different configurations, as shown in *figure 66.*

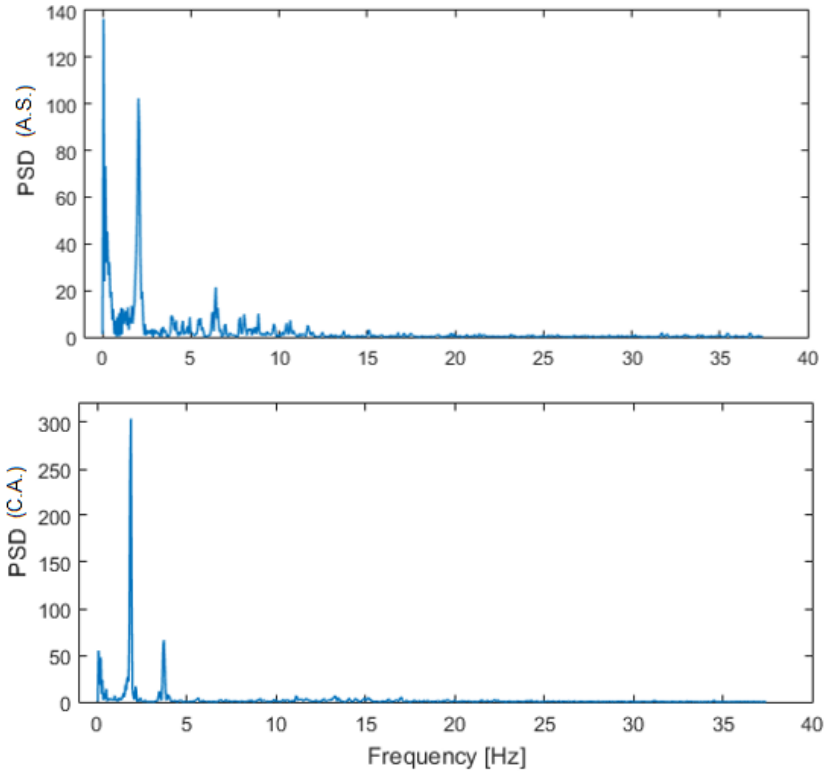

Figure 66. *PSD trends. Upper graph (A.S.) the push frequency occurs in the second highest peak; lower graph (C.A.) the push frequency relates to the highest peak.*

Spectrum of different players differ in their values, but this is not relevant since the important information in the present case, is the order of peaks of frequency. In some cases (5 over 19), the first peak has the highest value within the spectrum (*figure 66*, A.S.) but the most common situation is the second one (*figure 66,* C.A.), in which push frequency corresponds to the highest peak. This seems not to be related to the point of classification.

Player showing the first situation in all the three 20 m tests are: A.S., B.M., D.A., F.A., G.D: among them, there are no 3.5 points. F.P., F.S., Z.L. present this situation in only one of the three trials. All the other players present the second situation. Considering as example A.S., filtering its forward acceleration signal with an elliptic low pass filter with cutoff frequency at the most powerful energy frequency (0.0549 Hz), it shows an increasing trend reaching a maximum of 0.25 m/s^2. This value does not affect the measure, and could be related to an effective increasing of the acceleration or to an error of the sensor.

The push frequency of each single player was extracted as an average between the push frequencies of the three trials. *Table 8* contains the results. The push frequency locates between 1.18 and 2.67 Hz; with an average of 2.079 Hz (SD ±0.360). There is no correlation between the push frequency and the point of classification, as shown in *figure 67*. Apart from 1.0 points who exhibit a very close value, the other points do not present a homogeneous value, and frequencies are comparable between all points.

INITIALS	CLASSIFICATION POINT	PUSH FREQUENCY [Hz]	SD
A.S.	1.0	2,001	0,111
B.A.	3.5	2,537	0,057
B.N.	2.0	2,217	0,253
B.M.	2.5	2,158	0,011
C.A.	1.5	1,709	0,146
D.A.	1.5	2,591	0,097
F.P.	1.0	1,899	0,141
F.A.	0.5	1,907	0,051
F.S.	3.5	2,302	0,368
G.D.	1.5	2,291	0,008
G.M.	2.5	2,046	0,034
K.H.	1.0	1,919	0,072
M.P.	3.5	1,685	0,031
Q.V.	2.5	2,309	0,047
S.P.	0.5	1,178	0,094
T.G.	1.0	2,040	0,084
T.N.	2.5	2,672	0,098
V.L.	2.5	1,768	0,179
Z.L.	2.5	2,273	0,070

Table 8. *Push frequencies (mean and SD) of each player, with their classification points.*

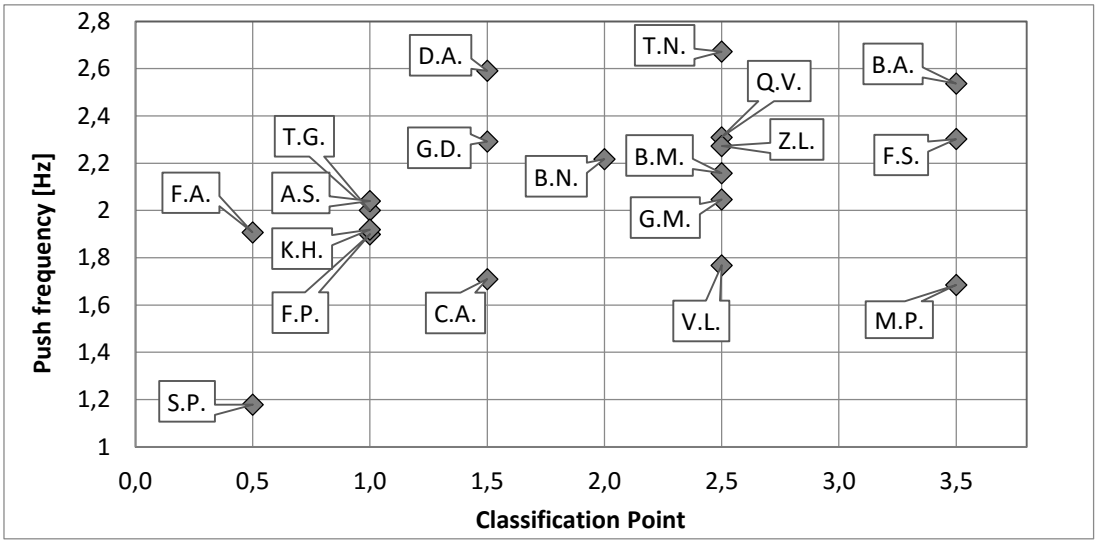

Figure 67. Push frequency in relation to classification point.

5.4.3 Dynamic tests

Dynamic tests with inertial sensors are described by parameters of forward acceleration and angular velocity. In particular, 20 m sprint and eight track give values of max and mean acceleration: these values, multiplied by the body weight of the athlete, give the expression of a force. In the data analysis and the comparison between different athlete's performance, it is important to rely to this value of force instead of the acceleration values. In fact in a dynamic test the acceleration trend depends, besides that, on the mass of the athlete-wheelchair system. For example, if athlete A transmits to his wheelchair a certain value of mean acceleration, which is the same value transmitted by athlete B having a half of his body weight, A is impressing a double force on his system with respect to the B, and this fact has to be taken into account in the comparison between them.

There are many parameters influencing the acceleration trends: mass of the system, inertial forces, friction (wheels-floor, with the air, in the axles), wheelchair structure, physical parameters and properties of the person and many others. Each value of force gives an expression of the force an athlete has to use to overcome the resistance given by all these factors.

For each test, force values were put in a descending order, giving for each athlete in the specific exercise, the rank. In the following graphs (*figures 68,69,70,71*) the force results for the force values in 20 m sprint and eight track are represented.

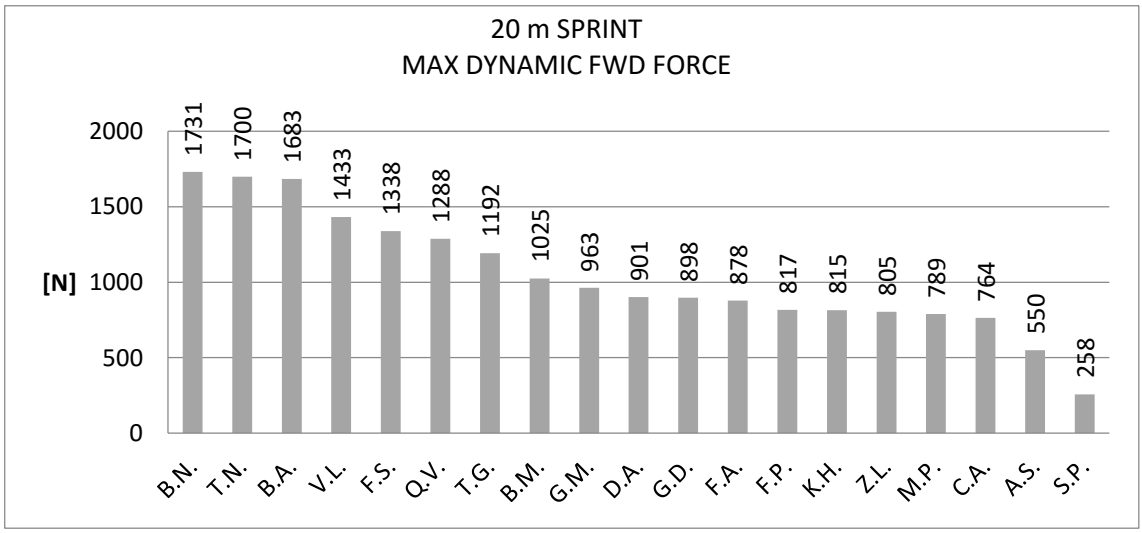

Figure 68. *Max dynamic forward force in 20 m sprint.*

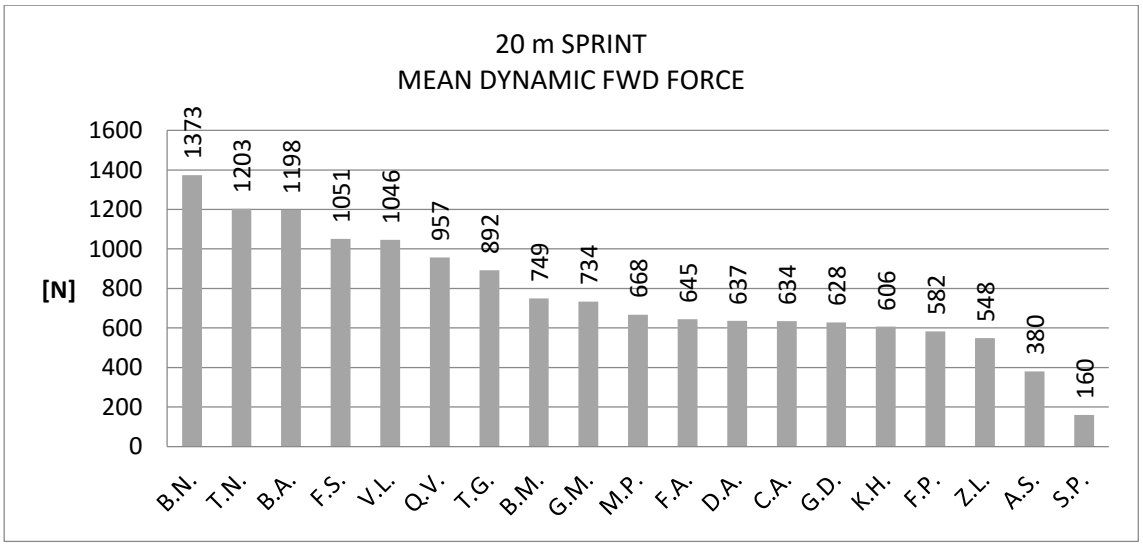

***Figure 69**. Mean dynamic forward force in 20 m sprint.*

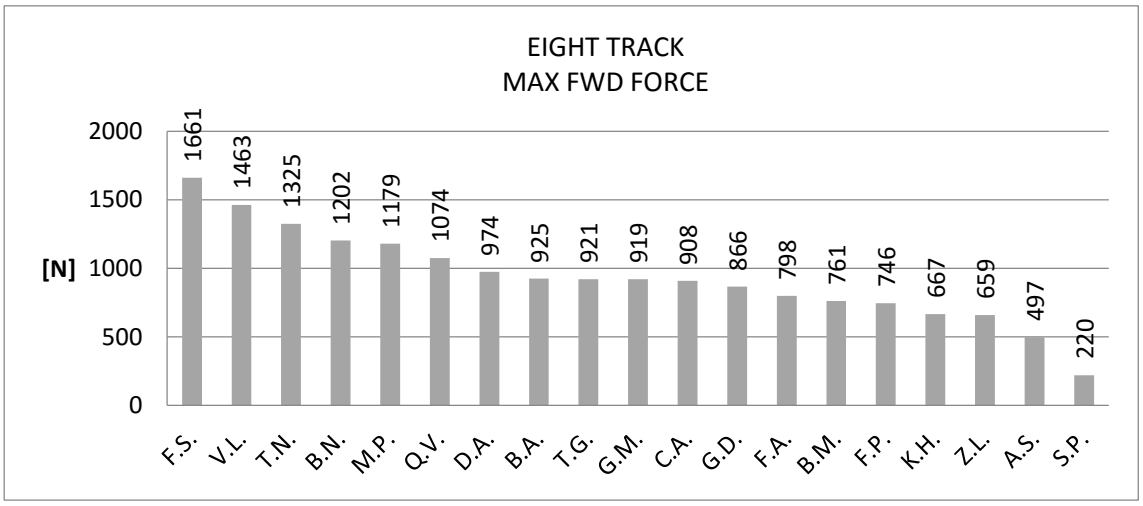

***Figure 70.** Max forward force in eight track.*

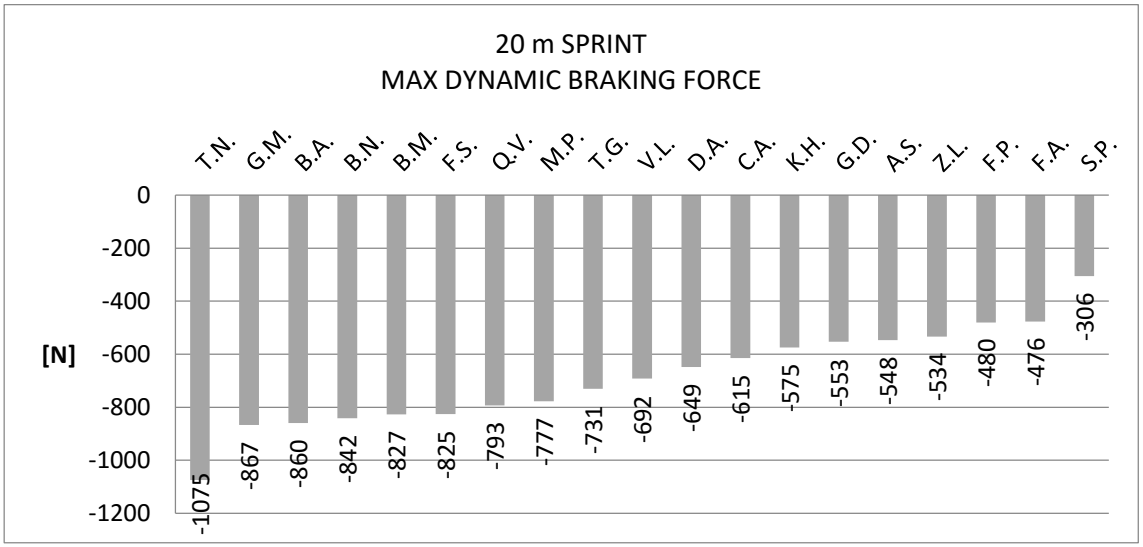

***Figure 71.** Max braking forward force in 20 m sprint.*

The maximum and mean dynamic forward force rankings generally agree. Two of the 3.5 points (B.A., F.S.) are in both cases among the first five places; the exception is M.P. that situates at the 16th place in the max force, and in the 10th place in the mean force. The reason can be found in the comparison between the isometric force, in the next paragraph. The braking force ranking agrees with the forward force ones.

The results for the rotation and eight track are represented in the following graphs (*figures 72, 73*).

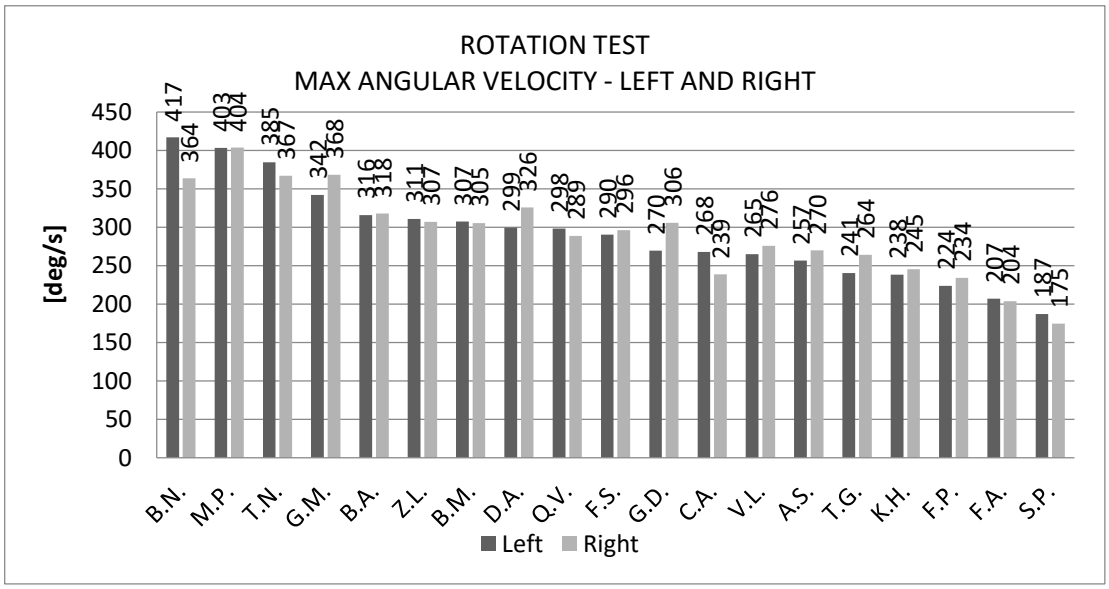

Figure 72. *Angular velocity values in the rotation test, sorted by the left side.*

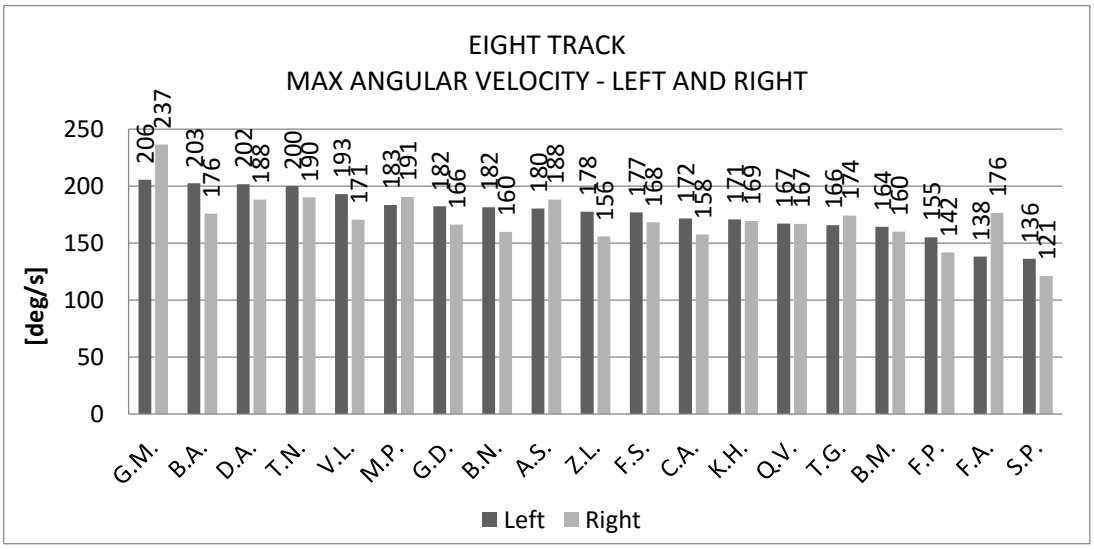

Figure 73. *Angular velocity values in eight track, sorted by the left side.*

The angular velocity force values for the rotation are, in average, 80% higher than eight track values: this was expected, since the rotation took place around the Z axis of the wheelchair-player system on place, while in the eight track the player had to turn around a

fixed point, external to his system and coming from a forward acceleration phase. The situation was different also because, in the rotation test, the subject had to equally use his arms, in different directions, to execute the movement while in the eight track, turning around a cone, while an arm is pushing the opposite is braking. In general, players do not present high differences between the left and right side performance.

The following graphs (*figures 74, 75, 76*) show the push frequency ranking in a 20 m sprint and time rankings in 20 m and eight track.

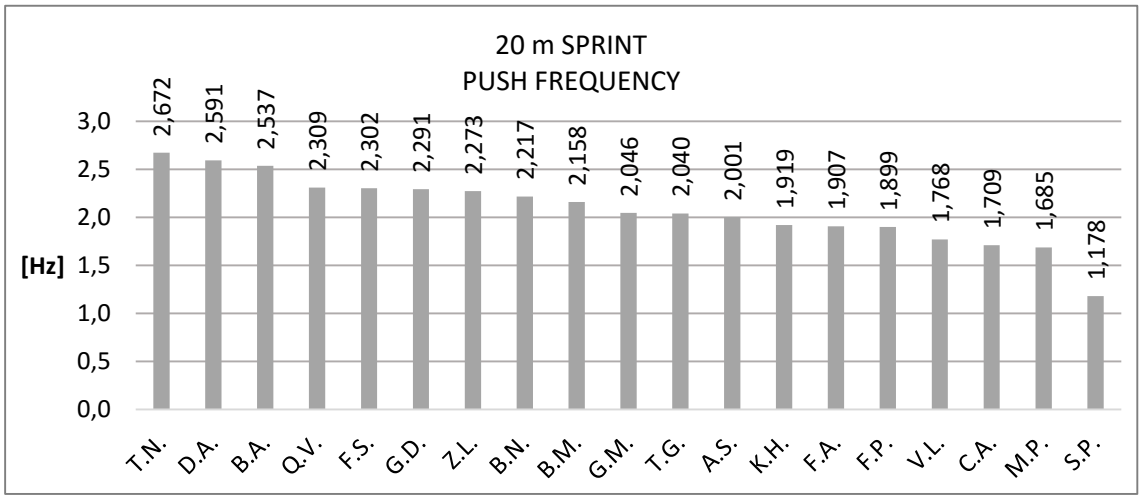

Figure 74. *Push frequency in 20 m sprint.*

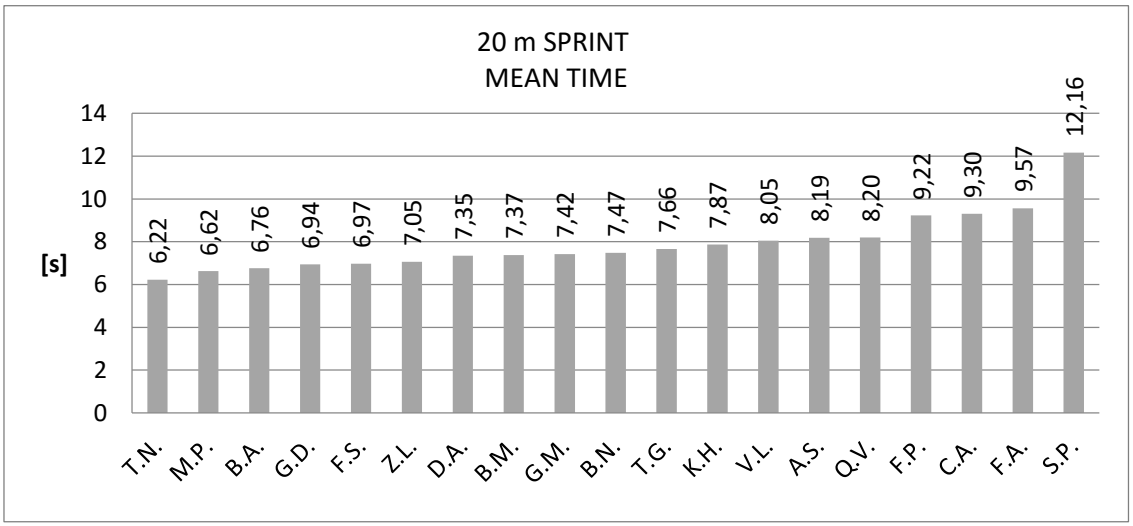

Figure 75. *Mean time in 20 m sprint.*

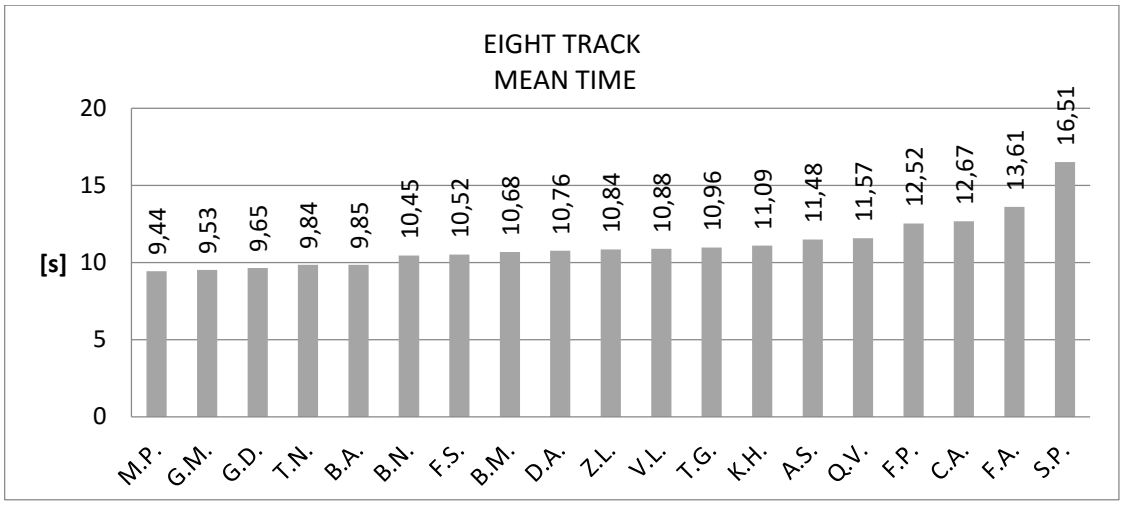

Figure 76*. Mean time in eight track.*

Time rankings of 20 m sprint do not completely correspond to the ranking of the mean forward force. For example, M.P. has a low position in the force ranking, but he is at the second place in time; G.D. and Z.L. present similar situations. This could mean that their movement are very efficient since with low forces they can reach low times: this could also mean that with the application of a higher force, they could even reduce their time. On the contrary, B.N. exerts the highest dynamic forward force, but places in the middle of the time ranking: this could mean that his movement is inefficient since his high force dissipates fast. In fact, his push frequency places in the middle of the ranking. The comparison with the isometric force is needed.

It is worth to notice that players that were in the last part of the ranking for the 20 m force values like M.P. and Z.L., position in the first places in the angular velocity results: this means that a player cannot be evaluated from only one performance, but the whole athletic actions must be taken into account. These results also underline which are the points of force of the team: some people can express a higher acceleration and thus be strong in a sprint to the goal line, others can express a higher angular velocity thus being able for example, to move on the court avoiding the opponents' blocks.

There are some differences in the maximum forward force expressed during a 20 m sprint and in an eight track, as shown in *figure 77*. Most of people locates in the bisector line; some (M.P., F.S.) express a higher force during the 20 m sprint, others (B.A., B.N.,T.N., T.G, Q.V., B.M.) express more than 20% of force in the eight track. This could be explained with the fact that an eight track is more similar to a game situation respect to a sprint, and maybe the motivation is higher.

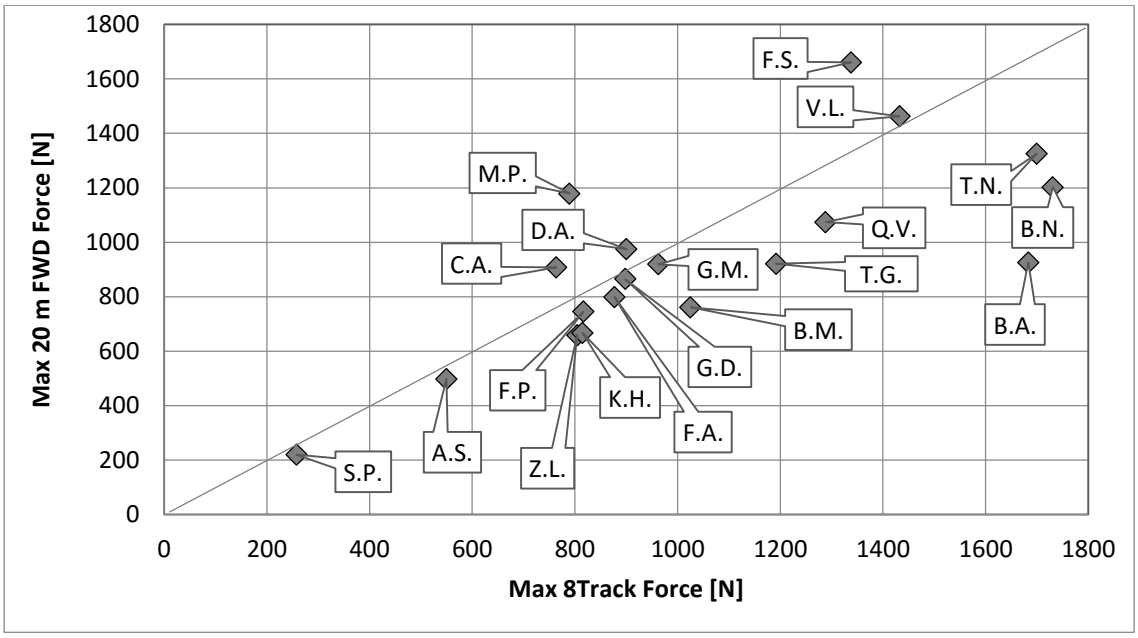

Figure 77. *Max eight track force vs max 20 m forward force. The grey line represents the bisector.*

The following graph (*figure 78*) shows the relation between the point of classification of each player and his mean FWD force in the 20 m sprint. The tendency line, obtained with a three order polynomial fit, reveals that there is a correlation between the point and the explicated force: the 3.5 points express double force respect to the 0.5 points. Nevertheless, some situations must be noticed: the 3.5 points express, on average, the same force of the 2 and 2.5 points (a linear regression, as done for the isometric push forward force, was avoided since it could not show this fact). Assuming that the increment between points should be linear, this means that the aim is to increase the pendency of the last part of the curve, by improving the performance of the higher points.

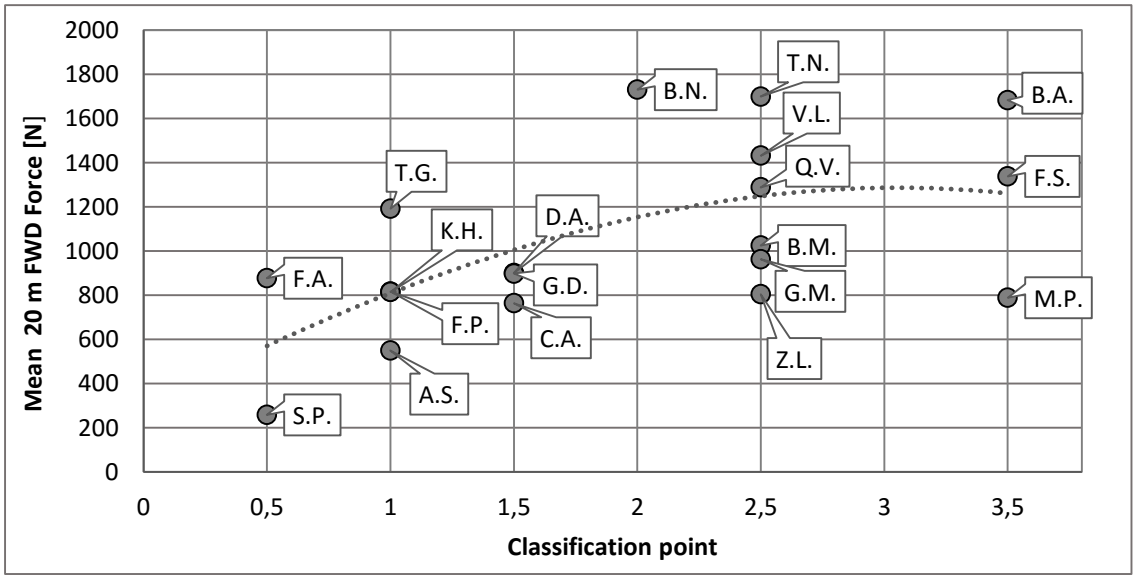

Figure 78. *Point of classification vs mean FWD force in a 20 m sprint. Dashed line: tendency line.*

5.4.4 Dynamic Vs isometric force values

In comparing the results found for the dynamic tests with the isometric tests, it is worth making some considerations. The graph in *figure 79* represents the isometric push forward force vs the mean 20 m forward force. The tendency line reveals that the mean dynamic force is 2.21 times higher than the isometric push force.

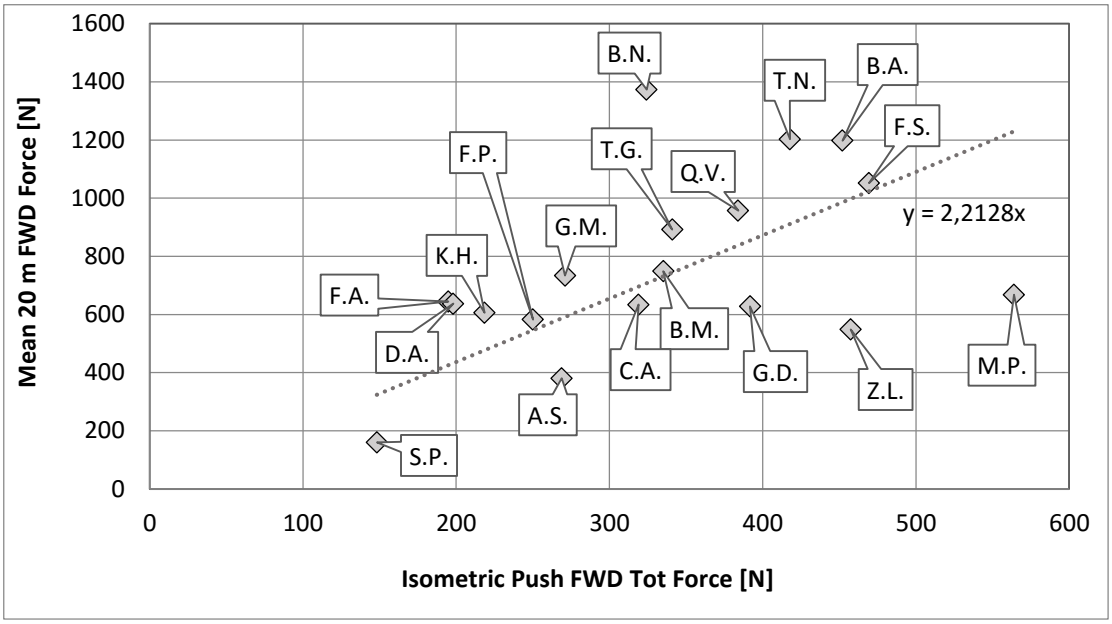

Figure 79. *Isometric push forward force vs mean forward force in 20 m sprint.*

Most of players are close to the regression line, but in some cases the difference between dynamic and isometric values is important. Subjects that collocate under the line exert more force in isometric contraction, subjects above the line are more skilled in dynamic conditions. People as M.P. and Z.L. potentially have the higher isometric force values, but they do not express them in dynamic conditions: this can be related to an inefficient pushing technique, or to a wrong wheelchair setting. Their training should be focused on the improvement of performance in dynamic conditions, and eventually in a revision of their wheelchair dimensions. People as B.N. on the contrary, present a high dynamic force and their work seems to be more efficient. This could mean that increasing the isometric force with focused force training, their dynamic performance could further improve.

The reason why dynamic values are more than double respect to the isometric force values might be explained with the fact that in the dynamic test, many inertial factors influence the performance: these do not occur in the isometric test. The player starts from a still position and after some pushes, he reaches a regime trend. The mean forward force was calculated by considering the higher peak of acceleration for each push, and making an average of them. Nevertheless, these peaks does not correspond to a situation in which the subject starts from a static position as it is for the dynamic test: he comes from a positive

acceleration that gives him inertial force. For this reason, the situation within a dynamic sprint which is more similar to the isometric test condition, is the beginning of the exercise, when the player exerts the first push. The peak of the first push is actually lower than the following since it is not affected by inertial factors (*figure 80*).

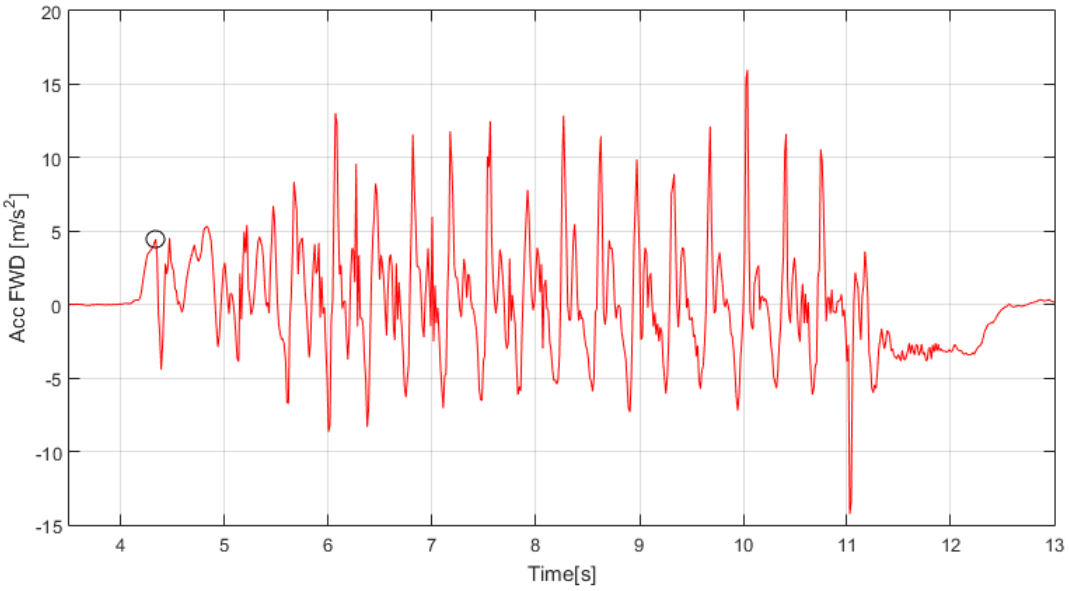

Figure 80. *Forward acceleration in a 20 m sprint (T.N.); black circle: first positive peak.*

Table 9 shows the comparison between the first peak of force in dynamic situations, the mean peaks value and the isometric force value. The force in the first peak was obtained through an average between the first positive peak values of the three trials of the 20 m sprint forward acceleration (multiplied for the body weight), for each player. *Figure 81* represents the linear regression of the isometric force values vs first peak of force, and of isometric force values vs mean dynamic force.

INITIALS	20 m SPRINT FIRST PEAK FORCE [N]	ISO PUSH FWD FORCE TOT [N]	20 m SPRINT MEAN FWD FORCE [N]
A.S.	234,59	268,95	380,29
B.A.	565,81	452,00	1197,97
B.N.	441,80	324,30	1372,90
B.M.	254,06	335,20	748,89
C.A.	255,43	318,90	633,90
D.A.	262,15	198,10	636,83
F.P.	243,04	250,00	582,44
F.A.	284,40	195,00	644,88
F.S.	290,50	469,30	1051,46
G.D.	336,91	391,80	627,94
G.M.	295,11	271,10	734,08
K.H.	226,10	218,60	606,26
M.P.	421,16	563,83	667,58
Q.V.	396,69	384,03	957,01
S.P.	85,97	148,30	159,95
T.G.	309,06	341,07	892,39
T.N.	386,71	417,83	1203,17
V.L.	374,47	83,77	1046,06
Z.L.	313,17	457,47	548,38

Table 9. *Force values from the first push in 20 m; isometric push forward force; mean dynamic forward force.*

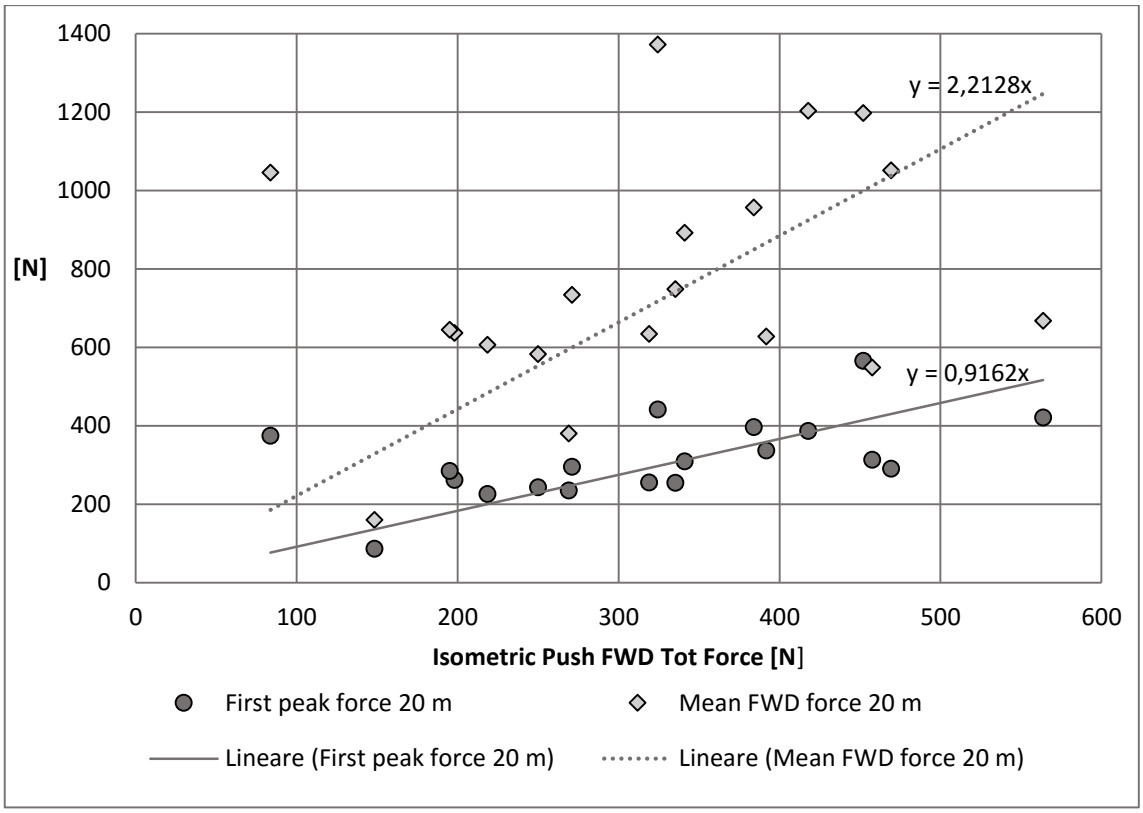

***Figure 81**. Isometric push forward force VS mean 20 m forward force (light grey symbols, dashed line); Isometric push forward force VS first push force (grey circles, solid line).*

The first positive acceleration values found in the 20 m sprint are comparable to the isometric force, more than the mean force values: the linear regression shows a high correspondence (92%) between the two trends. Some differences occur, since the first push of the 20 m sprint does not come from an isometric contraction, the friction of the floor is lower than the one received during the isometric test, the position of arm and trunk are different. In conclusion, this result give an additional confirm that the high difference between isometric and dynamic values is owed to inertial factors.

5.4.5 Match

The results coming from the match analysis are limited to eight athletes playing the first and the second time, and represented in *figure 82*. The first observation is that the maximum forward acceleration values were higher than the values found in the dynamic tests: this was expected, since the match creates different game situations and adds the motivation. Another observation is that each player has his different distribution of peaks.

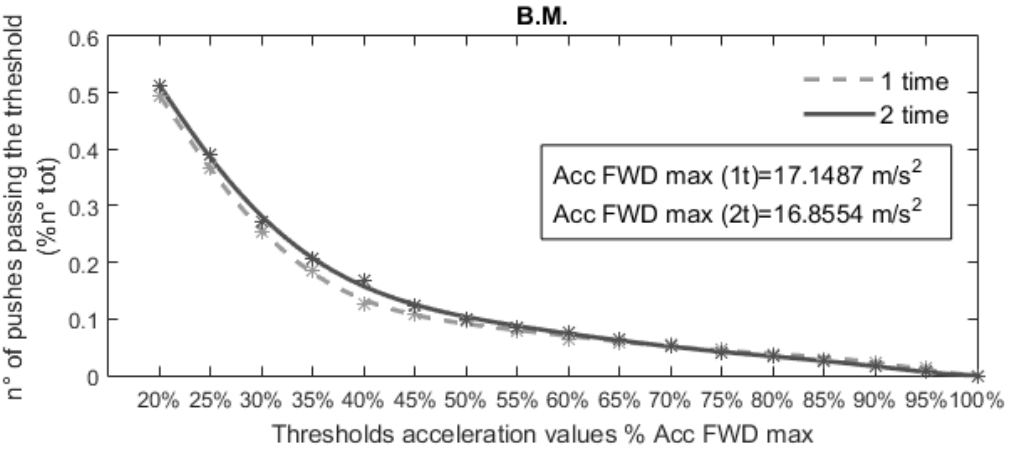
B.M.
n° of pushes passing the trheshold (%n° tot)
1 time
2 time
Acc FWD max (1t)=17.1487 m/s2
Acc FWD max (2t)=16.8554 m/s2
Thresholds acceleration values % Acc FWD max

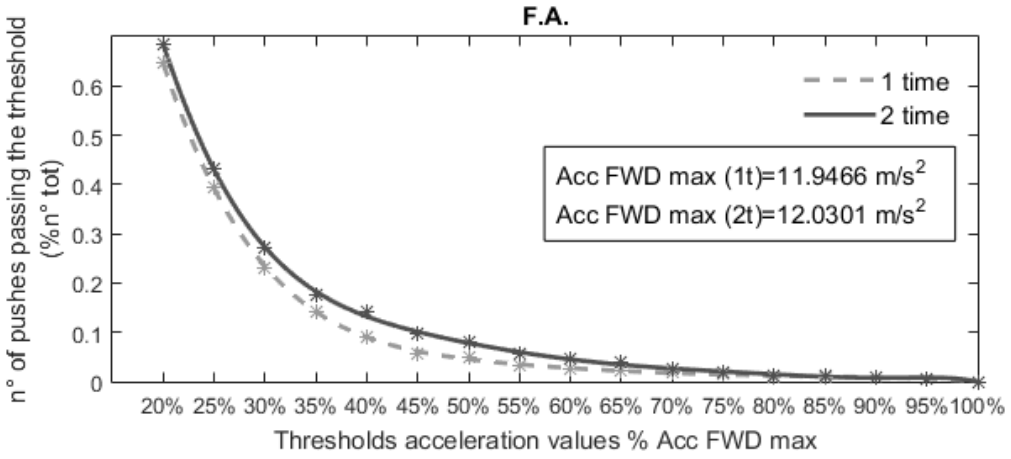
F.A.
n° of pushes passing the trheshold (%n° tot)
1 time
2 time
Acc FWD max (1t)=11.9466 m/s2
Acc FWD max (2t)=12.0301 m/s2
Thresholds acceleration values % Acc FWD max

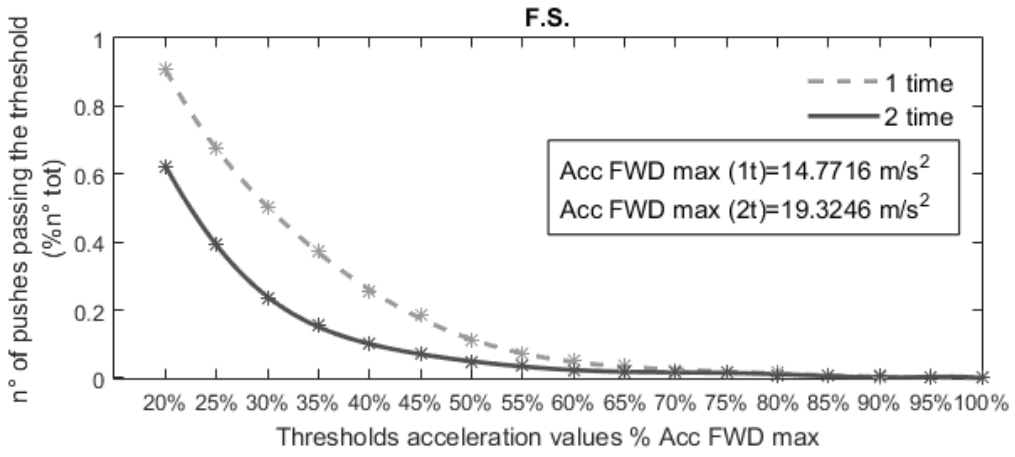
F.S.
n° of pushes passing the trheshold (%n° tot)
1 time
2 time
Acc FWD max (1t)=14.7716 m/s2
Acc FWD max (2t)=19.3246 m/s2
Thresholds acceleration values % Acc FWD max

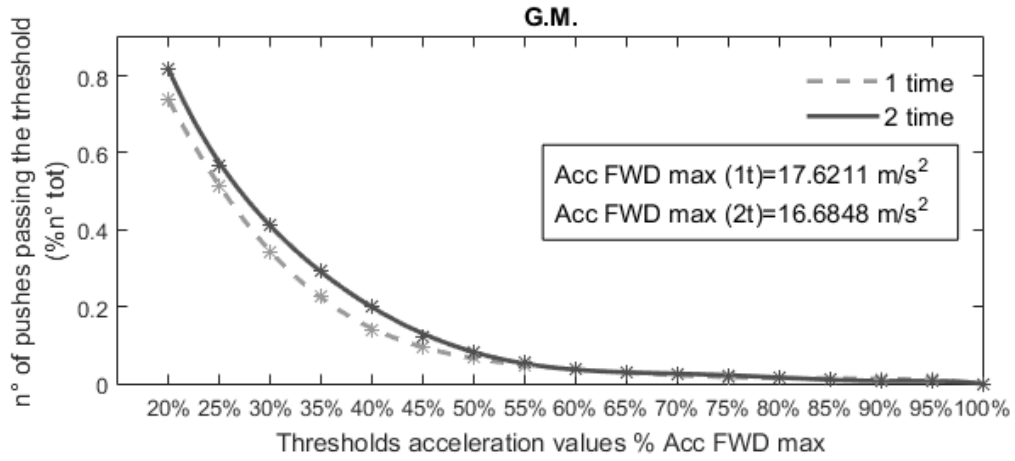
G.M.
n° of pushes passing the trheshold (%n° tot)
1 time
2 time
Acc FWD max (1t)=17.6211 m/s2
Acc FWD max (2t)=16.6848 m/s2
Thresholds acceleration values % Acc FWD max

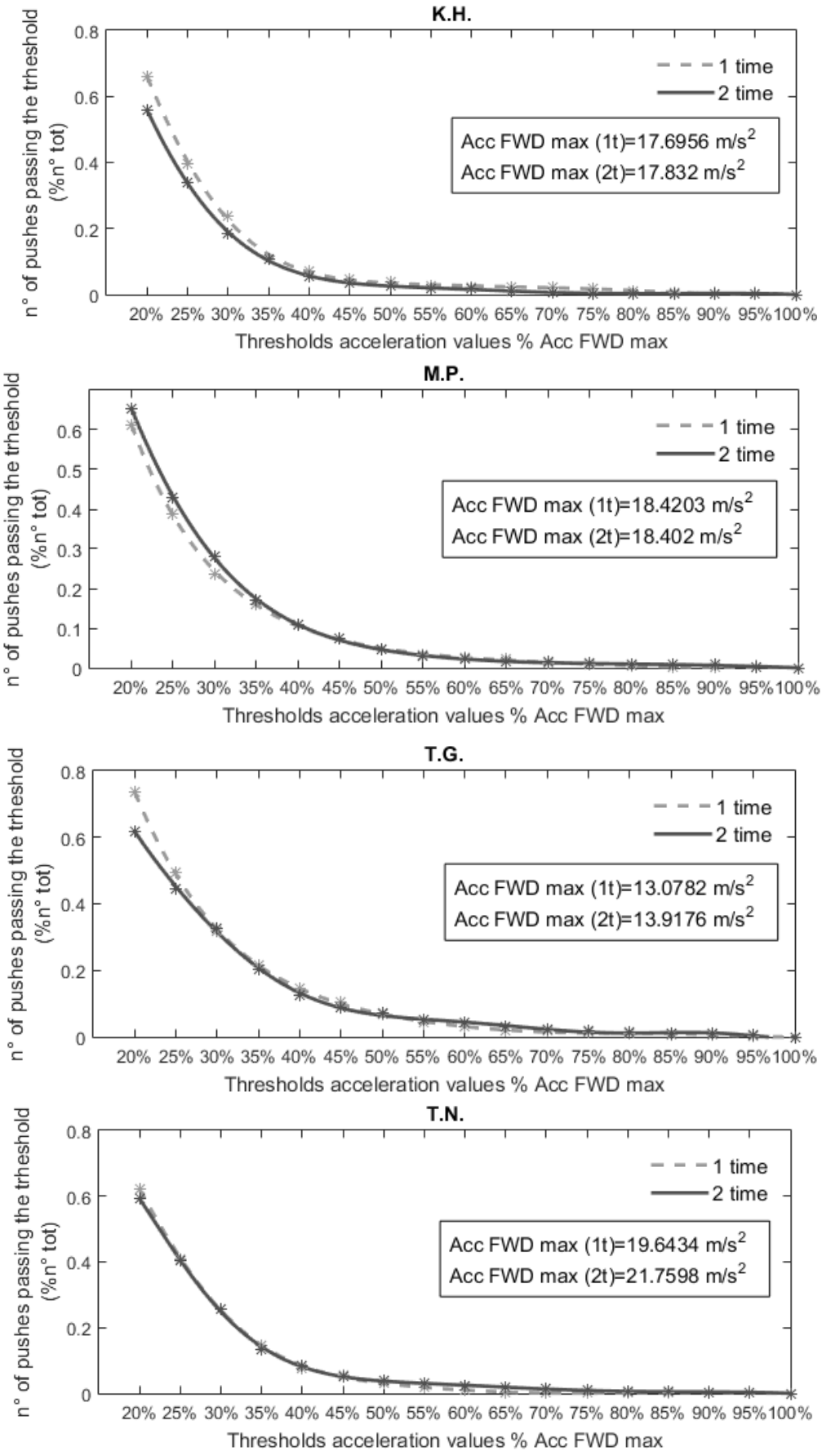

***Figure 82**. Cumulative distribution of the eight players of the match. The first time is the dashed line; second time is the solid line.*

The rapid decrease (high slope) of the initial part of the curve, observed in all cases, shows that players mostly work at very low acceleration: their pushes are on the majority lower than the maximum.
Another relevant factor is the percentage at the 20% threshold: values at the 0.8 (T.G., G.M.) indicate that the majority of pushes are more than 20% of the maximum acceleration. 0.6 or lower values, observable in most cases (B.M., M.P., K.H., T.N.) indicate that the 40% of pushes are at less than 20% of the max acceleration: this could mean that the player does not work at his best, and he should improve his court performance.

The difference between first and second time trends is generally low: curves are comparable, in particular for the higher values of acceleration (more than 50%). F.S. is the only case who reached very high values of acceleration in the first time (more than 0.9 of pushes were more than 20% of the max acceleration) and low values in the second (0.5): this might be imputable to a lack of physical resistance in the second time. Moreover, maximum acceleration values in the first and second time are comparable, apart for F.S. and T.N. who both present higher values in the second time.

A future development of these measures is the fixation of inertial sensors on wheel axles (as explained in the previous paragraphs) during a match, to determine the total distance covered by the wheels. Analysis of the covered distance made for eight tests gave results that are exportable in the analysis of an entire match, in which the path is unknown and the situations are more complex. It is important to acquire the signal coming from both wheels, since the obtained distance may have differences caused by the prevalence of rotations in left or right direction.

CHAPTER 6

Project activity 3: pressure tests

During trainings and matches, a player passes all his time seated on his sport chair: wrong ways of sitting, due to an incorrect physiological posture or to the pillow, can bring to posture problems which can also affect the performance. For this reason, the distribution of the pressure on the seat, in the different situations that can occur during a match, was investigated through the use of a pressure mat. With the same instrumentation, it was possible to evaluate the position of the Centre of Pressure (COP) on the seat plane: during a simulated set of pushes, the horizontal and vertical displacement of the COP were recorded.

Research question: What is the pressure distribution on the wheelchair seat in different static positions? What is the horizontal and vertical COP displacement while pushing?

6.1 Instrumentation

This paragraph describes the pressure mat and its placement on the wheelchairs seat for data acquisition.

6.1.1 mFlex pressure mat

The mFLEX system allows measuring the distribution of pressure in the seat of a wheelchair, and to evaluate the position of the COP. The system consists of:

- mFLEX Sensor mat: a pressure-sensing mat comprised of thin, flexible fabric piezo resistive pressure sensors and covered with polyurethane coated nylon (*figure 83*). The mat has a cable that attaches to 34-pin plug to the interface module. The sensing area is a 43x43 cm square, divided into 16x16 pressure sensors. The system was calibrated from 0 to 200 mmHg, but a proper instrumentation allows calibrating the mat at different pressures, depending on his use.

***Figure 83**. Mflex pressure mat*

- Interface module: the electronic communicator between the mat sensors and the computer. The interface module connects to the computer via USB cable, and it needs a constant charging, supplied with the system.

- Computer software to view, register and export file information gathered by the sensors. The software automatically saves the file of acquisitions with *.mfl* extension. On the output, the square of the mat is visualized on real time (*figure 84*); after a video recording, also the statistical data about the pressure distribution with their time plot are available.

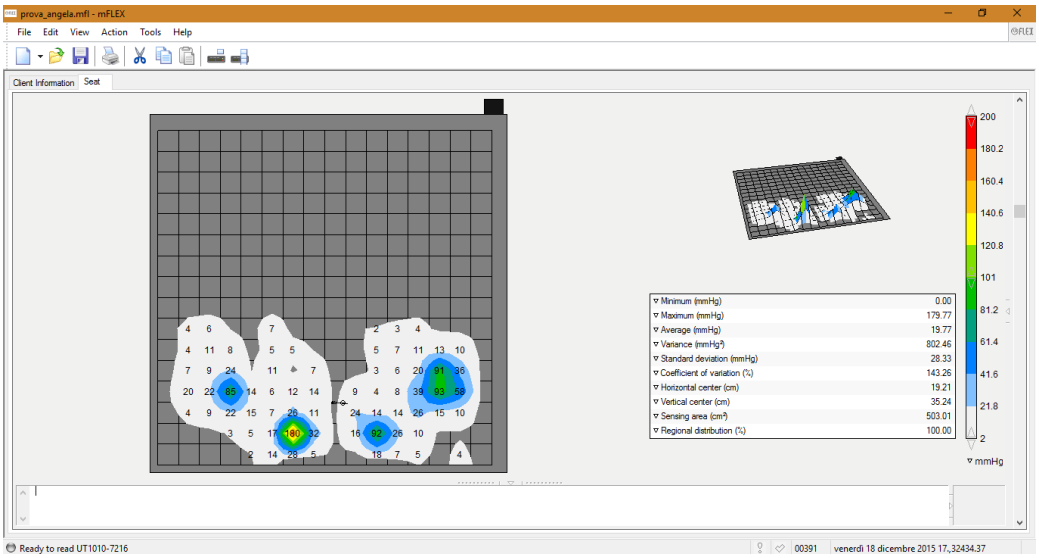

Figure 84. *mFlex software.*

6.1.2 Mat placement

The subject was asked, with some help, to move from his wheelchair, to easily place the mat in the correct way on his seat. The pillow was removed, to better position the mat on it minimizing folds, and rolling its extremities up the sides of the pillow. The mat's cable was kept on the front-right side, to avoid any impediment for the movement. The instrumentation (PC, interface module) was placed in front of the athlete, to have no obstacle with the cables, and to allow him seeing the output on the PC screen during the exercises. The subject was asked to prepare himself as if he had to play, with all the straps and gloves. Once the mat was positioned, a set of acquisition to track the edge of the pillow in the mat, was executed: this should avoid an incorrect interpretation of data for the presence of artefacts. Then, the subject could execute the whole set of exercises.

6.2 Methods

Pressure tests were executed for 14 of the 19 participants to the project, plus one extra player (P.S.) who made available for the test.

6.2.1 Tests description

Two kind of test were executed: a static test, to see the distribution of pressure in different positions, and a dynamic test to analyse the displacement of the centre of pressure (COP) during a simulated set of pushing.

6.2.1.1 Static tests

The subject was asked to execute a set of static movements. Starting from a normal sitting position, he had to move backward, forward, right and left, imaging during each situation, to have the need of picking up the ball from the floor (this was asked to avoid unnatural movements). Each position was maintained for 5 seconds, and between two different movements he always passed through the rest position, staying for 5 seconds:

1. normal rest position, with hands on wheels (5s)
2. forward position (5s) *(figure 84a)* + rest position (5s)
3. backward position (5s) *(figure 84b)* + rest position (5s)
4. left position (5s) *(figure 84c)* + rest position (5s)
5. right position (5s) *(figure 84d)* + rest position (5s).

The whole set was recorded as a video in the acquisition software.

a)

b)

c)

d)

***Figure 84**. Set of positions for the static test. a) Forward; b) backward; c) left; d) right.*

6.2.1.2 Dynamic tests

This kind of test simulated a real set of pushing. A wooden thickness with a plastic mat above it were placed under the rear castors to suspend them, allowing the wheels not to touch the ground. To create a friction for wheels, a resistance was simulated with two plastic mats, one for each wheel, placed in contact with the floor and the wheel. Starting from the normal rest position, the athlete was asked to execute a number of pushes, then to return to the rest position:

1. normal rest position (5s);
2. 10 pushes;
3. normal rest position (5s).

The whole set was recorded as a video by the software.

6.2.2 Data analysis

The data extracted from each static test were the graphical distribution of pressure on the seat, for the five assumed positions: normal, forward, backward, left and right. The video sampling frequency was 5 Hz, so each position was assumed, approximatively, for 25 samples. Excluding the first samples in which the subject came from the previous position and is not well positioned, a screenshot of the distribution when the position is graphically stable, was chosen.

For the dynamic tests, the position of the COP was evaluated. The software records, for each video sample, the horizontal and vertical position of the COP (in cm), considering the zero as the exit of the cable, which is always shown on the PC screen (*figure 85*). The lower

base of the output square always correspond to the seatback, the upper base correspond to the knees.

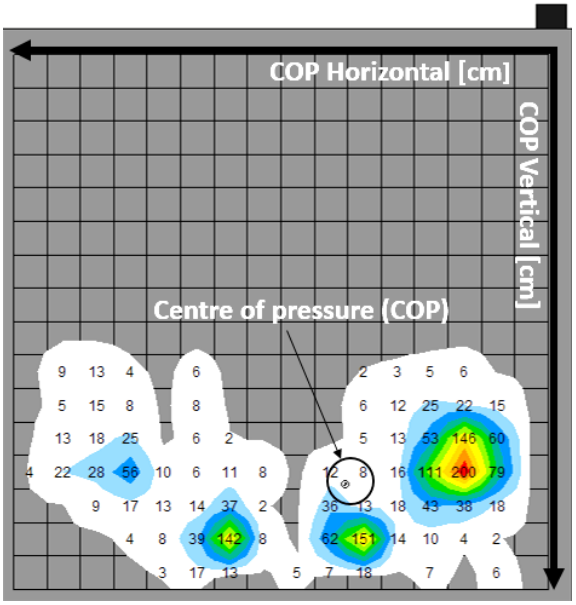

***Figure 85**. Mat pressure distribution, COP vertical and horizontal coordinates.*

For each dynamic test, the maximum vertical and horizontal displacement within the set of pushes was extracted by considering the time fit given by the output. For both the horizontal and vertical centre trend, the difference between maximum and minimum values within the pushes, was extracted.

6.3 Results

The results must be interpreted taking into account the protocol for the data collection: the graphical output pressure distribution, indeed, can be influenced by some artefacts (*figure 86*).

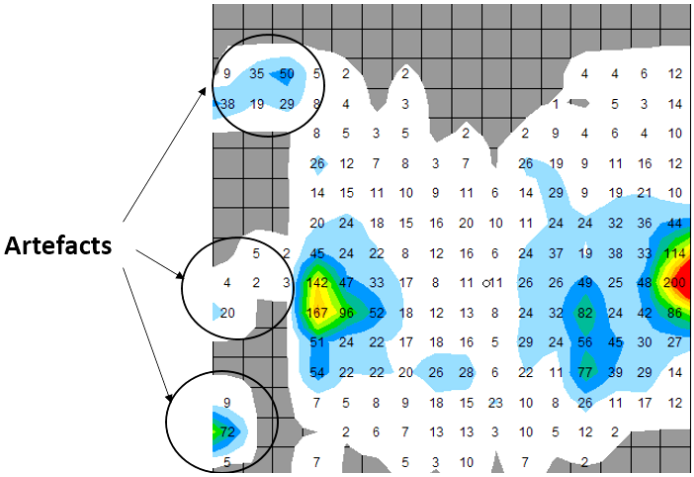

***Figure 86**. Artefacts in a graphical output.*

Therefore, the main problem within the mat placement was the presence of some folds of the mat: its adaptation to the pillow creates zones in which the pressure is positive. This happened because mat dimensions are higher than the dimensions of the common rugby wheelchair pillows, and obligates the mat itself to be rolled around the pillow. Other artefacts could be generate by straps that players use to fix them to the chair, which in some cases interfere with the mat, or to additional cushioning around or under the pillow, added to a more comfortable position.

Despite the presence of artefacts, static results highly differ among the tested subjects: this is owed to many factors. Firstly, in relation to the type of cushion (thickness, dimensions, material, overuse), the distribution and the peak of pressure vary. Then, physical structure of the person determines larger or narrower pressure distribution. Generally, the sensor corresponding to ischial tuberosities show higher values of pressure. For some subjects this values are low (40 mmHg), for others they reach the saturation (200 mmHg). With the left and right movements, the corresponding values increase. An example is shown in *figure 87*.

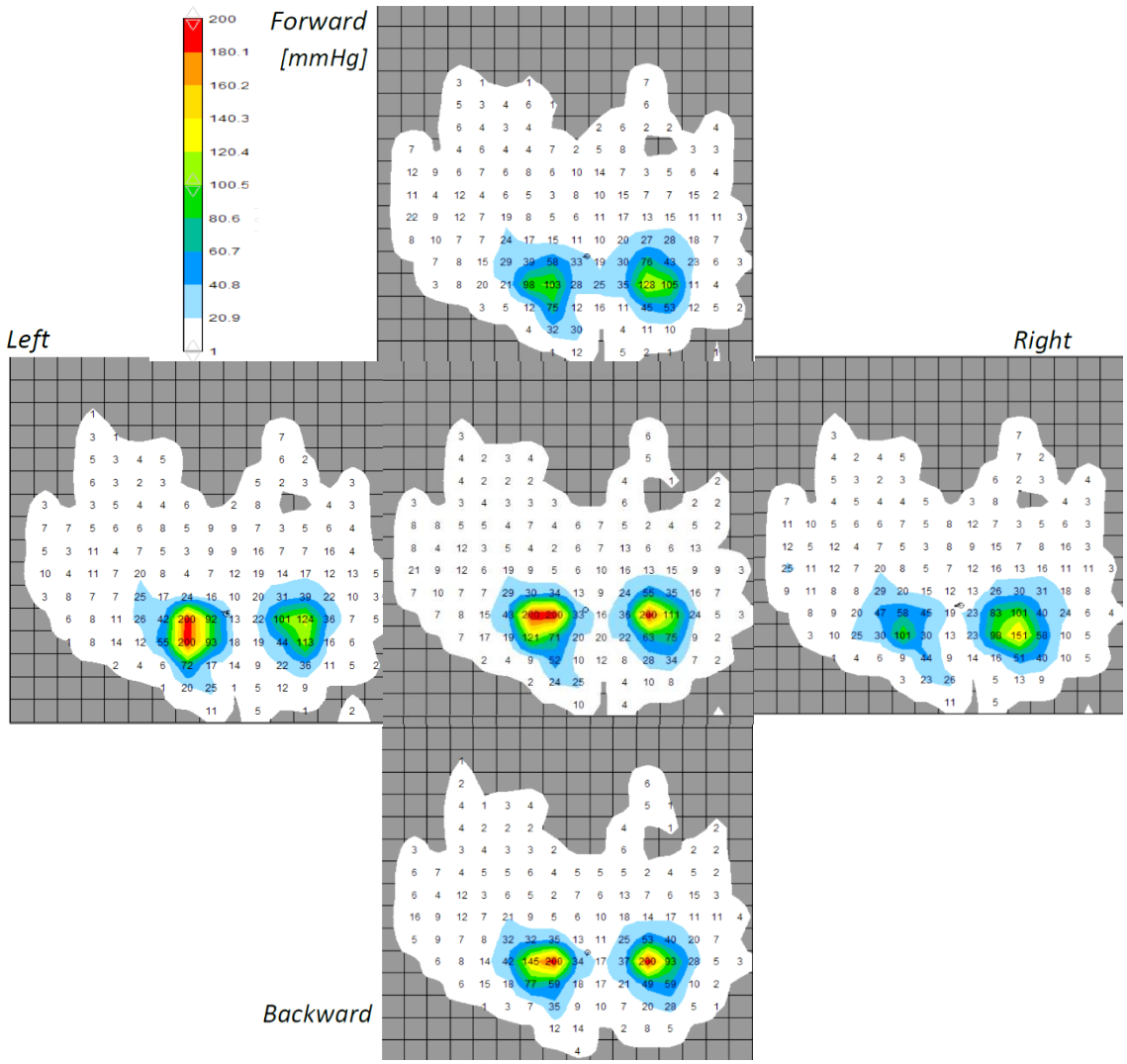

Figure 87. *Pressure distribution in static test (F.A.); centre: rest position.*

It is possible to notice that rest pressure distribution is symmetrical, but shows saturation values in correspondence to ischial tuberosities. The left movement creates a higher left peak in the left ischial tuberosity and lower values in the right one, and this happens symmetrically for the right movement. In the forward position, the same zones have lower values than in rest position, without reaching the saturation. In backward movement, the distribution is very close to the rest one: the subject, indeed, does not have the full control of his trunk and so his backward movements are very limited.

In other cases, the higher pressure values correspond to the contact of the thighs with the edge of the pillow. An example is represented in *figure 88*.

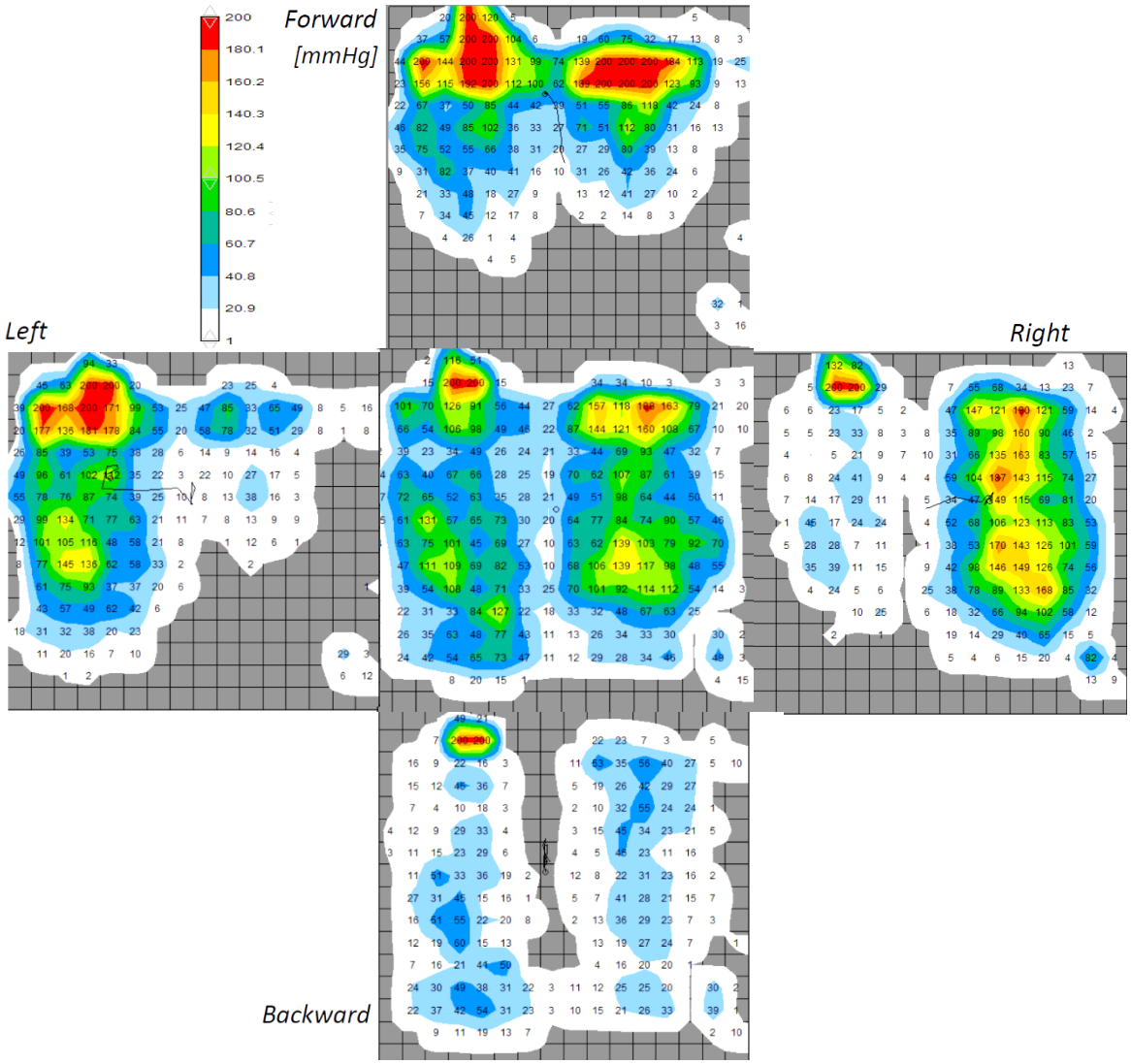

Figure 88. *Pressure distribution in static test. (N.B.); centre: rest position.*

In this case, the non zero values are more spread, and the whole pressure distribution assumes, on average, higher values than the previous case (*figure 87*). The movements are wider since the subject have the control of his trunk: the forward and backward position highly differ from the rest position. The rest pressure distribution is quite symmetrical, apart

for a peak of pressure in the distal part of the left thigh, which reaches saturation values not only in forward and left position, but even when the movement is backward or to the right. In this case, even in dynamic conditions, that zone maintains the same saturation value. This could be associated to a wrong posture and should be further investigated: a limited region with constant and high pressure value, could produce tissue damage.

There is no agreement on a pressure threshold for tissue damage. The existent studies were executed for daily wheelchair; some researchers indicated that tissue damage occur with a peak of pressure (PP) of 45 mmHg with friction, and 67.5 mmHg without friction. Nevertheless, many studies recorded PP greater values than the tissue damage thresholds reported in literature [30,31,32]. Differences between static and dynamic seat interface pressures were recorded: PP in static seat was lower than in dynamic tests. According to the research by Kalpen [32], reduced PP was found with an air-filled cushion compared with foam. Static PP was 18kPa (135mmHg) on the air cushion and 25kPa (187.5mmHg) on foam. The maximum PP was approximately 40% greater for the foam cushion than for the air. Kernozek found PP values of 16.2 kPa (121.5 mmHg) in static seat, and 20.3 (152.3) in dynamic seat. The values found in this work are sometimes higher. Apart for Q.V, K.H, F.P, G.D., all the subjects presented PP saturation values (200mmHg) in at least one of the static positions: this mean that those values can be even higher. This could be associated, as reported in literature, to the foam cushion that is usual for rugby wheelchairs and could be moreover, a pressure able to induce tissue damages. Nevertheless, the cited studies refer to daily use wheelchairs, in which tissue damage is owed to the fact that the user sits for long time in the same position, and with a pressure distribution that varies only in relation to limited movements. This situation highly differs from the large range of movement that a rugby player exhibits during a match: in this case, pressure distribution varies primarily because of the propulsion movement, and the risk for tissue damage should be lower since it does not involve long times in the same position. The presence of eventual zone with constant saturation values should be further examined.

From the data analysis of the dynamic test, the maximal horizontal and vertical displacement of the COP (*figure 89*) during a set of 10 pushes, were extracted and represented in *table 10.* These values give information about the personal pushing technique. The COP position is calculated by the software as a weighted average between the sensors' pressure values: therefore, its position in the mat square is influenced by artefacts. Nevertheless, the displacement is not affected by this problem, since it was calculated as a difference, and its absolute position within the square is not relevant.

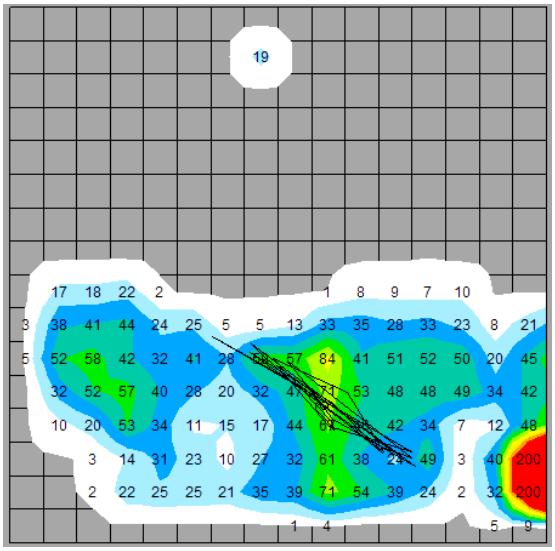

***Figure 89**. Displacement of the COP during dynamic tests (G.M.).*

		DELTA COP [cm]	
INITIALS	**POINTS**	**HORIZONTAL**	**VERTICAL**
B.A.	3,5	13,39	3,88
B.N.	2	2,94	2,96
B.M.	2,5	1,90	5,92
F.P.	1	3,35	2,62
F.A.	0,5	0,75	0,65
G.D.	1,5	2,21	1,83
G.M.	2,5	16,37	10,44
K.H.	1	5,54	3,64
M.P.	3,5	4,81	4,43
P.S.	1,5	3,33	0,99
Q.V.	2,5	4,29	7,71
T.G.	1,5	4,29	4,46
T.N.	2,5	7,60	7,33
V.L.	2,5	4,59	5,07
Z.L.	2,5	2,84	2,61

***Table 10**. Horizontal and vertical displacement of the COP during dynamic tests.*

No correlation between the point of classification and the COP displacement were found: this mean that the COP displacement is related to the personal pushing technique, to the posture in the chair, the pillow and many other factors and cannot be compared.

The use of the trunk itself, is not a discriminant factor since players who fully use their trunk (as M.P, Q.V) have comparable values to those who do not have a full control of their trunk (T.G., K.H.). The higher values were recorded from G.M. (2.5 point of classification): visually, his pushing technique consists of deep movements, and he has the total control of his trunk. The lower values were recorded for F.A. (0.5): he does not have the control of his trunk, and for his physical characteristics, his movement are not wide.

In conclusion, the mat used in this study was not appropriate for these tests: its dimensions fits in a daily use wheelchair seat, but rugby chairs seat is more narrow. Moreover, the presence of straps and border of the seat creates many artefacts and the consequent difficulty to data interpretation, since is not always clear if a zone is generated by the body pressure distribution or by other factors. Moreover, the mat must be calibrated at higher pressures since with the maximum scale value at 200 mmHg, all player reached the saturation so the correspondent values are probably higher.

CHAPTER 7

7.1 Conclusions

A Wheelchair Rugby player is the sum of many different aspects. The present work is comprised in a wider project which investigates this high number of features. Isometric measures of unilateral and bilateral pushing forward, and shoulder/elbow flexion/extension, combined with medical investigations, allowed assessing the presence of asymmetries in contralateral joints, and defining sportive and therapeutic training based on each need. Moreover, they allowed identifying situations at risk of infortune, and programming the recovery of the damaged function to avoid eventual relapses owed to a premature return to the sportive activity.

The tests of 20 m sprint underlined the presence of different pushing techniques, determined the push frequency, the maximum force exerted in a dynamic situation. Rotation tests identified the ability of spinning, and the analysis of eight track showed that some people are more skilled in spinning than in accelerating. From all tests, force rankings were complied, to give a general view of the present situations, and determine which are the points of force of the team.

Forces in dynamic tests were compared with isometric forces, underlining the fact that in dynamic conditions, inertial effects play an important role on force generation. In both cases, the correlation between force and point of classification is not always linear: this means that each player could improve his force with a proper training.

Pressure tests on wheelchair seats underlined the presence of high peaks of pressure if related with literature studies: nevertheless, the mat was not appropriate for the present study for its dimensions and the consequent presence of artefacts.

7.2 Future developments

Biomechanical analysis performed in this work will continue in the next team meetings. Meanwhile, players are undergoing a program of training based on the improvement of force, resistance and skills related to the game.

Isometric force tests will be repeated, to determine the efficacy of sport training, with the adoption of a more standardize acquisition protocols: all subjects must perform the

exercise with the same angles of shoulder, elbow and trunk flexion/extension, same position for wristbands, and minimizing any force compensation effect that could distort measures.

Dynamic tests will be repeated with the same conditions. Wheel sensors will be placed also during a match, to obtain the total distance covered by players. Moreover, the application of a heart rate monitor together with an inertial sensor could synchronize heart rate with forward acceleration and give more information about court performance.

Further analysis comprise the study of trunk movement: with an inertial sensor it is possible to determine trunk angles and acceleration in a sprint, and synchronize it with the forward acceleration of the system. This allow understanding if some oscillations in the forward acceleration trend are owed to the trunk.

The project of a rugby wheelchair ergometer is in program, to allow executing metabolic tests in conditions that are more similar to the real situations, instead of an arm ergometer; moreover, it would make possible the MoCap analysis of the propulsion.

The realization of an inclining platform with force plates will allow determining the spatial localization of the centre of mass of the wheelchair-player system. Starting from that, a study on the stability of the system will be executed.

The use of a Smart Wheel could have different applications: as example, in dynamic conditions, for the synchronization of force signals on the handrim with the forward acceleration, and on the ergometer, to perform test also with the MoCap for a deeper and complete study.

The analysis of performance is carrying on with investigations about strikes: the understanding of the maximal loads applied on the wheelchairs, allows starting a FEM study which should end in the proposal of modifications to improve the frame structure.

The biomechanical analysis performed in this study, moreover, wanted to increase the knowledge about Wheelchair Rugby, which lacks of research studies: this sport is still not well known.

Sport for people with physical disability can help them finding an autonomy and a higher knowledge of their potentialities, which are helpful also in their daily activities. For this reasons it is necessary to continue the study, and to spread information about Paralympic sports which are as important as sports for able-bodied. Moreover, in Paralympic sports, where the personal difficulty is higher, the dedication and the final satisfaction could be even greater. As Pierre de Coubertin, founder of the modern Olympic Games, stated: "*The sport goes looking for the fear to dominate it, the effort to surmount it, the difficulty to win*".

REFERENCES

[1] International Wheelchair Rugby Federation. IWRF Classification Manual. 3rd Edition; Revised 2015.

[2] Athens 2004 Organising Committee for the Olympic Games. The Paralympic Games from 1960 to 2004.

[3] International Wheelchair Rugby Federation. International Rules for the Sport of Wheelchair Rugby 2015.

[4] Official site of IWRF: http://www.iwrf.com/

[5] LHV van der Woude, HEJ Veeger, AJ Dallmeijer, TWJ Janssen, LA Rozendaal. Biomechanics and physiology in active manual wheelchair propulsion. *Medical Engineering & Physics* 2001; 23: 713-733.

[6] CC Campbell, MJ Koris. Etiologies of shoulder pain in cervical spinal cord injury. *Clin Orthop Relat Res* 1996; 322:140-5.

[7] IH Sie, RL Waters RH Adkind, H Gellman. Upper extremity pain in the postrehabilitation spinal cord patient. *Arch Phys Med Rehabil* 1992; 73:44-8.

[8] Y Vanlandewijck, DTheisen, D Daly. Wheelchair Propulsion Biomechanics: Implications for Wheelchair Sports. *Sports Med* 2001; 31(5):339-67.

[9] American Colleague of Sports Medicine. Resource manual for guidelines for exercise testing and prescription. Philadelphia: Williams & Wilkins, 1993. 2nd ed.

[10] X Devillards, P Calmels, B Sauvignet, A Belli, C Denis, C Simard, V Gautheron. Validation of a new ergometer adapted to all types of manual wheelchairs. *Eur. J. Appl. Physiol*. 2001; 85, 479-485.

[11] LHV Van der Woude, G De Groot, AP Hollander, GJ Van Ingen Schenau, RH Rozendal. Wheelchair ergonomics and physiology testing of prototypes. *Ergonomics* 1986; 29(1):1561-73.

[12] KT Assato, RA Cooper, RN Robertson, JF Ster. Smartwheels: development and testing of a system for measuring manual wheelchair propulsion dynamics. *IEEE Trans Biomed Eng* 1993; 40: 1320-4.

[13] HEJ Veeger, LHV van der Woude, RH Rozendal. Load on the upper extremity in manual wheelchair propulsion. *J Electromyogr Kinesiol* 1991; 1 (4): 270-80.

[14] HW Wu, FC Su. An instrumented wheel for the kinetic analysis of wheelchair propulsion. *J Biomed Eng* 1998; 120:533-5.

[15] K Roeleveld, E Lute, HEJ Veeger, T Gwinn, LHV van der Woude. Power output and technique of wheelchair athletes. *Adapt Phys Act Quart* 1994; 11(1):71–85.

[16] HEJ Veeger, EM Lute, K Roeleveld, LHV van der Woude. Differences in performance between trained and untrained subjects during a 30-s sprint test in a wheelchair ergometer. *Eur J Appl Physiol Occup Physiol* 1992;64(2):158-64.

[17] HEJ Veeger, LHV van der Woude. Force generation in manual wheelchair propulsion. In: XIII Southern Biomedical Engineering Conference, 1994:779-82.
[18] HEJ Veeger, LHV van der Woude. Force generation in manual wheelchair propulsion. In: H Van Coppenolle, Y Vanlandewijck, J Simons, et al., editors. Proceedings of the First European Conference on Adapted Physical Activity and Sports: a white paper on research and practice; 1994 Dec 18-20: Leuven. Leuven: Acco, 1995: 89-94.
[19] LY Guo, KD Zhao, FC Su, KN An. Moment generation in wheelchair propulsion. *Proc Inst Mech Eng H*. 2003;217(5):405-13.
[20] WJ Rankin, AM Kwarciak, WM Richter, RR Neptune. The influence of altering push force effectiveness on individual muscle demand during wheelchair propulsion. *J Biomech.* 2010; 43(14): 2771–2779.
[21] AJ Dallmeijer, LHV van der Woude, HEJ Veeger, AP Hollander. Effectiveness of force application in manual wheelchair propulsion in persons with spinal cord injuries. *Am J Phys Med Rehabil* 1998; 77 (3): 213-21.
[22] AJ Dallmeijer, YJ Kappe, HEJ Veeger, TW Janssen, LH van der Woude. Anaerobic power output and propulsion technique in spinal cord injured subjects during wheelchair ergometry. *J Rehabil Res Dev* 1994; 31 (2): 120-8.
[23] FCT van der Helm, HEJ Veegert. Quasi-static analysis of muscle forces in the shoulder mechanism during wheelchair propulsion. *J Biomech*. 1996;29(1):39-52.
[24] CC Usma-Alvarez, FK Fuss, A Subic. Effects of rugby wheelchair design on output velocity and acceleration. *Procedia Engineering* 2011. 13: 315–321.
[25] YC Vanlandewijck, AJ Spaepen, RJ Lysens. Wheelchair propulsion efficiency: movement pattern adaptations to speed changes. *Med Sci Sports Exerc* 1994; 26 (11): 1373-81.
[26] AJ Spaepen, YC Vanlandewijck, RJ Lysens. Relationship between energy expenditure and muscular activity patterns in handrim wheelchair propulsion. *Int J Indust Ergon* 1996; 17: 163-73.
[27] HEJ Veeger, LHV van der Woude, RH Rozendal. Wheelchair propulsion technique at different speeds. *Scan J RehabilMed* 1989; 21: 197-203.
[28] LHV van der Woude, HEJ Veeger, RH Rozendal. Propulsion technique in hand rim wheelchair propulsion. *J Med Eng Tech* 1989; 13: 136-41
[29] YC Vanlandewijck, AJ Spaepen, M Heister. Maximal exercise responses and manual wheelchair propulsion: cardiorespiratory and movement pattern adaptations to slope and velocity changes. In: Van Coppenolle H, Vanlandewijck Y, Simons J, et al., editors. Proceedings of the First European Conference on Adapted Physical Activity and Sports: a white paper on research and practice; 1994 Dec 18-20: Leuven. Leuven: Acco, 1995: 73-8.
[30] M Kosiak. A mechanical resting surface: its effect on pressure distribution. *Arch Phys Med Rehabil* 1976; 57:481-4.
[31] TW Kernozek, JE Lewin. Seat Interface Pressures of Individuals With Paraplegia: Influence of Dynamic Wheelchair Locomotion Compared With Static Seated Measurements. *Arch Phys Med Rehabil.* 1998; 79(3):313-6.

[32] Kalpen A, Bochdansky T, Seitz E. The dynamic body pressure distribution in a moving wheelchair. Workshop MW04: RESNA Conference, June 7-12, 1996.
[33] MNX MEMS and Nanotechnology exchange: https://www.mems-exchange.org
[34] M Andrejasic. Mems Accelerometers. Seminar at Ljubljana University 2008.
[35] G Bellusci, F Dijkstra, P Slycke. Xsens MTw: Miniature Wireless Inertial Motion Tracker for Highly Accurate 3D Kinematic Applications. *Xsens Technologies* 2013; Version 29.
[36] F Hintzy, N Tordi. Mechanical efficiency during hand–rim wheelchair propulsion: effects of base-line subtraction and power output. *Clinical Biomechanics* 2004; 19:343-349.

APPENDIX 1

Power Spectral Density

The analysis in the frequency domain is a strong and useful instrument for signal elaboration. In fact, for some kind of signals, time description can be insufficient to understand their properties. In this work, the calculation of Power Spectral Density (PSD) is an important mean to extract some characteristics of the signal that, in time domain, would have been very difficult to extract.

PSD allows understanding the strength of the variations as a function of frequency: it shows at which frequencies variations are strong, and at which they are weak. The unit is energy per frequency. To evaluate PSD it is first necessary to introduce some elements of signal analysis, as Fourier Transform, energy and power.

Let x(n), $-\infty < n < +\infty$, be a real discrete signal, obtained from the sampling of the continuous signal x(t); the continuous Fourier Transform of x(n) is:

$$X(\omega) = FT\left[x(n)\right] = \sum_{n=-\infty}^{\infty} x(n)e^{-j\omega n}$$

It is a complex function of the real variable ω (pulsation *ω=2π/f, f* is the frequency). For a real signal as *x(n)* is, the FT has even module and odd phase: it is sufficient to represent its module and phase in the interval of frequencies of 0-π, or, in terms of frequencies, 0-0.5. In the continuous domain, with sample frequency Fs, the correspondent intervals are 0-π Fs for ω and 0-0.5*Fs for frequency.

Given *x(n)* as a discrete signal with a finite number of samples, n=0,1,…N-1, next the FT it is possible to calculate the Discrete Fourier Transform with the following expression:

$$X(k) = DFT\left[x(n)\right] = \sum_{n=0}^{N-1} x(n)e^{-j\frac{2\pi}{N}nk}$$

k=0,1,..N-1. It is a complex signal with N samples. From the comparison between FT and DFT, it is clear that X(k) represents the sequence on N samples of X(ω) in the interval of 0-2π, as shown in *figure 90.*

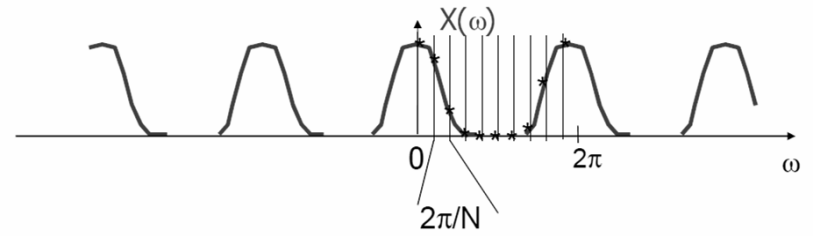

Figure 90. *Graphical representation of discrete Fourier Transform of a signal.*

Let x(t) be a deterministic continuous signal, defined in $0 < t < \infty$, its energy is:

$$E = \int_{-\infty}^{+\infty} x^2(t)dt$$

Form Parseval theorem considering the Fourier transform (FT) of x(t), being $X(\Omega) = FT(x(t))$, energy density is:

$$E = \int_{-\infty}^{+\infty} x^2(t)dt = \frac{1}{2\pi}\int_{-\infty}^{+\infty} |X(\Omega)|^2 \, d\Omega$$

And energy spectral density has the following expression:

$$S(\Omega) = \frac{1}{2\pi}|X(\Omega)|^2$$

This expression, integrated in a certain interval of frequencies Ω_1- Ω_2 , gives the energy contained in x(t) and associated to those frequencies.

Nevertheless, some signals (stationary and stochastic) have infinite energy, so it becomes necessary to evaluate power, with this expression:

$$P = \lim_{T\to\infty} \frac{1}{2T}\int_{-T}^{T} x^2(t)dt$$

And Power Spectral Energy:

$$P(\Omega) = \frac{1}{2\pi}\lim_{T\to\infty}\frac{1}{2T}\left|\int_{-T}^{+T} x(t)\, e^{-j\Omega t}\, dt\right|^2 = \lim_{T\to\infty}\frac{1}{2T}E$$

This expression, integrated in a certain interval of frequencies Ω_1- Ω_2, gives the power contained in x(t) and associated to that band.

The literature offers many instruments to calculate PSD: parametrical methods, based on FT (indirect methods using the autocorrelation function, or direct methods), or non parametrical, based on the use of models. In this work, PSD was calculated with the direct method of the periodogram.

The formulas to calculate PSD, as shown in the previous expression, implicates the evaluation of energy and its infinite limit: since the signal x(t) is not defined in an infinite number of samples, an estimator is defined, as:

$$\hat{P}_{PER}(\omega) = \frac{1}{N}\left|\sum_{0}^{N-1} x(n)e^{-j\omega n}\right|^2 = \frac{1}{N}|X(\omega)|^2$$

In a practical field, this value is calculated through the Discrete Fourier Transform (DFT):

$$\hat{P}_{PER}(k) = \frac{1}{N}\,|DFT[x(n)]|^2 = \frac{1}{N}\left|\sum_{n=0}^{N-1} x(n)\, e^{-j\frac{2\pi}{N}nk}\right|^2 = \hat{P}_{PER}(\omega)\,\Big|_{\omega=\frac{2\pi}{N}k}$$

k=0,1,…N-1.

In this work, in Matlab environment, PSD of the acceleration signal was obtained via the Matlab function for the fast Fourier Transform *fft(x)*.

APPENDIX 2

Matlab code

2.1 Peak detection for forward acceleration analysis

This appendix contains the data analysis, with Matlab R2015a, performed for signal of forward acceleration in 20 m sprint tests, with the importing of text file and peak detection algorithm.

```
close all
clc
clear all

%% Import data from text file
% Initialize variables.
filename = 'C:....\MT_00200108_000-000_00341101.txt'; %file path
delimiter = '\t';
startRow = 6;

% Format string for each line of text:
formatSpec = '%f%f%f%f%f%f%f%f%f%f%[^\n\r]';

% Open the text file
fileID = fopen(filename,'r');

% Read columns of data according to format string.
dataArray = textscan(fileID, formatSpec, 'Delimiter', delimiter,
'EmptyValue’,NaN,'HeaderLines' ,startRow-1, 'ReturnOnError', false);

% Close the text file.
fclose(fileID);

% Allocate imported array to column variable names
PacketCounter = dataArray{:, 1};
SampleTimefinish = dataArray{:, 2};
Acc_X = dataArray{:, 3};
Acc_Y = dataArray{:, 4};
Acc_Z = dataArray{:, 5};
Gyr_X = dataArray{:, 6};
Gyr_Y = dataArray{:, 7};
Gyr_Z = dataArray{:, 8};
Roll = dataArray{:, 9};
Pitch = dataArray{:, 10};
Yaw = dataArray{:, 11};
```

```
% Clear temporary variables
clearvars filename delimiter startRow formatSpec fileID dataArray ans;

%% Signal elaboration

%Time axis
freq=75; %sampling frequency [Hz]
n_sample=size(Acc_X,1); %number of samples
Ttot=n_sample/freq; %total time of acquisition
t_sample=1/freq;    %time period
t=0:t_sample:Ttot-t_sample; %time axis

Acc=Acc_Y;  %Forward acceleration
Acc_max=max(Acc);
figure
plot(Acc)
grid on

%Elimination of drift values
ind_drift=input('Choose drift indexes: '); %selection of Acc indexes
drift=mean([Acc(ind_drift(1)) Acc(ind_drift(2))])
Acc=Acc-drift;

%Selection of acceleration period to analyse
period=input('Choose time period to analyse: ');
start=period(1);
finish=period(2);

%PSD extraction
Acc2=Acc(start:finish); %acceleration to analyse
N=n_sample;
Acc_ft=fft(Acc,N);  %Fourier Transform
freq_ft=0:freq/N:freq-freq/N;   %frequency domain
PSD=(abs(Acc_ft).^2)/N;   %Power Spectral Density
PSD=PSD(1:N/2);
freq_ft=freq_ft(1:N/2);

figure
plot(freq_ft,PSD)
hold on

%Push frequency extraction
n_sample2=length(Acc2);
[val,ind_ord]=sort(PSD,'descend');
freq_peaks=freq_ft(ind_ord);
freq_push=0;
for i=1:length(freq_peaks)
    plot(freq_peaks(i),val(i),'+')
    ans=input('Accept the peak? y/n ','s');
    if ans=='y'
        freq_push=freq_peaks(i);
        break
    end     %if
end   %for
hold off

t_push=1/freq_push; %push period
Ttot_acc=t(finish)-t(start)+t_sample;
M=round(Ttot_acc/t_push);    %number of pushes
n_acc=round(n_sample2/M);   %number of samples for each push
```

```
figure
plot(Acc2)
grid on
hold on

%Division of acceleration in push periods
ind_peaks=[];
peaks=[];
k=1;
for i=1:M
    [c,d]=max(Acc2(k:k+n_acc));
    ind_peaks=[ind_peaks d+k-1];
    peaks=[peaks Acc2(ind_peaks(i))];
    k=k+n_acc+1;
    if k+n_acc>n_sample2
        [c,d]=max(Acc2(k:end));
        ind_peaks=[ind_peaks d+k-1];
        peaks=[peaks Acc2(ind_peaks(i+1))];
            break
    end     %if

end   %for

threshold=0.5*max(peaks);
hold on
plot(threshold*ones(n_sample2),'-b')
p=find(peaks>=threshold);
plot(ind_peaks(p),Acc2(ind_peaks(p)),'*r')

Acc_mean=mean(peaks(p));
```

2.2 Covered distance

After the extraction of each wheels covered distance with the function *integral*, following lines contain the code for the extraction of distance covered by the wheelchair-player system, represented by the middle point (MP) of the beam connecting wheels axles.

```
function y=integral(x,start,finish)
%%Trapezoidal integral of signal x.
%%x: signal to integrate
%start, finish: initial and finale indexes of integration

freq=75;    %sample frequency
n_sample=size(x,1);
Ttot=n_sample/freq;
t_sample=1/freq;
t=0:t_sample:Ttot-t_sample;

x_int=x(start:finish);   %signal to integrate

%Integration
y(1)=trapz(t(start:start+1),x_int(1:2));
k=1;
for i=start:finish-1
```

```
    y_temp=trapz(t(i:i+1),x_int(k:k+1));
    y(k+1)=y_temp+y(k);
    k=k+1;
end %for

end %function
```

%%Calculation of wheelchair covered distance

```
load('Right_wheel');  %Gyr_right, distance_right
load('Left_wheel');   %Gyr_left, distance_left
load('MP_Frame');  %Gyr_frame, start and finish indexes, time axis

diameter_inches=input('Insert wheels diameter (inches): ');
      %generally, 24 or 25 inches
diameter=diameter_inches*0.0254;

%Average between wheels angular velocities
Ang_vel_med=0;
for i=1:length(Gyr_right)
    Ang_vel_med(i)=(Gyr_right(i)+Gyr_left(i))/2;
end   %for

%Integration of Ang vel med
distance_med=integral(Ang_vel_med,start,finish);
distance_med=distance_med/360*(diameter*pi);

%Results
figure
subplot(211)
plot(b,Ang_vel_med(start:finish),'-r')
grid on
ylabel('Ang vel med [deg/s]')
subplot(212)
plot(b,distance_med,'b-')
hold on
plot(b,distance_right,'-b','LineStyle','--')
plot(b,distance_left,'-b','Linestyle',':','LineWidth',1.5)
xlabel('Time [s]')
ylabel('Distance [m]')
legend('Average','Right wheel','Left wheel')
grid on
hold off

distance_tot_right=distance_right(end); %right wheel distance
distance_tot_left=distance_left(end);   %left wheel distance
distance_tot_MP=distance_med(end);  %wheelchair middle point (MP)
distance
```

RINGRAZIAMENTI

Ringrazio prima di tutto la mia famiglia: i miei genitori, i miei fratelli Andrea e Arianna, e i miei nonni, che mi sono stati vicini in tutti questi anni di studi, dandomi la forza di continuare nei momenti più difficili, e gioendo assieme a me per ogni piccolo traguardo raggiunto.

Tutti i miei amici e le persone importanti che ho incontrato in questi anni nella mia strada, che con la loro pazienza mi hanno supportato sempre ed hanno creduto in me. Senza i tanti bei momenti passati con loro, staccando dallo studio, non sarei arrivata a questo traguardo.

Ringrazio il prof. Petrone e tutti i ragazzi incontrati ad Ingegneria Meccanica, assieme ai quali ho passato questi ultimi mesi imparando molto sia dal punto di vista scolastico che umano.

Infine i ragazzi del Wheelchair Rugby, grazie ai quali ho scritto questa mia tesi e conosciuto un mondo che sempre porterò con me.

Maria Laura